ENERGY RECOVERY FROM ORGANIC WASTEWATER VIA MICROBIAL FUEL CELL TECHNOLOGY: A NOVEL APPROACH

Samuel Putra

University of Oxford

Trinity College

Department of Engineering Science

A thesis submitted for the degree of

Doctor of Philosophy

Michaelmas 2022

Abstract

One promising technology that offers a potential breakthrough in terms of energy recovery from wastewater efforts is Microbial Fuel Cells (MFCs). This technology exploits the ability of microorganisms, usually bacteria, to oxidise organic matter contained in wastewater and harness the produced electrons to generate electricity. However, despite its promise, current bottlenecks such as long start-up time, low power output and limited understanding of microbial communities central to the process, prevent this technology to achieve its maximum potential. Through this DPhil project, we have expanded our understanding of the underlying science and mechanisms behind Microbial Fuel Cell technology, as well as pushing towards its applications as a simultaneous solution for wastewater treatment and energy crisis problems in industrial scale.

In this project, two main Extracellular Electron Transfer (EET) mechanisms for *S. oneidensis* MR-1 – mediated electron transfer (MET) and direct electron transfer (DET) were evaluated and analysed for their contributions. The results confirm that electron transfer via mediator contributed 70% of power output, and genetic engineering of cells to include additional flavin-production gene from *B. subtilis* increased the power output by over two-fold. In addition, the *in-situ* transfer of flavin-overexpression genes into the bacterial cell using ultrasound in an MFC setup was achieved for the first time. This study has also demonstrated a significant scale-up to ultrasound gene transfer technology – with working volume of 300 mL, providing ~150X scale-up than those previously reported elsewhere.

Furthermore, the ability of *S. oneidensis* MR-1 to utilise acetate as sole carbon and energy source in an MFC setup was demonstrated. A voltage of 0.032 ± 0.011 V was generated across 1kΩ resistor with 20 mM sodium acetate as the sole carbon source, with maximum power output that reached 1.2 ± 0.1 mW/m^2. The acetate utilisation by *S. oneidensis* was also demonstrated when using anaerobic digester liquor as MFC substrates – with 16.2 ± 4.1 mg/L

of acetate content consumed within 5 days, resulting in ~11% coulombic efficiency. This is a novel finding – as there are no previous literatures that report successful utilization of pure culture *S. oneindensis* to degrade acetate from real AD liquor for electricity generation. Furthermore, this further supports claims that have been made by other researchers – that acetate utilization by MR-1 is not limited only under aerobic condition.

Finally, the viable application of magnetic nanoparticles (MNPs) in MFC setup was demonstrated. The deployment of silica-coated Iron-Oxide Nanoparticles (ION) prevented oxidative nature of the iron core, while maintaining the magnetic property of the nanoparticles. The combined result of these characteristics enabled the use of nanoparticles to form engineered biofilm on the electrode surface without compromising its electricity production. A voltage of ~40 mV was achieved using *E. coli* – *S. oneindensis* MR-1 consortium to degrade glucose, with maximum power production of 39.8 ± 2.4 mW/m^2. The biofilm composition was found to have shifted towards a community predominated by the favoured electrigen which is MR-1 strains, reaching 38.3 ± 7.0% of total cell population – around 5-fold higher compared to 7.4 ± 4.2% of that the control where the nanoparticles were not present. To the best of our knowledge, this is the first reported study of MNP application in MFC as coating agent for bacterial cell – for the purpose of selective biofilm formation of electrigen-enriched electrode.

Future research trends should be focused on the advancement of electrode materials towards cheaper, more biocompatible, and higher effective surface area which promote better biofilm attachment, and further understanding of the biology within bacteria consortium that is often very complex – coupled with genetic engineering and modifications to implement capabilities across bacterial species for complex substrate degradation and enhanced electricity generation capabilities. This study has contributed majorly to some of these aspects through its novel result and findings, although further studies, sensitivity analyses and development

are still required to reach our target end-state. In the future, we believe that the application of MFC should not be limited to wastewater treatment, but also form part of important integrations with other technologies such as biosensory systems, anaerobic digester as well as energy storage and chemical productions. All these milestones should be achieved as we advance our understanding of the science and underlying mechanisms behind the technology.

Acknowledgement

First and foremost, I would like to thank those who are closest to me – my family, for being there when I needed them. It is an understatement to say that without them, I simply would not have survived, let alone made it this far to the very end of my DPhil journey. To Athira – you are my rock, my motivation, and my source of strength.

Secondly, I would like to thank Wei and Ian for their continuous support as my supervisors. I do realise that I was not the easiest student to handle, but their kindness, professionalism and understanding has helped me through all the ups-and-downs and enabled me to achieve things that I did not think I could. I would forever be grateful for the opportunities that you both have given me, and I sincerely wish you good health and success for many years to come.

I would also like to thank the entire Begbroke family – for all their helps and friendships for the past 5 years. I do learn from every single one of you, and I wish you all great success in your future career.

Finally, I would like to thank Jardine Foundation, as the financial sponsor of my DPhil study. I am grateful for their continuous support, especially for granting me a scholarship extension when the Covid-19 pandemic hits. Without them, this whole thing would not have been possible.

Table of Contents

List of figures *1*

List of tables *4*

List of abbreviations *5*

Chapter 1: Introduction *7*

1.1. Background **7**

1.2. Research aims and objectives **8**

1.3. Knowledge gaps and relevant achievements **9**

1.4. Structure of the thesis **10**

1.5. List of publications and paper in preparation **12**

Chapter 2: Literature Review *13*

2.1. Wastewater: Current treatment and future projection **13**

2.2. Microbial fuel cells (MFCs) **13**

2.3. Performance of MFC **15**

2.4. MFC Designs and components **20**

2.5. Bacteria and substrate for MFC application **26**

2.6. Genetic modification for MFC performance improvement **35**

2.7. MFC challenges, limitations, and opportunities **39**

2.8. Integration of MFC with other technologies **42**

2.9. Magnetic nanoparticles (MNPs) **45**

Chapter 3: Selective biofilm formation on electrode surface of microbial fuel cell using iron-oxide magnetic nanoparticles *49*

3.1. Introduction **49**

3.2. Materials and methods **51**

3.3. Results and discussion **62**

3.4. Conclusion **74**

Chapter 4: Genetic engineering biofilms in situ using ultrasound-mediated DNA delivery *76*

4.1. Introduction **76**

4.2. Materials and Methods **79**

4.3. Results and discussion **87**

4.4. Conclusion **94**

Chapter 5: Current generation in microbial fuel cells by Shewanella oneidensis MR-1 via assimilation of acetate *100*

5.1. Introduction **100**

5.2. Materials and Methods **104**

5.3. Results and discussion 109
5.4. Conclusion 117
Chapter 6: Conclusion, limitations, and future directions 120
6.1. Conclusion 120
6.2. Limitations 121
6.3. Future directions 122
References 125
Appendices 151

List of figures

Figure 2.1: Schematic diagram of MFC

Figure 2.2: MFC reactors type and architecture

Figure 2.3: Extracellular electron transfer (EET) mechanisms of *S. oneidensis* MR-1

Figure 2.4: Proposed EET pathways of *S. oneidensis* MR-1

Figure 2.5: Alternative EET pathways of *S. oneidensis* MR-1

Figure 2.6: Bioelectrochemical system comprising of bioanode (oxidation of organics; wastewater) and biocathode (i.e. reduction of CO_2 into acetate)

Figure 3.1: Growth curve of *E.coli* and *S.oneidensis* MR-1 in different carbon source (LB, Glucose, Lactate, Acetate and Formate) at a) 30^{o}C and b) 37^{o}C

Figure 3.2: Bioproduction of iron-oxide magnetic nanoparticles via iron reduction with *S. oneidensis* MR-1

Figure 3.3: Colony forming unit (CFU) of the target system and negative controls of the iron reduction experiment

Figure 3.4: SEM images of MR-1; a) MR-1 in free suspensions; b) MR-1 with self-produced iron-oxide nanoparticles clumped on its cell wall

Figure 3.5: Iron reduction experiment with iron (III) concentration of 20, 25, 30, 35 and 40 mM (from left to right)

Figure 3.6: CFU of bacterial cells at varying concentration of Iron (III) NTA for iron reduction experiment

Figure 3.7: a) Size distribution of PAH-coated ION; Measured in duplicates (blue and red) through zetasizer. Average size 34.6 ± 14.6 nm (zeta potential 56.8 ± 4.4 mV); b) Luminescence per OD via bacterial ATP assay; three negative controls (water, minimal media (MM) and MNPs used as baseline. Luminesce of MNP-MR1 samples was measured for 7 days with no noticeable change in activity, indicating longevity in viability post MNP-

coating; c) Coating efficiency of PAH-coated ION for low cell concentration of 100 cells/mL (blue) and 10 cells/mL (orange) at time of 15 min, 60 min and 24 hr

Figure 3.8: a) TEM images of PAH-SiO2-ION; images were taken using JOEL TEM 2100, with 200 kV beam; b) FT-IR spectrum of PAH-SIO2-ION

Figure 3.9: a) Voltage of MFC systems across 1 kΩ resistor for 5 days; Positive controls *MR1_E.coli_Glu* (blue) and *MR1_For* (grey), and both MFC with PAH-SIO2-ION (yellow and light yellow) all reach steady state voltage of ~40 mV. Other MFCs dropped to ~5 mV. Data shown were the mean value of triplicate measurements; Negative controls and error bars were not shown for simplicity; b) Polarisation curve and c) power curve of *Si_MNP-MR1_E.coli_Glu*

Figure 3.10: a) Concentration of glucose consumed (blue bar) and cell density of anodic culture (orange line) of different MFC systems; b) %occupancy of MR1 cells on electrode surface of MFC anodes; measurement was taken at the end of MFC experiment (day 5)

Figure 4.1: a) Electric current density *I* versus elapsed time, b) polarisation curve (current density vs. potential) and c) power density curve of MFC reactors with *S. oneidensis* MR-1 WT (blue), MR-1/YYDT-C5 mutant (orange) and MR-1 Δ*bfe* strains (grey) with 20 mM sodium lactate as sole carbon source

Figure 4.2: a) Measured optical density at 600nm (OD_{600}) of anodic culture of MFC reactors utilising *S. oneidensis* MR-1 WT, MR-1/YYDT-C5 mutant and MR-1 Δ*bfe* strains with 20 mM sodium lactate as sole carbon source. Measurement were done using 1 cm cuvette (1 mL sample size). b) Biofilm quantification using crystal violet assay: optical density at 595nm (OD_{595}) of cell-bound crystal violet solution from anodic biofilm cells of the MFC reactors. c) The amount of lactate consumed by each reactor.

Figure 4.3: Schematic diagram of ultrasound-based DNA delivery (UDD) into bacterial cells of mature biofilms established in microbial fuel cell (MFC)

Figure 4.4: a) Electric current density *I* of double-compartment MFC reactors running at 1kΩ load with 20 mM initial concentration of sodium lactate; b) extracellular flavins concentration of MFC reactors after 14 days of operation

Figure 5.1: a) Voltage of Lactate-fed MFC across 1 kΩ resistor over time; the resistance was increased gradually to establish a polarisation curve. *MR1_Lac* system (green) showed a step increase in voltage each time the resistance was increased, whereas *NoMR1_Lac* system did not generate any current; b) Polarisation curves of *MR1_Lac* system showing a maximum attainable power of 2.39 ± 0.61 μW/cm^2; c) Concentration of lactate (solid) and acetate (dash) over time in *MR1_Lac* (green) and *NoMR1_Lac* (yellow) systems

Figure 5.2: a) Voltage of Acetate-Fed MFC systems over time across 1kΩ resistor for 6 days, *MR1_Ac* (orange) and *NoMR1_Ac* (blue) was fed with 20 mM acetate whereas *MR1_NoAc* (grey) has no carbon source; b) Polarisation curve of *MR1_Ac* established on day 6 with potentiostat showing maximum power output of 0.12 ± 0.01 μW/cm^2; c) Concentration of acetate in the anodic compartments of *MR1_Ac* (orange) and *NoMR1_Ac* (blue) on day 0 (stripes) and day 6 (dots); d) Optical density at 600 nm wavelength (OD_{600}) of anodic culture of *MR1_Ac* (orange) and *MR1_NoAc* (grey) on day 0 (stripes) dan day 6 (dots)

Figure 5.3: a) Voltage of MFC systems fed with AD liquor across 1kΩ resistor for 5 days, all systems were injected with 1.1 mL AD liquor to achieve initial acetate concentration of 30 mg/L inside the reactors. Wild-type strain (blue) reached a voltage of 0.033 ± 0.002 V, consistent with acetate-fed MFC result (fig. 2); *pYYDT-C5* strain (green), *dBFE* (yellow) and negative control *No Bac* (orange); b) Concentration of acetate inside MFC reactors at day 0, 3 and 5. Acetate concentration in *no Bac* reactors remained unchanged; c) optical density of anodic culture at day 0, 3 and 5

Figure 5.4: a) Scanning Electron Microscope (SEM) image of *Shewanella oneidensis* MR-1 biofilm on carbon cloth electrode; b) thick biofilm was found at some parts of the electrode surface; c) planktonic *S. oneidensis* isolated from the anodic media

List of tables

Table 2.1: Examples of previous MFC studies with pure culture bacteria

Table 2.2: Examples of previous MFC studies with multi-species consortium

Table 2.3: List of experiments performed to engineer *S. oneidensis* for MFC improvement

Table 3.1: Description of the two targets and 5 negative controls of the iron reduction experiment with *Shewanella oneidensis* MR-1

Table 3.2: Explanation of the different MFC systems being experimented in chapter 3

Table 3.3: Anaerobic growth result of single strain and co-culture of *E. coli* and *S. oneidensis* MR-1, with glucose and fumarate as carbon source and electron acceptor

Table 3.4: Plate count result of *S. oneindensis* coated with PAH-coated ION; CFU of MNP-MR1 was almost identical to those of the control, indicating full biocompatibility

Table 4.1: List of strains and plasmid used in Chapter 4 experiment

Table 4.2: The steady-state bioelectrical current density and maximum output power density (power per unit electrode surface area) of the MFC running with MR-1 wild-type and mutants

Table 4.3: Final electric current density (current per unit electrode surface area) and extracellular flavin concentrations of UDD-treated MFC systems

Table 5.1: Bacterial strains and plasmids used in Chapter 5 experiment

List of abbreviations

AD	Anaerobic Digester
ATP	Adenosine Triphosphate
CC	Carbon Cloth
COD	Chemical Oxygen Demand
DET	Direct Electron Transfer
DO	Dissolved oxygen
EET	Extracellular Electron Transfer
GC	Gas Chromatography
HPLC	High Performance Liquid Chromatography
ION	Iron Oxide Nanoparticles
LB	Lysogeny Broth (for cell culture)
LC	Liquid Chromatography
MET	Mediated Electron Transfer
MFC	Microbial Fuel Cell
MM	Minimal media (for cell culture)
MN	Magnetic Nanosphere
MNP	Magnetic Nanoparticles
MR1	*Shewanella oneidensis* MR1
OCV	Open-Circuit Voltage
PAAH	Poly(allylamine hydrochloride), polymer for nanoparticles coating
PEM	Proton Exchange Membrane
PHB	Polyhydroxybutyrate
PTFE	Polytetrafluoroethylene

SEM	Scanning Electron Microscope
UDD	Ultrasound DNA Delivery
VFA	Volatile Fatty Acid

Chapter 1: Introduction

1.1. Background

Based on 2021 annual reports published by 12 water and sewerage companies in the UK, every day in the UK over 16 billion litres of wastewater are generated from homes, municipal, and commercial and industrial premises [1]. In most, if not all cases, wastewater contains potentially valuable energy locked within it in a form of organic matters. Typical wastewater contains organic matters that is equivalent to chemical energy content of around 13 MJ/kg COD [2]. Despite this huge potential, ironically wastewater treatment processes today are still net energy consumers. Globally, wastewater treatment plants (WWTP) consume larges amount of energy, estimated at between 1 – 3% of global energy output [3]. Although some technologies, such as anaerobic digestion [4]–[6], biogas utilization [7], [8], sludge handling processes [9]–[12] and thermal hydrolysis process [13], [14] have been utilised to recover some portion of energy from wastewater, most of the useful energy within it remains unrecovered, leaving significant rooms for further improvement in energy recovery technologies. Through this DPhil, we focused our studies on Microbial Fuel Cell (MFC) as one of the promising solutions to the simultaneous wastewater and energy problems. Through better understanding of the science and mechanisms behind how MFC operates – we hoped to push the barrier of our current knowledge on MFC – its potential, limitations and opportunities / specific efforts needed for it to fulfil its true potential of industrial scale applications. Hence, this DPhil study was intentionally focused on works within laboratory scales, and less on industrial applications – to enable more efficient knowledge transfer with previous studies/reports and content build-up.

1.2. Research aims and objectives

The aim of this DPhil research is to push further the development of Microbial Fuel Cell (MFC) technology as a viable solution to renewable energy alternative using wastewater as the sustainable energy source – through better understanding of its science and mechanisms. To achieve this, we focused our works within laboratory scales and less on industrial applications – to enable more efficient knowledge transfer with previous studies/reports and content build-up. Nonetheless, we hoped that our results and findings through this study could act as a foundation to improve the feasibility and long-term viability of MFC applications for industrial applications – taking this technology to its full potential.

In this study, a comprehensive view of relevant objectives is considered and pursued, considering three fundamental scientific factors – biological, chemical, and physical. The three research objectives are set as the following:

1. Biological modification of key bacterial genes (i.e., genetic engineering) to maximise extracellular electron transfer (EET) for greater power recovery
2. Investigation of alternative carbon source for energy generation in MFC system via chemical analysis of short-chain organic acids
3. Physical manipulation and control of biofilm architecture on electrode surfaces to favour electrogenic bacteria build-up for higher electrode usage efficiency

Objective (1) was addressed through determination of the most dominant EET mechanism of studied bacteria, followed by identification of relevant genes required to enhance such mechanism, and novel *in-situ* gene transfer technique via ultrasound. Objective (2) was addressed thorough chemical analysis of MFC metabolites, validated with appropriate electrochemical experimentations with anaerobic digester liquor as the experiment substrate. Objective (3) was addressed via synthesis and selection of suitable magnetic nanoparticles,

key characterisation of synthesised nanoparticles and their application in multi-species microbial fuel cell setup to degrade complex organic matters.

1.3. Knowledge gaps and relevant achievements

The identified **knowledge gaps** found prior to this study includes the following:

1. Determination of the most dominant extracellular electron transfer (EET) mechanism of studied bacteria (i.e., *Shewanella oneidensis* MR-1) in a dual-chamber MFC setup – on-going debate of mediated electron transfer (MET) vs. Direct electron transfer (DET) being the dominant extracellular electron transfer (EET) mechanism
2. Lack of feasible approach for *in-situ* genetic modification in MFC setup
3. On-going debate whether pure culture *S. oneidensis* MR-1 is able to utilize acetate as sole carbon source in MFC setup i.e., limited publication on acetate utilisation for power generation in MFC systems with single culture *S. oneindensis* MR-1
4. No publications on application of magnetic nanoparticles (MNP) as coating agent for bacterial cell for the purpose of selective biofilm formation in MFC setup; previous studies on nanoparticles application on MFC have mostly focused on electrode surface modifications and mostly used non-magnetic nanoparticles

This DPhil project has **contributed to the field by filling the identified gaps above, and achieved the following** through detailed experimental studies:

1. Successful demonstration of use of magnetic nanoparticles (MNP) to encourage selective biofilm formation in a multi-species MFC setup (*S. oneidensis* – *E. coli* consortium), increasing the coverage of electrode area by electrigen by over 5X fold, generating 39.8 ± 2.4 mW/m^2 with glucose as carbon source

2. Use of silica-coating as protective layer for iron-oxide nanoparticles core, to prevent its redox nature which competes with electrode as electron acceptors
3. Determination of flavin-mediated electron transfer (MET) as the key EET mechanism for *S. oneidensis* in lactate-fed MFC dual-chamber setup, contributing up to 70% of total power output
4. Successful demonstration of *in-situ* ultrasound gene transfer in MFC setup, increasing current density level by 61% after addition of flavin-bioproduction genes with significant Ultrasound DNA Delivery (UDD) application scale-up through 300mL working volume
5. Confirmation of acetate as a viable carbon source for electricity generation in MFC using single-culture *S. oneidensis* MR-1, generating 4.89 ± 0.34 $\mu A/cm^2$ with anaerobic digester liquor as the source of acetate

1.4. Structure of the thesis

This thesis was structured as to provide a clear run-through of what was done and achieved through the DPhil project – written in chronological order so reader can follow the logics and development of the study:

- Chapter 1: Introduction (this chapter).
- Chapter 2: Literature review – conducted as a base of our research, to populate the current knowledge and understanding of the technology and to identify the gaps relevant to our research objectives.
- Chapter 3: Selective biofilm formation on electrode surface of microbial fuel cell using iron-oxide magnetic nanoparticles – our experimental effort started with development of biocompatible magnetic nanoparticles – synthesized through chemical and biological methods. The produced nanoparticles were then used in

multi-species MFC to promote selective biofilm formation to enrich electrogenic bacteria occupation on electrode surface for improved MFC performance.

- Chapter 4: Genetic engineering biofilms *in situ* using ultrasound-mediated DNA delivery – our second experimental study focused on 1) determination of dominant EET mechanism, through study of different MR-1 mutants in lactate-fed MFC; and 2) Once key mechanism was determined, we implemented a novel gene transfer method via ultrasound to transfer flavin-synthesis pathway plasmid into wild-type *S. oneidensis* to enhance electricity generation.
- Chapter 5: Current generation in microbial fuel cells by *Shewanella oneidensis* MR-1 via assimilation of acetate – our final experimental study focused on further utilization of acetate as the intermediate product of lactate metabolism by *S. oneidensis*, for further electricity generation, thus expanding the substrate envelope for MR-1 application in MFC system.
- Chapter 6: Conclusions, limitations, and future directions – At the end of all experiments and analysis, we summarized the key results and takeaways of our work and provide recommendation and future directions for this technology development.

1.5. List of publications and paper in preparation

1. Ng CK*, Putra SL*, Kennerley J, Habgood R, Roy RA, Raymond JL, Thompson IP, Huang WE. 2021. Genetic engineering biofilms *in situ* using ultrasound-mediated DNA delivery. Microbial Biotechnology 2021 14(4):1580-1593. https://doi.org/10.1111/1751-7915.13823. (*The two first authors contribute equally to the manuscript)
2. Putra SL, Thompson IP, Huang WE. 2022. Current generation in microbial fuel cells by *Shewanella oneidensis* MR-1 via assimilation of acetate. (In preparation).
3. Putra SL, Thompson IP, Huang WE. 2022. Selective biofilm formation on electrode surface of microbial fuel cell using iron-oxide magnetic nanoparticles. (In preparation).

Chapter 2: Literature Review

2.1. Wastewater: Current treatment and future projection

Based on 2021 annual reports published by 12 water and sewerage companies in the UK, every day in the UK over 16 billion litres of wastewater are generated from homes, municipal, and commercial and industrial premises [1]. In most, if not all cases, wastewater contains potentially valuable energy locked within it in a form of organic matters. Typical wastewater contains organic matters that is equivalent to chemical energy content of around 13 MJ/kg COD [2]. Despite this huge potential, ironically wastewater treatment processes today are still net energy consumers. Globally, wastewater treatment plants (WWTP) consume larges amount of energy, estimated at between 1 – 3% of global energy output [3]. Although some technologies, such as anaerobic digestion [4]–[6], biogas utilization [7], [8], sludge handling processes [9]–[12] and thermal hydrolysis process [13], [14] have been utilised to recover some portion of energy from wastewater, most of the useful energy within it remains unrecovered, leaving significant rooms for further improvement in energy recovery technologies.

2.2. Microbial fuel cells (MFCs)

One promising technology that can offer a breakthrough in energy recovery from wastewater is microbial fuel cells (MFCs). Such technology was first reported in 1910 – where bacteria was shown to be able to produce electricity [15]. Further concepts and practical developments were explored since, including Cohen's 35-unit setup in 1931 [16], Karube et al. catalyst study in the 70's [17] and works on synthetic mediators by Benetto et al. in the 80s-90s which resulted in the development of so-called "Analytical MFC" that is known till this date [18]. Microbial fuel cells (MFCs) exploits the ability of microorganisms, usually

bacteria, to oxidise organic matters contained in wastewater and harness the produced electrons to generate electricity. In nature, bacteria grow by catalysing chemical reactions and harnessing and storing energy in the form of adenosine triphosphate (ATP). In bacteria, organic matters are oxidised and electrons are produced. These electrons then flow down a respiratory chain – a series of enzymes that moves protons across an internal membrane to create a proton gradient. Due to this gradient, the protons then flow back into the cells through enzyme ATPase, creating 1 ATP for every 3-4 protons. As the last step, the electrons are released to electron acceptors available, usually oxygen. The two half-reactions that happen during the process (taking acetate as the organic substrate) are summarised in Equation 2.1 and 2.2. Note that *Equation 2.1* is written as a reduction reaction (due to the international convention), although an oxidation reaction is what really takes place.

$2HCO_3^- + 9H^+ + 8e^- \rightarrow CH_3COO^- + 4H_2O$ Eq. 2.1

$E_{an} = -0.296$ V ($C_{species}$ = 5 mM; pH = 7)

$O_2 + 4H^+ + 4e^- \rightarrow 2H_2O$ Eq. 2.2

$E_{cat} = 0.805$ V ($pO_2 = 0.2$; pH = 7)

In an MFC, the bacteria and the organic substrate are contained inside the anodic chamber in the absence of oxygen or any other electron acceptors except the anode. Driven by the potential difference between the electrodes, the produced electrons then flow through an external circuit to reach the electron acceptors that are made available in a separate chamber, the cathode. These flowing electrons, i.e., electrical current, is the energy recovered by the MFC. The produced protons (H^+) flow from the anode through an ion exchange membrane, or sometimes salt bridge, to the cathodic compartment and recombine with the electrons and its acceptor to form reduced products (water, for example, when the electron acceptors are oxygen). The process is illustrated in Figure 2.1.

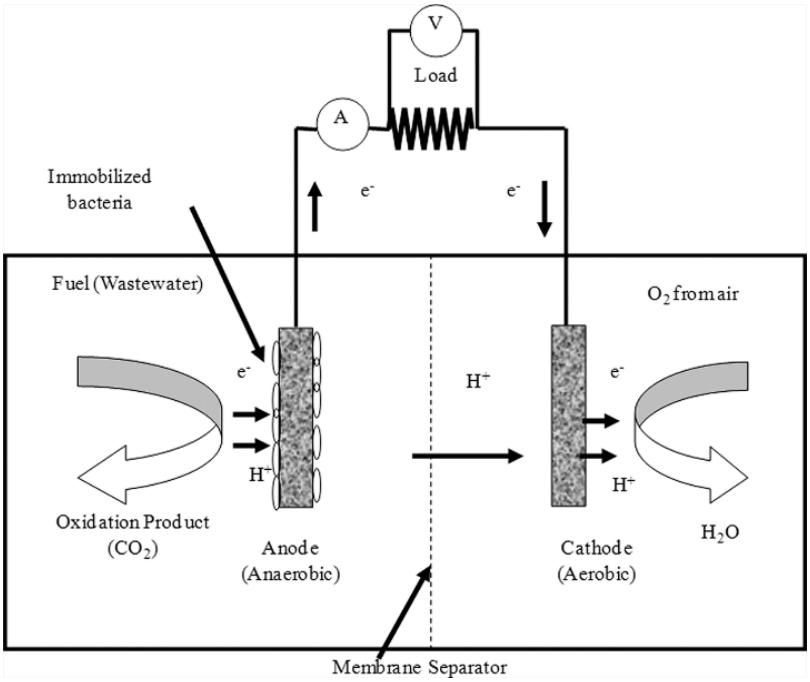

Figure 2.1: Schematic diagram of MFC [19]

The difference in redox potentials of the reaction occurring in each chamber creates the electromotive force E_{emf} ($E_{cat} - E_{an}$) within the MFC, which drives the current to flow. Thermodynamically, positive E_{emf} means that the reaction is spontaneous and electricity is generated. When acetate ($C_{species}$ = 5 mM; pH = 7) is the organic substrate and oxygen (pO_2 = 0.2; pH = 7) acts as the electron acceptors, the cell E_{emf} is = 0.805 – (-0.296) = 1.1 V. This calculated E_{emf} provides the upper limit for the cell voltage.

2.3. Performance of MFC

2.3.1. Open-Circuit Voltage (OCV)

The cell E_{emf} is a thermodynamic value that does not consider potential losses. Open-circuit voltage (OCV) is the actual potential measured between the anode and cathode in the absence of current. In theory, OCV should approach E_{emf}. In practice, however, OCV will be lower than E_{emf} due to various potential losses. These losses are usually referred to as overpotentials, which is the difference between potentials at equilibrium and the actual

measured potentials. For example, a typical measured potential of oxygen reduction reaction at a cathode at pH 7 is about 0.2 V (vs SHE), which is significantly lower than the potential under equilibrium conditions (0.805 V). In this case, the cathode overpotential is 0.805-0.2 V = 0.605 V.

2.3.2. Cell voltage (E_{cell}) and internal resistance

When the circuit is closed, current starts to flow through the external circuit. Due to the internal resistance of the MFC, the cell voltage generated will be lower than OCV and can be calculated using Equation 2.3. [20]

$$E_{cell} = OCV - i.R_{int}\ ; \qquad Eq.2.3$$

Where E_{cell} is cell voltage (V), R_{int} is the internal resistance of the MFC (Ω) and i is the current (A). Besides ohmic losses, R_{int} also includes other current-dependent losses that occur at the electrodes. These losses could be categorised as follows: i) activation losses; ii) mass transport losses; iii) bacterial metabolic losses.

2.3.2.1. Ohmic losses

The ohmic losses in MFCs consist of resistance to the flow of electrons through the electrodes and connection equipment, as well as the resistance to the proton flow through the anodic and cathodic medium and exchange membrane (if present) [21], [22]. Ohmic losses can be reduced by minimising the spacing between the anode and cathode, using high conductivity electrode and low resistivity membrane, and increasing the conductivity of the electrolytes to the maximum tolerated by the bacteria [23]–[26].

2.3.2.2. Activation losses

Activation losses are attributed to the energy required to initiate the redox reaction at both electrodes. At the anode, the transfer of electrons from the bacteria to the anode has been the major source of activation loss [27]. At the cathode, the same problem occurs with the high-energy barrier to pass the electrons to its acceptor, e.g. oxygen [28], [29]. Activation losses can be reduced by increasing the electrode surface area, improving electrode catalysis, and through the establishment of enriched biofilm on the anode surface [30]–[32].

2.3.2.3. Mass transport losses

Slow mass transfer rates of the chemical species from the bulk fluid to the electrode surface (and vice versa) cause further loss in MFC. At the anode, mass transport losses are caused by limited supply of substrate to the electrode, and by limited discharge of oxidised species from the anode surface [28]. At the cathode, lack of dissolved oxygen (DO) on the cathode surface often become major limitation in power generation of MFC [29], [33]–[35]. In continuous MFC, mass transfer resistance can be reduced by having higher feed flowrate [36], [37]. In batch MFC, stirring can help enhance the mass transport of chemical species to and from the electrodes [38], [39]. However, stirring and higher flowrate require energy which could sometimes be higher than the energy generation of the MFC itself, hence careful consideration is needed.

2.3.2.4. Bacterial metabolic losses

In MFC, the actual anodic potential is higher, i.e. less negative, than the substrate potential since some potentials are “stolen” for cell growth and reproduction. The higher the difference between the substrate and the anode potentials, the greater the energy gain for bacterial metabolic activities, but the lower the maximum recoverable potential for the MFC. To

maximise voltage generation of MFC, the anode potential needs to be kept as low as possible. However, if the anode potential is too low then electron transport will be inhibited, and fermentation reaction may be favoured [20], [40].

2.3.3. Power generation

There are several ways to evaluate the performance of MFC; principally through power output and coulombic efficiency. The power output is calculated as

$$P = i.E_{cell}\ ; \qquad Eq.2.4$$

Where P is the power output (W). When a fixed resistor is used as load, the current can be evaluated using Ohm's Law:

$$i = \frac{E_{cell}}{R_{ext}}; \qquad Eq.2.5$$

Where R_{ext} is the external resistance (Ω). Hence power output can be evaluated as follow:

$$P = i.E_{cell} = \frac{{E_{cell}}^2}{R_{ext}}\ ; \qquad Eq.2.6$$

The performance is usually expressed in terms of power density, that is the power output normalised with respect to the anode area:

$$P^* = \frac{{E_{cell}}^2}{A_{An}R_{ext}}\ ; \qquad Eq.2.7$$

where P^* is power density (W/m^2) and A_{An} is the anode total surface area (m^2).

2.3.4. Polarisation curve

Polarisation curve is needed to evaluate the maximum attainable power of an MFC. In polarisation curves, cell voltage is plotted as a function of current. Polarisation curves can be

obtained by using potentiostat, where one can control the voltage of the fuel cell and observe the generated current. If potentiostat is not available, a variable resistor box can offer an alternative. By measuring the cell voltage and current (using Ohm's Law) at different resistance value, polarisation curves can be generated. Caution needs to be taken when using variable external resistance technique, that measurements must be taken only when steady-state conditions have been achieved (i.e. constant generation of current). In reality, the produced current will rarely reach steady state - especially when operated in batch mode where substrate concentration is finite [41]. Hence, pseudo steady-state is often satisfactory to conduct the analysis e.g., changes less than 1% after 15 minutes [42]. From polarisation curves, power as a function of current can be calculated easily. From this power curves, then the maximum point at which MFC generates maximum power can be identified.

2.3.5. Coulombic Efficiency

Coulombic efficiency represents the ratio between the total coulombs recovered in electricity generation to the maximum possible coulombs if all substrate removal produced current. The total coulombs obtained is calculated by integrating the current over time, whereas the maximum possible coulombs are calculated using Faraday's Law of electrolysis. The coulombic efficiency for a batch system is calculated using Equation 2.8.

$$\in_c = \frac{M \int_0^{t_b} i \, dt}{\Delta C . V . z . F} \; ; \qquad Eq. 2.8$$

Where $\in_c$ is coulombic efficiency, M is molar mass of the substrate (gr mol^{-1}), ΔC is change of concentration of substrate (gr m^{-3}), V is anodic chamber volume (m^3), F is faraday constant (96485 C mol^{-1}), z is the number of moles of electrons generated per mole of oxidised substrate (for acetate, then z = 8), and t_b is total time of operation.

Coulombic efficiency is reduced by utilisation of alternate electron acceptors by the bacteria besides anode, either those present in the medium (i.e. wastewater) or those diffusing through

the exchange membrane (for example, oxygen). Other factors that decreases the efficiency are alternative processes such as fermentation and/or methanogenesis and bacterial growth [43], [44].

2.4. MFC Designs and components

2.4.1. MFC reactors type and architecture

Many types of reactors have been tested in MFC systems, but they all share the same operating principle. Different configurations of MFCs have been/are being developed using a variety of materials. As always, each type has some advantages over the others at a certain operating condition. Generally, MFC reactor type could be classified into three categories: i) double-compartment MFCs; ii) single-compartment MFCs; iii) Up-flow MFCs;

2.4.1.1. Double-compartment MFCs

This is the most widely used design consisting of two chambers with the anode and cathode compartments separated by an ion exchange membrane. This design is generally used in lab-scale research [45]–[47], as in this project, as the cathodic chamber often needs to be aerated, requiring an input of energy which in practice would minimize the purpose of its industrial applications. Furthermore, some literatures also suggest that the power output from these systems are generally low due to relatively substantial energy / electrical losses, often created by high internal resistance and large separations of the electrodes [48], [49]. An example of a double-compartment MFC is shown in Figure 2.2 a).

2.4.1.2. Single-compartment MFCs

One-compartment MFC eliminates the need for the cathodic chamber by exposing the cathode directly to air. This offers simpler designs hence easier to scale-up, also remove the

energy requirement needed to aerate the cathodic chamber that happens in double-compartment MFCs. In some studies [50]–[53], single-compartment MFCs could generate higher power compared to the double-compartment ones, due to much shorter and simpler connection between the anode and cathode in single-compartment MFCs, which reduces the internal ohmic losses. However, single compartment MFCs often experience low coulombic efficiency, due to leakage of oxygen into the anodic chamber [54], [55]. An illustrative diagram of a single-compartment MFC is shown in Figure 2.2 b).

2.4.1.3. Up-flow MFCs

For continuous operation, up-flow MFCs offer some advantages. This cylindrical MFC consists of an anode (bottom) and a cathode (top), separated by microporous and chemically-stable materials such as glass wool and glass beads layers. The feed is supplied from the bottom of the anode, the effluent passes through the cathode and exits at the top. Due to the vertical design, the air that is bubbled from the top is unlikely to reach the anode, hence oxygen contamination is minimal [56], [57]. Furthermore, bacterial cells remain at the bottom of the cylinder due to its weight and the physical barrier [56]. The schematic diagram of an up-flow MFC is given in Figure 2.2 c).

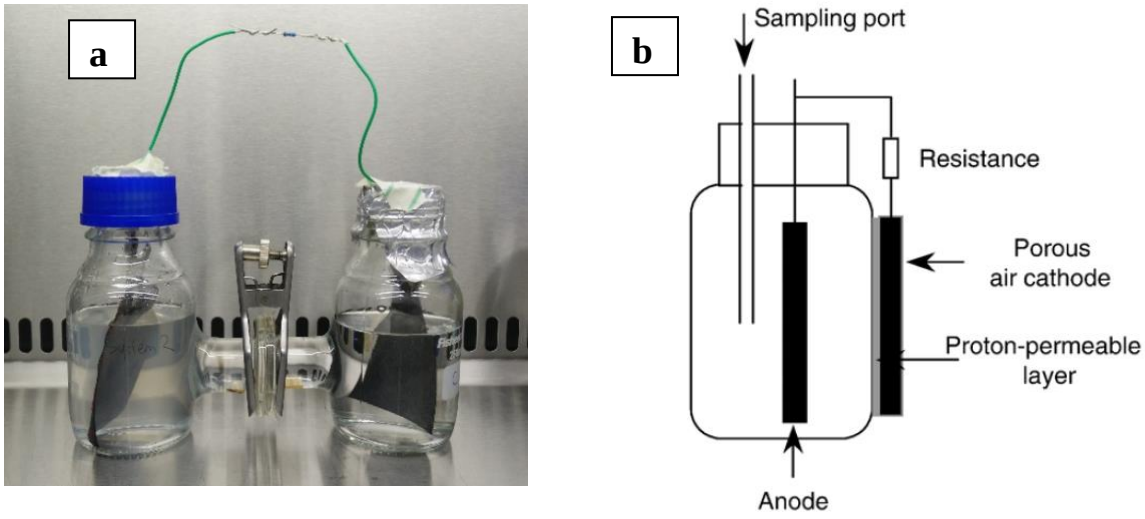

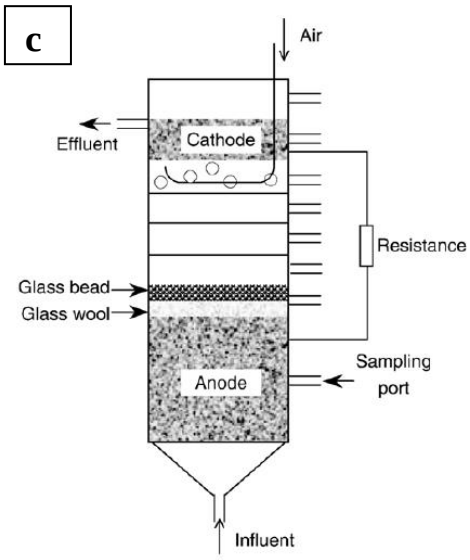

Figure 2.2: a) Double-compartment MFC; b) Single-compartment MFC [58]; c) Up-flow MFC [59]

2.4.2. Anode material and medium

For MFC systems, an ideal anode should have the following features: (i) good conductivity and low resistance; (ii) good biocompatibility; (iii) good chemical stability and corrosion-resistant; (iv) large surface area; and (v) appropriate mechanical strength and toughness [60]–[62]. To achieve this, several materials have been investigated, including carbon, metals and composites [60], [63]–[67]. Although metals present high conductivities, most of them can suffer from corrosion and have lower microbial attachments compared to carbon materials [61], [68], [69]. Therefore, optimization efforts have been conducted to get the best combined features of both metals and carbon materials, including coating of metals with biocompatible materials, such as carbon and polyaniline, grafting with chemical mediators through surface hydrophilization and heat treatment [69]. Recent research has also been conducted on carbon materials that were treated with metal, or metal oxide nanoparticles as electrode support to improve electron transfer [70]–[73]. Carbon materials are an attractive option, due to their biocompatibility, chemically stable and can present a high surface area. The conventional

carbon-based electrodes used in MFC includes carbon cloth, paper, rod, brushes and activated carbon [63], [74]. Carbon brushes offer 3D configuration, providing a higher area for biofilm attachment which in turn increasing the direct electron transfer [75]. However, a trade-off will occur between 3D structure vs. flat electrodes, as the former often result in larger distance between the electrodes which increase the internal resistance, despite providing higher surface area [75].

Besides organic substrates, anodic medium must also contain ions and minerals to sustain bacteria lives. Moreover, the presence of ions will also enhance the conductivity of the electrolyte. However, the ions' concentration must not be too excessive to avoid cells shrinkage. Although one could simply use tap water to provide the ions, the unspecified composition of ions in tap water will leave an unknown factor in MFC study. Furthermore, tap water might also contain microbes which will contaminate the pure culture. In most studies, the minimal media (MM) solution is chosen as medium for cell growth and MFC operation. MM solution is a standard medium for bacterial culture. It contains the necessary ions to provide the suitable osmotic pressure for the bacteria to live [76].

2.4.3. Cathode material and medium

The electrons generated by the microbes would be flowing to the cathode through an external circuit, where it will combine with protons and the electron acceptor to produce reduced products. Since there are no microbes or substrate inside the cathodic chamber, a cathode does not have to exhibit good biocompatibility. The main criteria for a good cathode are: i) low resistance and good conductivity; ii) low reaction overpotential [61], [62]. Platinum (Pt) is a great material for cathode because it provides good catalysis for oxygen-reduction reaction [77]. This results in much lower activation energy hence more energy could be recovered. However, it is too expensive to be commercially attractive [78]. Carbon-based

materials are relatively cheaper, and they offer good conductivity. However, they often introduce high reaction overpotential hence require the presence of catalysts [65], [79]. As a result, work on this field has been focused on finding low costs catalysts as replacement of Pt [80], [81]. Among them, activated carbon is the most commonly used cathode materials due to its low price [82]–[85]. More recently, more studies have been conducted on metal-nitrogen-carbon complex, and metal-organic framework as catalyst for cathodes, showing their ability to fulfil the needs for efficient oxygen reduction reaction [86]–[88].

The efficiency of the cathodic reaction is also determined by the concentration and species of the electron acceptor and the proton availability in the cathodic chamber. Besides oxygen, other chemicals such as hydrogen peroxide and potassium ferricyanide ($K_3[Fe(CN)_6]$) could be used as electron acceptors [89]. The advantage of using ferricyanide is its low overpotential in a plain carbon-based electrode, resulting in high power output [89]. However, such chemical needs to be continuously renewed, hence increasing operational cost. In this study, oxygen (from air) was chosen as the final electron acceptor, because of the cost (it is free) and safety considerations. Similar to anodic medium, cathodic medium must also be electrically conductive to support ions flow.

2.4.4. Proton Exchange Membrane / Separator

Separator is an important component in an MFC to prevent electrical contact between anode and cathode, avoiding short-circuits and increasing the open circuit voltage [62]. It also prevents oxygen diffusion towards the anode, which negatively affects the anaerobic environment within it. Proton exchange membranes (PEMs) are widely used for this application - semi-permeable membranes designed to conduct protons (H^+) while being impermeable to gases such as nitrogen or oxygen [90]. It is used in MFC systems to allow the

produced protons at the anode to travel to the cathode and react with the electrons and its acceptor. The most commonly used material for PEM in MFCs system is Nafion®.

However, they are not totally selective to protons, allowing the crossover of undesirable species that are present in substrates used on the anode side, which accumulates on the cathode side. This will lead to catalyst poisoning, pH change and decrease in cathode reaction e.g., oxygen reduction rate [62]. Therefore, alternative separators such as cation exchange membranes, CMI-7000 from Ultrex, agar salt bridges, sulfonated polyimides, polyethylene and its derivatives, chitosan, nylon and glass fibres, and unconventional materials like natural rubber or even laboratory gloves have been used [88], [91]–[95].

More recently, researchers have tried to attempt an eco-friendlier solution by building membrane separators with sustainable materials such as cellulose [96], [97]. The presence of exchange membrane, however, introduces physical barrier to the flow of H^+. This creates a large resistance to the system and is sometimes the dominant source of the cell's internal resistance [28]. To avoid this, scientists have tried to not use them [98], [99]. In single-compartment MFC [51], although power generation could be increased by not using exchange membrane, the coulombic efficiency was found to be greatly reduced due to the oxygen leakage to the anodic chamber. Furthermore, potential biofilm development at the cathode could greatly decrease the MFC performance [100].

2.4.5. Energy harvesting method for MFC

To complete the circuit and harvest the energy generated by the MFC, a fixed resistor is usually used to represent external load. In MFC studies, resistors are chosen because they are cheap and easy to model [20]. The only drawback of using resistor is that the energy is dissipated as heat, which is not practically useful. Other energy-harvesting devices have been proposed to replace resistor [101], but such devices require further knowledge, and often

involve more complicated operations. Because of these reasons, most studies on MFC use a fixed resistor to absorb the generated power [20]. *Note that resistors are only useful for study purpose; for real world applications, other energy harvesting circuits are required to collect usable energy.*

2.5. Bacteria and substrate for MFC application

Many bacteria possess the ability to oxidise organic compounds and transfer the produced electrons to the anode. Different bacteria work more effectively with a certain organic compound than the others, hence a choice of bacteria in MFCs system is crucial depending on the composition of substrate used. Some examples of bacteria that have been investigated for MFC application are listed in Table 2.1. Please note that the power densities that were delivered by different bacteria across different studies as mentioned in Table 2.1 are not to be compared – as these studies were conducted under different operating parameters, with different optimization objectives.

Table 2.1 Examples of previous MFC studies with pure culture bacteria

Culture	**Substrate**	**Wastewater the substrate is usually contained in**	**Power (mW/m^2)**	**Ref.**
Citrobacter sp. LAR-1	Sodium acetate	Domestic, pharmaceutical	610	[102]
Citrobacter freundii Z7	Citrate	Domestic / municipal	204.5	[103]
E.coli (DH5α)	Glucose	Domestic / municipal	1606	[104]
Shewanella oneidensis MR-1	Lactate	Domestic, pharmaceutical	6,600	[105]
Shewanella oneidensis MR-1	Sodium lactate	Domestic, pharmaceutical	1460	[106]
Shewanella oneidensis MR-1	corn straw	Food industry	660	[107]
Geobacter sp.	Glucose	Domestic / municipal	1296	[108]
Rhodopseudomonas palustris DX-1	Complex organics	Industrial, pharmaceutical	2720	[109]
Escherichia coli	Glucose	Domestic / municipal	2420	[110]
Chlorella vulgaris	Microalgae powder	Medical, textile	1926	[111]
Anaeromusa spp.	Cellulose	Paper industry, textile	3220	[112]
Rhodoferax ferrireducens	Glucose, xylose, sucrose, maltose	Municipal wastewater	158	[113]
Pseudomonas aeruginosa	Glucose, Fructose, Sucrose	Municipal wastewater	136	[114]
Klebsiella pneumoniae L17	Glucose	Municipal wastewater	41.7	[115]

Table 2.2 Examples of previous MFC studies with multi-species consortium

Culture	**Substrate**	**Wastewater the substrate is usually contained in**	**Power (mW/m^2)**	**Ref.**
Gammaproteo and Shewanella affinis	Cysteine	Domestic, textile	36	[118]
Clostridium celluloticum and G. sulfurreducens	Carboxymethyl cellulose (CMC)	Paper industry, textile	500 mA/m^2	[119]
Rhodococcus spp. and Paracoccus spp.	Glucose	Domestic / municipal wastewater	7000 mA/m^2	[120]
E.coli K-12 and manure leachate	Cattle manure	Farming industry	215	[121]
Mixed culture of cellulose degrading bacteria (CDBs)	Rice straw	Food industry	190	[122]
Desulfobulbus and *Clostridium*	Rice straw	Food industry	138 mA/cm^2	[111]
S. oneidensis CP2-1-S1 (mutant) + *E.coli*	Xylose	Food industry, municipal	728.6	[123]
G. sulfurreducens and E.coli	Acetate	Domestic wastewater, pharmaceutical	918	[124]
G. sulfurreducens and C. cellulolyticum	Carboxymethyl cellulose (CMC)	Paper industry, textile	143	[125]
S. oneindensis + S. cerevisiae	Glucose	Municipal / domestic wastewater	123.4	[126]
S. oneindensis + K. pneumoniae	Glycerol	Pharmaceutical, industrial	19.9	[127]
Engineered MR-1 + Engineered K. pneumoniae	Glucose + Xylose	Municipal / domestic wastewater	104.7	[128]
Saccharomyces cerevisiae + Bacillus subtilis	Glucose	Municipal / domestic wastewater	287	[130]
E. coli + P. aeruginosa (*+ Chlorella vulgaris* in cathodic chamber)	Acetate	Municipal, pharmaceutical, industrial	190 (248)	[116]

Multi-species / community-based MFCs have also been studied to degrade more complex organic compounds, as often one bacterial species does not have all the metabolic pathways to degrade these complex chemicals completely, hence inter-species collaboration is required to ensure complete degradation and better electron recoveries [116], [117]. Examples of studies done on multi-species MFC are given in Table 2.2.

Study conducted by *Gurung et al.* [122] utilized a mixed culture of cellulose degrading bacteria (CDBs) isolated by transferring 1gr of fertile soil to modified Dubos salt medium – amended with carboxymethyl cellulose (CMC) as sole carbon source for inoculation. Double chamber MFC with working volume of 160 mL was used, with carbon paper of 5.5 x 5.5 cm^2 used as both anodes and cathodes. Reactors were inoculated with 5mL of mixed culture of CDBs, with rice straw of 1 g/L concentration (cellulose ~50%, hemicelluloses ~25% and lignin ~25%) used as sole carbon source in the anodic chamber, and potassium ferricyanide in the cathode as terminal electron acceptors – generating maximum potential of ~0.6 V and max. power density of 190 mW/m^2 with measured coulombic efficiency of 37%. A different study on mixed culture of genetically modified *Shewanella oneidensis* and *Saccharomyces cerevisiae* was able to produce 123.4 mW/m^2 power density, utilizing glucose as sole carbon source [126]. In this study, ethanol pathway gene of *S. cerevisiae* was knocked out, replaced with lactic acid biosynthesis pathway to enable glucose-to-lactate conversion. A porin protein encoded by oprF gene from *P. aeruginosa* was incorporated into *S. oneidensis* to enhance membrane permeability and its hydrophobicity to facilitate biofilm formation. The power generated was ~2X higher compared to its wild-type counterpart. More recently, a co-culture of *Escherichia coli* and *Pseudomonas aeruginosa* was employed to degrade acetate in dual-chamber MFC system [116] – generating power density of 190 mW/m^2 which was higher than when each bacteria was employed individually under the same setup (139 mW/m^2 for *E. coli* and 159 mW/m^2 for *P. aeruginosa*). Moreover, inoculation of photosynthetic alga

Chlorella vulgaris in the cathodic chamber improved electricity generation to 248 mW/m^2, a further ~40% rise vs. control. This has shown a promising synergistic effect when the co-cultures were coupled with biocathode *C. vulgaris* towards better MFC performance. Similarly, it is worth noting that the power generation by different mixed cultures across different studies in Table 2.2 are not to be compared, neither with one another nor with the studies done on single cultures as outlined in Table 2.1 – as the operational set-up, parameters and study objectives were vastly different from one another.

2.5.1. Real vs. Synthetic wastewater

One of the most significant potential applications of MFC is in power generation from wastewater treatment. Besides using real wastewater (either domestic or industrial), researchers have also used synthetic wastewater in their experiments for good reasons [131]–[133]. Synthetic wastewater is usually chosen as opposed to the real one, because of 1) unavailability of real wastewater; 2) unknown composition of real wastewater; 3) changing concentration and composition of wastewater, depending on when and where it is sampled. These difficulties make consistent analysis extremely difficult, and sometimes impossible. Synthetic wastewater used in MFC studies usually contains a single organic substrate with known concentration, which constitute as the major carbon source present in a typical wastewater. Table 2.1 and Table 2.2 summarises some previous MFC studies that have been done, along with the substrate chosen and the type of wastewater it usually exists in.

2.5.2. Interaction between bacteria and anode

Understanding the electron transfer mechanism between the bacteria and the anode is key to MFCs development. Generally, the mechanisms can be divided into two main categories: 1) contact-independent; and 2) contact-dependent electron transfer.

2.5.2.1. Mediated electron transfer (MET)

Some bacteria do not possess the ability to transfer electrons to the electrode by themselves. For these types of bacteria, electrons must be transferred to the anode with the help of mediators. Mediators, or sometimes refered to as *electron shuttles,* are chemicals capable of receiving electrons from cells and transport it to the electrode. These compounds can either enter the cells and receive the electrons intracellularly (For bacteria uncapable of transferring the generated electrons to their outer membrane) [134], [135]; or take the electrons from the cell's outer membrane via interaction with the OM multiheme c-type- cytochromes (for exoelectrogenic bacteria) [59], [136]. Mediators are important in MFCs that use bacteria such as *Escherichia coli*, *Bacillus*, *Proteus*, and *Pseudomonas* species that are unable to effectively transfer electrons gained from their metabolism to the outside of the cell [137]. Examples of artificial mediators include thionine, benzylviologen, 2,6-dichlorophenolindophenol, 2-hydroxy-1,4-naphthoquinone and various phenazines [89], [117], [137]. However, application of artificial mediators has several major drawbacks. For continuous operation, the mediator needs to be continuously added which adds operational expenses. Furthermore, some artificial mediators are known to be toxic to human, hence handling and disposal are not so straightforward to perform [117], [138]. In some cases, bacteria can produce their own mediators to promote extracellular electron transfer. In metal reducing environment, *Shewanella* spp is known to produce flavin mononucleotide (FMN) and its hydrolysed product, Riboflavin (B2) to help conduct remote electron transfer [139]–[141]. Other bacteria such as *Geothrix ferementans* [142], *Lactobacillus* and *Enterococcus* [143] species are also capable to produce mediators. However, such processes often require a substantial amount of energy [144]. The illustration is given in Figure 2.3 a).

2.5.2.2. Direct electron transfer (DET)

Many studies have also been focused on bacteria that possess the ability to attach to the electrode, i.e. forming biofilm and transfer electrons to the electrode directly [145]–[150]. Once attached, bacteria can transfer the electrons by: i) direct contact of outer-membrane c-type cytochromes; and/or ii) contact via conductive pili or *nanowires.* C-type cytochromes are water-soluble proteins that have been well studied as one of the most important components of the electron transport chain inside bacterial cells. In some bacterial species, such as *Thermincola potens* [148], *Cellulomonas fimi* [149], *Geobacter sulfurreducens* [146], [147], [151] and *Shewanella oneidensis MR1* (the subject of this experiment), these cytochromes also appear at the outer membrane, enabling direct electron transfer to electrode surface. Several studies have also observed the appearance of conductive pili, or sometimes referred to as *nanowire*, produced by *G. sulfurreducens* [147], [152] and *S. oneidensis* [145], [153], that helps the bacteria transfer electrons to electrode surface. This is particularly useful in thick biofilms where some cells are not directly attached to the electrode. The cells in the 2nd, 3rd (and so on) layer of the biofilm is able to transfer the electrons through the *nanowires.* The ability of bacteria to transfer electrons directly to the electrode surface greatly reduces the internal resistance of MFCs, therefore enhancing power generation [145], [147]. The illustration of EET mechanisms is shown in Figure 2.3 b).

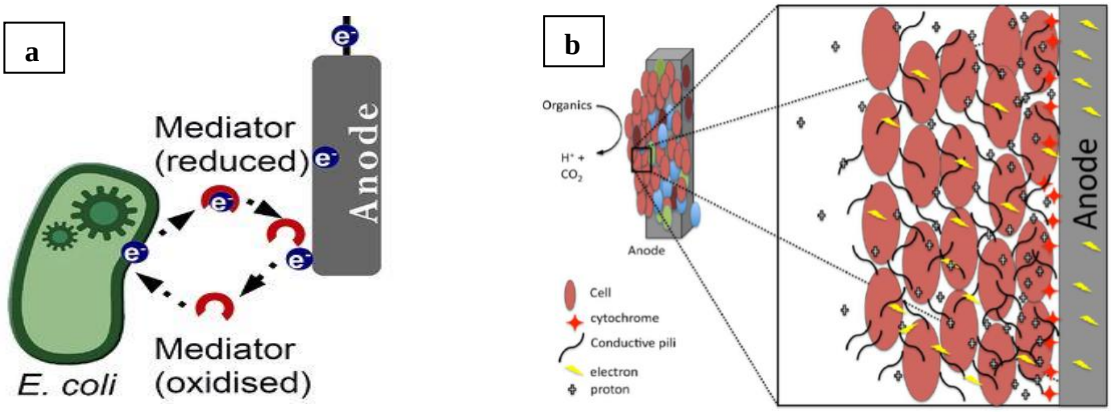

Figure 2.3: a) Mediated electron transfer [154]; b) Biofilm attachment on anode surface, electrons are transferred using c-type cytochrome and conductive pili [155].

2.5.2.3. Extracellular electron transfer (EET) mechanism of S. oneidensis MR-1

Shewanella oneidensis MR-1 is one of a few bacteria that are capable of combining both direct and remote EET mechanisms in its anaerobic respiratory purposes [140], [156]. Although the suggestion that *nanowires* may play a role in EET is still controversial up to this day [153], [157], both mechanisms share the same respiratory pathway which governs the anaerobic respiration of the cell [158]. In the absence of oxygen, electrons are produced via oxidation of carbon source inside the cell and passed on through a series of conductive proteins to the cell outer membrane to reach extracellular electron acceptors. In this pathway (Mtr Respiratory pathway), electrons (from NADH, the intracellular electron carrier) flow through the menaquinol pool, CymA (inner membrane [IM] tetraheme c-type cytochromes), MtrA (periplasmic decaheme c-type cytochromes), MtrB (β-barrel trans-OM protein) and finally to MtrC and OmcA (two OM decaheme c-type cytochromes). The illustration is given in Figure 2.4 [158] .

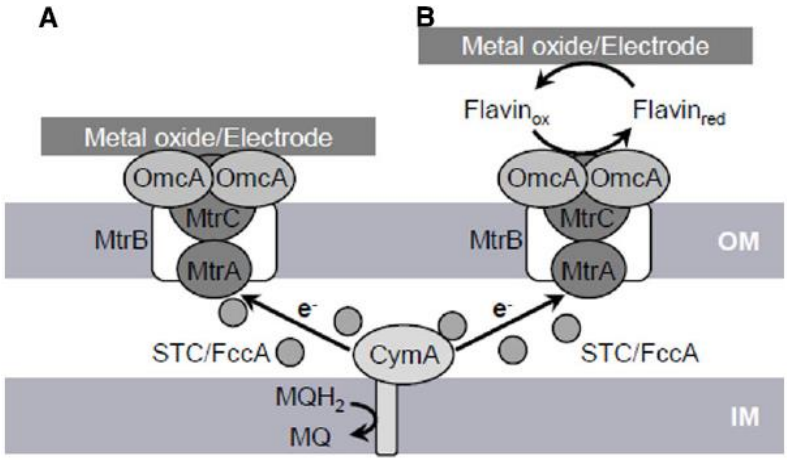

Figure 2.4: Proposed EET pathways (Mtr Pathway) in *S. oneidensis* MR-1 involved in A) direct EET; and B) mediated EET; MQH2, reduced form of menaquinone; MQ, oxidised form of menaquinone [158]

It is worth noting, however, that several studies have observed the presence of other proteins (MtrD, MtrF, DmsE) that could be involved in EET which are not listed in the primary pathway. These proteins serve as alternatives when one or more of the primary proteins are absent [159]. The proposed alternative pathways are illustrated in figure 2.5.

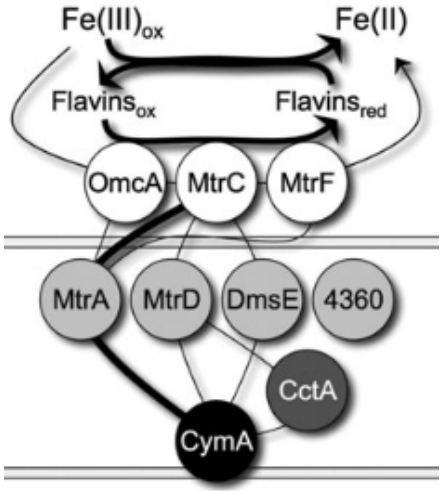

Figure 2.5: Electron flow map for EET pathways; thick lines indicate primary pathway while thin lines indicate pathways observed in their absence [159]

2.5.2.4. On-going debate; which one is the key EET mechanism for S. oneidensis?

In bioelectrochemical systems, there has been an on-going debate regarding which of the EET mechanisms play the most dominant role. Although most believe that direct contact via c-type cytochromes is key [160]–[162], other studies suggest that electron shuttling is more dominant [163], [164]. In fact, both of these observations could be correct, as the most dominant mechanism could potentially be affected significantly by the choice of carbon source, reactors type and operating conditions [160], [164]. Unfortunately, most studies in this regard have been conducted separately by different research groups, making their comparison less informative [165]. Nonetheless, the determination of the most dominant EET mechanism is necessary to further understand how this technology works, and to optimise it

closer to its theoretical limit. If direct contact is the key, the establishment of biofilm would need to be optimised. However, if electron shuttling is key then the optimisation of electron shuttling, along with its production by the bacteria, are crucial for its improvement efforts.

2.6. Genetic modification for MFC performance improvement

Shewanella species synthesise FMN and Riboflavin via electron shuttle production pathway. This pathway requires the protein *ushA* that converts flavin adenine dinucleotide (FAD) into FMN in the periplasmic space of the cell. FAD is transported to the periplasmic space across the inner membrane via a multidrug and toxin efflux transporter called *bfe* (bacterial flavin adenine dinucleotide (FAD) exporter) [163]. Deletion of this gene would result in loss of ability to transport the FAD into the perisplasm where FMN is synthesised, thus severely reducing the extracellular flavins available for electron transfer. In contrast, enhanced bioflavin production in *S. oneidensis* is possible through the addition of synthetic flavin synthesis pathway from *Bacillus subitlis* [164]. This bacterium is one of the most robust industrial riboflavin producers, and its flavin biosynthesis pathway is well studied [164], [166]. This pathway could be encoded into plasmid pYYDT-C5, and inserted into *S. onediensis* via conjugation, with High EET efficiency was able to be achieved [164].

Another step forward of improving the EET is by coupling improved flavin synthesis, with metal-reducing conduit. A mutant encoding flavin biosynthesis gene cluster *rib*D-*rib*C-rib-BA-*rib*E with metal-reducing conduit biosynthesis gene *mtr*C-*mtr*A-*mtr*B were experimented and shown to improve EET efficiency and enhanced power generation of 3.5X compared to control, and ~2X fold compared to mutant with only either gene cluster [167].

Cyclic diguanylate (c-di-GMP) is a second messenger well-known for its function to regulates motility, biofilm formation, virulence and more in response to triggers from the extracellular milieu. Overexpression of this molecule would favour a sessile lifestyle, often

stimulating biofilm formation [168]. Plasmid pYedQ2 encodes *yedQ* gene from *E.coli* which is responsible for the formation of c-di-GMP [169]. The insertion of this plasmid can increase the production of cytoplasmic c-di-GMP, resulting in increased biofilm formation. It was also reported that a transposon mutant of *S. oneidenensis* MR-1 deficient in the biosynthesis of cell surface polysaccharides showed an increase ability to attach to carbon-based anode and generate 50% more current in MFC system [170]. In addition, an engineered MR-1, overexpressed a c-di-GMP biosynthesis gene MP biosynthesis gene *yde*H, significantly enhanced biofilm formation and EET efficiency [171].

Another approach to enhance biofilm formation is to enhance adhesiveness of cell outers to electrode by genetic modification. *S. oneidensis* mutant CP2-1S1 was adopted with highly hydrophobic cell outer feature, increasing its attachment to electrode. In a mixed consortium between *S. oneidensis* and *E.coli,* the numbers of *S. oneidensis* on electrode surface was increased by 3X, whereas the *E. coli* composition decreased by 99% [123]. Coupled with addition of synthetic riboflavin pathway from *B. subtilis*, the electricity generation is increased by almost 7X compared to wild-type control in the same setup.

Besides *S.oneindensis, P. aeruginosa* has also been favored by researchers because of its ability to produce its own mediators phenazine-1-carboxamide, PYO [172], [173] and pyorubrin [174]. PYO is a blue, phenazine-based soluble antibiotic and metabolite that serves as electron shuttles between sessile cells and electrode surface in MFCs [175], and that is absolutely required for biofilm formation since an enzyme PYO demethylase (PodA) was shown to inhibit *P. aeruginosa* biofilm formation [176]. Studies conducted by *Yong et al.* [177] has shown noticeable EET efficiency by overexpression of *phz*M, enhancing PYO synthesis pathway, achieving power density by 4X compared to control WT strain.

Another strategy of gene modification to improve electricity generations is by direct or indirect manipulation of the metabolism of electrogenic microorganisms [170], [178].

Nicotinamide adenine dinucleotide (NAD+) or nicotinamide adenine dinucleotide phosphate (NADP+) and their reduced products NADH and NADPH are essential cofactors and electron mediators that are involved with catabolic and anabolic reactions, and concomitant energy production [179]. Furthermore, NAD+ and NADH play a central role in biofilm EET and metabolic pathways [56] – hence altering the ratio of NADH and NAD+ is a strategy to improve MFC performance. It was reported that abolishment of the lactate biosynthesis pathway in *E.coli* increased the NADH/NAD+ ratio, thus generating higher electrical output of MFCs [180]. It was also found that the availability of intracecullar NAD+/NADH cofactor pool that increased through overexpression of *nadE* (NAD+ synthetase gene), resulted in 3X higher power generation compared to wild type [172]. In other bacteria, heterogenous expression of formate dehydrogenase gene for NADH regeneration was applied to *Clostridium ljungdahlii.* The resulted voltage generation is 3.8X higher compared to parent strain, attributed to higher NADH pool which facilitate electron transfer in the system [181].

Table 2.3 provides a long list of experiments that have been performed to engineer *S. oneidensis* for performance improvement of MFC.

Table 2.3 List of experiments performed to engineer *S. oneidensis* for MFC improvement

Elements	**Remarks**	**Power uplift vs. WT control (%)**	**Ref.**
Biofilm formation			
speF	Gene repression by CRIPSRi	51	[182]
uvrY	Gene repression by CRIPSRi	25	[182]
Metal reducing pathway			
mtrCAB	Overexpression through a medium-strength promoter	347	[183]
mtrC-mtrA-mtrB	Gene cluster for metal-reducing pathway amplified and overexpressed	270	[167]
Cytochromes *cymA*	Gene encoding c-cytochromes in *S. oneidensis*	18	[184]
Flavin biosynthesis			
ribADEHC	Overexpression of flavin biosynthesis pathway from B. subtilis	1321	[164]
ribD-ribC-ribBA-ribE	Gene cluster for flavin biosynthesis from *S. oneidensis* amplified and overexpressed	50	[167]
NADH regeneration			
pfLB-fdh-gapA2-mdh*	Plasmid constructed with both *pfLB* and *fdh**, with individual *placl*	304	[185]
Ycel-pncB	Genes encoding biosynthetic pathway to facilitate utilization of nicotinic acid and nicotinamide	134	[186]

Most frequently used method for plasmid / genes insertion into bacteria is conjugation [187]. In such method, plasmids were often firstly transformed into an intermediate / carrier bacteria or called donor cells using DNA transformation kit. The donor cells are often *E. coli* mutant whose toxicity features has been deleted [188], chosen for its high efficiency of introduction of DNA molecules into cells, rapid growth, and ability to express proteins at very high levels [188], [189]. Once the donor cells have carried the desired plasmids, often proven upon growing the bacteria with antibiotics (as the plasmid carries genes that enable antibiotic-resistance), the plasmid would be conjugated into recipient cells / target bacteria by growing the bacterial mixture together with appropriate antibiotics [189].

2.7. MFC challenges, limitations, and opportunities

2.7.1. Cost effectiveness

One of the largest bottlenecks in MFC scale-up efforts and eventual applications in larger industrial scale is its cost effectiveness. The capital costs of scale-up system vary between USD 735 /m^3 to 36,000 / m^3 [190], [191] – much larger than other typical fuel cell technologies. The electrode materials (especially cathode), and membrane separators have been the primary source of costs [192], [193]. Therefore, developing cost-effective MFC components from low-cost materials are key. More recently, focus of studies have been slowly moving towards membrane-less MFCs [194], [195], or MFCs with low costs membranes e.g., dynamic membrane [196], glass fibre separators [81] and nano filtration membranes [197]. Apart from capital costs, operational costs such as aeration and effluent pumping are also significant to energy usage and costs [198].

2.7.2. Low power output

MFCs are generally known to generate much lower energy output than other fuel cell technologies [199]. Moreover, as MFCs are scaled to deal with larger volumes, power generations tend to worsen [200], [201]. Due to the non-linear inverse relationship between power and size, stacking of small MFC reactors through series and/or parallel connections has been shown to improve voltage and electrical current outputs [202]–[205]. However, stacking often presents new issues due to kinetic imbalance i.e., shunt current formation, voltage, and current reversal [206]–[208]. Different circuit connections also often result in changes in microbial communities [203]. To solve these, recent studies have shown that such challenges can be addressed through careful design of circuitry, coupled with use of maximum power tracker and through usage of enriched electroactive microorganisms [206], [209], [210]. Despite this, more work still needs to be done to enable better understanding about molecular mechanisms of microbe-electrode interactions, biofilm compositions and its synergistic effect, especially in large volume, to make this technology competitive with other existing alternatives [199].

2.7.3. Operational stability and durability

In addition to high costs and low power delivery, there are also operational challenges, which require considerations of substrate characteristics, operating conditions, and durability. Plenty of studies have been explored to investigate and optimize operating conditions such as temperature [211], pH [212], [213], salinity [214], start-up [215] and retention time [216]. However, these studies are often focused on specific substrates, making the optimization efforts limited to case-by-case basis [199]. High salt content in typical wastewaters often cause inorganic fouling, due to blockage of the precipitates that are rich in calcium and

magnesium [217], [218]. Therefore, long-term durability remains a challenge, and further studies are required especially regarding corrosion, biofouling, and potential clogging [219].

2.7.4. Long start-up time

Typical MFCs start-up time ranges from 10s of hours, to a few months, depending on the inoculum, electrode materials, and other operating conditions [220]. Start-up time is defined as the time required for obtaining maximum and stable power output from the beginning of its operations [221]. Usually, the start-up time increases as the scale of the system is increased [221]. Although start-up time can be reduced by increasing the operating temperature [222], this reduces the dissolved-oxygen concentration in the cathode and could potentially harm the MFC equipment. Furthermore, the resistance of electrical components in the MFC increase with temperature. All these factors will result in reduction of power generation. Long start-up time can be caused by multiple factors, including: 1) lack of electron donor and terminal electron acceptor concentration; 2) low ionic strength of electrolytes; and 3) slow biofilm formation [223]–[225]. To promote biofilm formation and attachment to electrode surfaces – some studies have been done to improve electrode surface adhesion and biocompatibility [226]–[229], as well as surface modification and genetic modifications to enable quicker and stronger bacterial attachments on electrode surface [230]–[232]. Furthermore, application of lower external resistance was shown to promote biofilm formation, compared to open circuit condition [223]. Supplementary carbon sources such as glucose and acetate were often added to low-BOD wastewater to promote bacterial growth [233]–[235], and inoculum pre-treatment methods, such as chemical treatment, oxygen and loading shock, and infrared were used on a variety of mixed cultures to inhibits methanogens growth – which promotes current-producing biofilm formation for shorter start up time [236].

2.7.5. Cathodic limitations of MFCs

Typical MFCs utilise oxygen as the final electron acceptor in the cathode, giving out water molecule as given in *Equation 1.2*. The problem with this reaction is significant overpotential, and requirement of expensive catalysts such as Platinum to accommodate the reaction [77]. In some MFC systems, the internal resistance was dominantly contributed by the cathode [237]. To overcome this, researchers have tried alternative electron acceptors such as potassium ferricyanide, $K_3[Fe(CN)_6]$, or other oxidising agents. Although higher voltage could be generated, and the need for expensive catalysts can be exempted, such chemical needs to be continuously supplied hence not sustainable for real-life applications [89].

2.8. Integration of MFC with other technologies

In industrial scale, often MFCs have only been thought as wastewater treatment technology, but not yet as renewable power generator [238]. This is mainly due to the very low power density output, making MFCs not yet attractive to be considered for its energy recovery ability. Furthermore, a relatively low voltage output (~1 V) of a single MFC makes it unattractive to be applied as power source for direct-electrical appliances.

2.8.1. MFC with anaerobic digester

Studies have been carried out on the integration of anaerobic digesters (AD) with microbial fuel cells (MFC) for wastewater treatment. In those studies, AD acts as the primary unit whereas MFC acts as the secondary unit (taking effluent of AD as inlet). This integration is useful primarily because what are considered as by-products of AD, volatile fatty acids (VFA), are valuable substrates for MFC for electricity generation. Furthermore, COD of wastewater could be further reduced by treating the effluent of AD with MFC technology.

Around 16% extra COD removal has been observed by integrating AD with MFC, utilising swine wastewater [239]. In another study [240], mediator-less two chamber MFCs were constructed using dairy digester microbial population as biocatalyst in the anode to convert ground pine tree digestate at 2% (w/v) to electricity – with addition on bovine rumen microorganisms at 1% v/v dosage. Electricity generation reached power density between 17.6 – 67.2 mW/m^2. Separate study conducted by *Cerrillo et al.* [241] used pig slurry digestate to run the MFC reactor – achieved COD removal efficiencies of 50% during AD operation inhibition, with ammonia removal of 31%. It was identified that the main populations in the anode belong to *Bacteroidetes (Flavobacteriaceae), Chloroflexi (Anaerolineaceae)* and *Methanosarcinaceae*.

2.8.2. MFC with electrosynthesis

Voltage generation of a single MFC is usually considered too small for practical direct-electrical applications. Although stacking is possible, the resulted size of the stacked MFC is unfavourable. Other applications of MFC has been proposed, such as production of H_2 in Microbial Electrolysis Cell (MEC) [242]–[247], or other valuable chemicals from CO_2 reduction through electrosynthesis coupled with bioanode [248]–[251].

Electrosynthesis is a chemical synthesis process in an electrochemical cell. In bioelectrosynthesis process, where bacteria is used as biocatalyst in either anodic or cathodic chamber, or both, chemical compounds can be formed in the cathode using electrons recovered from wastewater degradation that takes place in the anodic chamber. Such illustration is given in Figure 2.6.

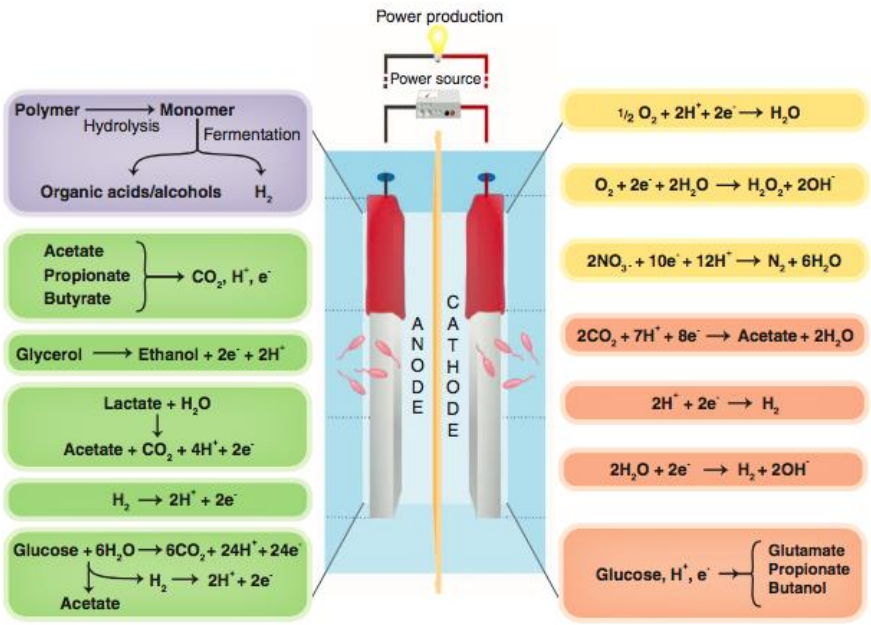

Figure 2.6: Bioelectrochemical system comprising of bioanode (oxidation of organics; wastewater) and biocathode (i.e. reduction of CO_2 into acetate). [252]

In the last decade, reduction of CO_2 to form organic compounds in the cathode has been very attractive thanks to its ability to reduce carbon emission. Reduction of CO_2 can either be physically/chemically assisted (abiotic) [253], microbially assisted (biotic) [254], [255], or both [256]. As opposed to conventional chemical catalysts and metal electrodes (abiotic system), microorganisms as biocatalysts offer great advantages such as higher efficiency [257], milder operating conditions [254] and higher flexibility of target products [258]. Whereas abiotic system is efficient to make C1-C2 organic compounds, biocatalysts (i.e. microorganisms) are much more efficient and sometimes the only way to make long-chain carbon molecules [258]. Some whole-cell bacteria such as *Methylobacteria* and *Acetogens* have been tested to produce formate [254] and acetate [257] from CO_2, respectively. Extensive studies on *Sporomusa ovata* have demonstrated the ability of the bacteria to utilise carbon dioxide and direct current as both carbon and energy source for synthesis of complex organic compounds such as Polyhydroxybutyrate (PHB) [256].

2.9. Magnetic nanoparticles (MNPs)

Nanoparticles technology has emerged as one of the most influential technologies for the future in almost every industrial sectors. Nanoparticles have enormous potential because they exhibit new and interesting properties (e.g. quantum entanglement, unique photonic, electronic and catalytic properties) that bulk materials lack [259]. Magnetic nanoparticles (MNPs) are a class of nanoparticles which can be manipulated using magnetic fields. Such particles are commonly made of magnetic elements such as iron, cobalt, and nickel and their chemical compounds. In recent years, MNPs have been the focus of much research because they exhibit unique properties which could see potential uses in the following sectors (please note this list is not exhaustive): i) medical diagnostic and treatments [260]–[262]; ii) environmental remediation [263]–[266]; and iii) data storage [267]–[270].

2.9.1. MNPs application in microbiology

In *NanoBio* hybrid systems, which is an integration of nanotechnology in biological systems, the combination of nanotechnology and microbiology endows bacterial cells with novel functions which are supposed to have many potential applications, including energy generation and biofuel production [271], optimisation of biosensors [272] and environmental remediation [273]. Some biocompatible MNPs which can coat bacteria without disrupting their viability have been discovered [272]–[274].

In MFC system, surface modifications of electrode with nanoparticles have shown concrete promises of MFC performance improvements. Stainless steel felt electrode treated with flame oxidation, which resulted in formation of iron nanoparticles on the surface, increased surface area of the electrode by ~2X and favoured formation of biofilm (~40 um), while no biofilm was produced without treatment – resulted in 16X higher current density vs. untreated control [275] – however, no such mechanism is revealed so far which describes the direct influence

of nanoparticles to facilitate EET [276]. Carbon nanotube hydrogel-modified carbon paper used as an anode increased the EET rate and improved current density by more than 3X compared to the control [277].

Nanoparticles application on electrodes not only affect the current densities, but also alter the diversity in bacterial community in the biofilm. For an example, application of gold nanoparticles on carbon paper used as anode in MFC, not only improved the power generation and coulombic efficiencies, but also encourage a more diverse microbial communities, as the amount of gold was increased [278]. Modifications of carbon paper with nanoflaky NiO made the surface more hydrophilic, improving the bacterial adhesion and was assumed to increase the DET between outer membrane cytochromes and electrode surface – producing 3X more power compared to control [279].

In addition, EET rates un MFCs can be further facilitated by biogenic inorganic nanoparticles to increase the power output. A study reported that *Shewanella* PV-4 in an MFC with biomineralized iron sulphide nanoparticles showed a substantial increase in density [280]. Moreover, an in-situ biosynthesis of iron sulphide nanoparticles (FeS and FeS_2) with mixed consortia in an MFC setup improved electricity generation and resulted in 519 mW/m^2 power generation, 2x higher compared to control under the same experimental setup [281]. Biosynthesis of palladium nanoparticles by *S. oneindensis* MR-1 in-situ within MFC system remained bound to the cell membrane, enhancing EET facilitation and showed an increase of power density by 75% [282]. Interestingly, it was also observed that larger size of Pd nanoparticles were produced with higher bacterial concentrations used for the biosynthesis.

Magnetite nanoparticles also have shown to enhance electocatalytic activity of electrigens – improving current production when used in MFC with *G. sulfurreducens* [283] and increased hydrogen production when used in MFC with *Desulfovibrio paquesii* as biocathode [284]. A traditional carbon felt electrode, modified with iron-oxide (Fe_3O_4) nanoparticles via facile

dip-and-dry methods, was able to improve power density of MFC employing sulfate-reducing bacteria (SRBs) of almost 2X compared to untreated electrode [285]. Such effects are thought to come from lower charge transfer resistance, higher conductance and increased number of catalytic sites [285]. More recently, study on transfermembrane and outer-membrane silver nanoparticles in a form of reduced graphene oxide-silver (rGO/Ag), was able to facilitate *Shewanella* attachment to the nanoparticles scaffolds to form dense biofilms, and produce *Nanobacteria* hybrid with greatly enhanced electron transfer efficiency [105]. The resulting MFC system delivered max. power density of 6.6 W/m^2, significantly higher to most of reported MFC studies previously. However, despite the great outcome of improvements, the complete mechanism underlying the stimulatory effect of these nanoparticles is still unclear and under debate [105].

Magnetic Fe_3O_4 nanoparticles have also been studied for its effect in EET. It was reported that the decolorization rate of *Aeromonas jandaei* strain SCS5 was significantly enhanced by cell aggregation immobilized with magnetic FE3O4 nanoparticles, compared to regular immobilization [286]. The possible reasons weer thought to be the ability of the nanoparticles to facilitate microbial EET to electron acceptors through aggregation. A 3D coating of anode with magnetite/multi-walled carbon nanotubes (MWCNT) composite enhanced electron transfer from *E.coli* to the anode, while attracting more bacteria on the anode through magnetic field created within the composite [287]. The result of this modification is 30% higher power density (1050 mW/m^2) vs control. Other studies involving magnetite nanoparticles reported its ability to wire up acetate-oxidizing bacteria to trichloroethane dechlorinating bacteria and result in 2-fold dichlorination rate [288]. Similarly, magnetite nanoparticles were also reported to facilitate IET from *G. sulfurreducens* to *Thiobacillus denitrificans* and promote acetate oxidation coupled with nitrate reduction [289].

In this project, we explored the application of magnetic nanoparticles (MNP) of iron-oxide (Fe_3O_4) as means to increase adhesion of bacterial cell to electrode surface, through magnetisation of the bacterial cell. To our knowledge, there is no reported study that has conducted the application of iron-oxide MNP in the same way that we did in this project (direct coating on bacterial cell by MNP for electrode attachment) – hence this study would expand the window of knowledge regarding application of MNP in microbial fuel cell setup.

Chapter 3: Selective biofilm formation on electrode surface of microbial fuel cell using iron-oxide magnetic nanoparticles

3.1. Introduction

In the real world, wastewaters contain dozens, if not hundreds of different organic matters, sometimes very complex and require a community of bacteria to degrade completely. For electricity generation, long carbon chain molecules are often degraded in a series of metabolic pathways, each contributed by certain species in the community, into simpler molecules such as small organic acids (ie. lactate, acetate, pyruvate, succinate) to be utilised by *exoelectrogens* to release electrons to the electrode. Studies regarding MFC have been done extensively using real wastewater, with inoculum coming from the wastewater itself. COD removal between 80% up to 99% [290] and electricity generation in order of ~100 up to >1000 mW/m^2 has been achieved [291]. Most optimization efforts on mixed culture have been done on works surrounding reactor design [292]–[294], membranes [290] and electrode materials [228], [230], [295]. Nonetheless, key bottlenecks remain such as slow start up time [223], [225], [296] and limited electrode surface utilization [123], [297] due to complex bacterial community and inefficient use of electrode surface i.e., mixture biofilm formation consist of many non-conductive bacteria.

It is known that biofilm formation on anodic surface is deemed as one of the key important factors in reducing MFC start up time and improve electricity generation [298]–[300]. Such optimizations effort in accelerating biofilm formations have been conducted, for example via surface modification of gold anodic electrodes [301], [302], manipulation of electrical circuit through variation of external resistances [303], [304], and surface-to-surface biofilm transfer [305]. Although it is only the *exoelectrogens* which contribute directly towards electricity

generation, other bacteria in mixed culture MFCs often occupy the electrode surface resulting in inefficient use of surface area [129], [306]. Hence, it is important to engineer the anodic biofilm such that only the *exoelectrogens* occupy the electrode surface.

To promote selective biofilm formation, the concept of bacterial separations and enrichment with MNPs is not uncommon, given such topic has been extensively studied in recent years [274], [307]–[309]. For example, MNPs functionalized with target molecules such as antibodies, bacteriophages and aptamers were used for bacterial separation and concentration [310]. In a separate study, use of magnetic nanospheres (MNs) was successfully demonstrated to achieve rapid and efficient enrichment of bacteria Salmonella typhimurium, while maintaining 100% MNs recovery within 1 min with a simple magnetic scaffold [307].

The combination of the above two well-known observations provides a clear argument and rationale of the ingoing hypothesis of this chapter – that is to use MNPs to accelerate biofilm formation through selective targeted species build up on the anode surface, that will in turn reduce start up time and enhance MFC performance.

In this study, *Escherichia coli* DH5*α* and *Shewanella oneidensis* MR-1 were employed to form a consortium to generate electricity by degradation of glucose. This is a proof-of-concept work to represent multi-species interaction to degrade rather complex organic matter. *E.coli* will degrade glucose and produce lactate and formate as metabolites – which in turn is used by *S. oneidensis* MR-1 for its metabolism and electricity generation. This symbiotic interaction is necessary as wild-type MR-1 is unable to grow on glucose [311], and *E. coli* DH5*α* is not able to generate electricity in MFC systems without mediators [312]. As it is only MR-1 that contributes directly towards electricity generation, it is of great benefit to engineer the anodic biofilm such that only MR-1 occupies the anode surface whilst keeping *E. coli* DH5*α* stays planktonic in the medium. Previous study has shown that without modification, surface coverage of the anode was almost 50:50 between MR-1 and *E. coli*

DH5*α*, resulted in ineffective utilisation of anodic surface [123]. In this work, Iron-Oxide Nanoparticles (ION) were employed to engineer biofilm formation selectively, to favour *S.oneidensis* build-up on the electrode surface.

The nanoparticles used in this work was iron-oxide magnetic nanoparticles (Fe_3O_4 MNP) – synthesized through both biological and chemical methods. Under anaerobic conditions, *Shewanella oneindensis* MR-1 was able to reduce metal to form its metallic form or reduced oxides - often nanosized with magnetic properties [313]–[315]. We also explored the coating of such nanoparticles with Silica layer, as an attempt to increase redox inertness of the nanoparticles to prevent them from competing with the electrode as electron acceptors.

3.2. Materials and methods

3.2.1. Bacterial strain and media preparation

Initial colonies of bacteria were grown by streaking frozen (-80^{o}C) stock on LB agar plates using an inoculation loop. *S. oneidensis* plates were kept in a 30^{o}C incubator for 24-48 hours, sealed with parafilm and stored in a fridge. Overnight cultures were prepared through single colony inoculation from the plate into 10 mL of LB media, grown at 30^{o}C for 12-16 hours. *E. coli* DH5*α* plates and overnight cultures were prepared in the same manner but were incubated at 37^{o}C.

LB plates were prepared by autoclaving 37 g of LB agar pellets in 1 L of deionised water (dH_2O). LB liquid media was used to grow overnight cultures of bacteria, prepared by autoclaving 20 g of LB pellets in 1 L of water. Glucose agar plates were used for anaerobic growth experiments – these were made by autoclaving 11.28 g of M9 minimal salts in 475 mL of dH_2O, and 12 g of 1.2% Agar Technical (Agar No. 3) in a separate 475 mL of dH_2O. After combining the mixtures, 10 mL of amino acids, minerals and vitamins were filtered in, plus 20 mL of 1 M glucose media. A 20 mM glucose media was prepared by autoclaving

5.64 g of M9 in 475 mL water, then filtering in 5 mL each of amino acids, vitamins and minerals, and 10 mL of 1 M glucose stock. The 1M stock was made by dissolving 36 g of D(+) glucose in 200 mL dH_2O.

3.2.2. Single strain growth experiment

A growth experiment was performed to determine the individual growth rates of *S. oneidensis* and *E. coli* DH5*α* in various media: LB, glucose, lactate, acetate and formate. This demonstrated the effect of different carbon sources on bacterial reproduction and used to determine the suitability of the bacteria and substrates in the MFC reactors.

1.5 µL of overnight cultures of each bacteria were transferred into 150µL of select media inside a 96-well plate. The OD_{600} of each well was monitored every 10 minutes over a 48-hour period using plate reader (Tecan Spark®). The experiment was performed at 30^{o}C and 37^{o}C to represent optimum grow temperature for *S. oneindensis* and *E. coli* respectively. Each system was done in quadruplicate.

3.2.3. Anaerobic growth

The metabolic interaction between *S. oneidensis* MR-1 and *E. coli* DH5*α* was tested anaerobically using glucose as the sole carbon source and fumarate as the electron acceptor. The OD_{600} and colony growth after series dilution were measured for each of the following samples:

1. 10 µL *S. oneidensis* + 8 mL of 20 mM glucose media + 2 mL of 1 M fumarate stock
2. 10 µL *S. oneidensis* + 1 µL *E. coli* + 8 mL M9 media + 2 mL of 1 M fumarate stock
3. 1 µL *E. coli* + 8 mL of 20 mM glucose media + 2 mL of 1 M fumarate stock
4. 10 µL *S. oneidensis* + 1 µL *E. coli* + 8 mL of 20 mM glucose media + 2 mL of 1 M fumarate stock

Samples 1 (*MR1_Glu_Fum*) and 2 (*MR1_E.coli_Fum*) were used as negative controls, whereas sample 3 (*E.coli_Glu_Fum*) was positive control. Sample 4 was the target system (*MR1_E.coli_Glu_Fum*). Each bacteria was taken from their overnight cultures. The 1:10 ratio between *E. coli* and *S. oneindensis* was selected to balance the much faster growth rate of *E. coli* compared to its counterpart. Each mixture was purged with N_2 for 20 minutes prior to incubation at 30^{o}C for 24 hours. After incubation, 3 mL of each sample was extracted – 1 mL was transferred to a cuvette for its OD_{600} measurement; A further 0.5 mL was transferred to an Eppendorf tube to be used for series dilution. The remaining volume was used for metabolite analysis using HPLC (acid column Hi Plex – H; Agilent. Eluent: 0.005 M H_2SO_4, flow rate of 0.6 mL/min, UV 210 nm detection at 55^{o}C).

The OD measurements were used to determine the number of series dilutions necessary for each sample. LB and glucose agars were used as plating medium. While both strains can grow in LB, only E. *coli* is able to grow in glucose. Hence, the difference of colonies numbers between the two plates would yield the number of *S. oneindensis* colonies.

It is important to note that high growth of *S. oneidensis* cells was unwanted, as this would have interfered with the efficiency of the MNP coating. The initial culture *S. oneidensis* cells would have been coated with sufficient MNPs to achieve a high efficiency. However, each daughter cell would only have a coating of half the amount of MNPs as on its parent cell. After a few rounds of replication, this would have led to an extremely low amount of coating on each cell, negating the magnetic properties. Hence for this project, a low *S. oneidensis* growth result was desired.

3.2.4. Iron-oxide magnetic nanoparticles (MNP) synthesis

3.2.4.1. Bioproduction of MNP via iron reduction

One of the key attributes of MR-1 is its ability to reduce metals, including iron. Under anaerobic condition, MR-1 was able to reduce Iron (III) into Iron (II) which would then mix to form nano-sized magnetite [316]. The bioproduction of iron oxide nanoparticles were conducted with Iron(III)-NTA as the complex ligand with lactate as the electron source. Two target systems *Target* and *Target_2* were set up – each contains 20 mM of lactate and 20 mM of Iron NTA in a 10 mL anaerobic tube, with initial OD_{600} of bacterial cell of 0.5 and 1.0 respectively. Several controls, *C1 – C5* were also experimented to further understand the effect of each key component in the system. The list of systems and controls with their description is given in Table 3.1.

Table 3.1: Description of the two targets and 5 negative controls of the iron reduction experiment with *Shewanella oneidensis* MR-1

System	Description	Comment
Target	MR-1 (OD 0.5) + 20 mM Iron (III) NTA + 20 mM Lactate + N2	
Target_2	MR-1 (OD 1.0) + 20 mM Iron (III) NTA + 20 mM Lactate + N2	Cell 2x
C1	20 mM Iron (III) NTA + 20 mM Lactate + N2 purge	No cell
C2	MR-1 (OD 0.5) + 20 mM Iron (III) NTA + 20 mM Lactate	Aerobic
C3	MR-1 (OD 0.5) + 20 mM Iron (III) NTA + N2 purge	No lactate
C4	MR-1 (OD 0.5) + 20 mM Lactate + N2 purge	No iron
C5	MR-1 (OD 0.5) + buffer solution + N2 purge	No both

Overnight cultures of MR-1 were mixed with appropriate volume of lactate and Iron-NTA, previously sterilized through 0.2 um-pore filter. Rubber stopper was placed to seal the tubes, then purged with N_2 for 20 min to remove oxygen. The tubes were incubated at 30^{o}C, 200 rpm for 12 hours. The MNP-coated cells were collected with strong magnet and washed with

PBS prior to plated on LB agar for cell counting to confirm the cell viability post-coating. The supernatant, along with all the controls were also plate-counted to compare the results. SEM images (Zeiss Merlin, FEG – SEM) were also taken to confirm the presence of iron particles on the cells wall.

3.2.4.2. Chemical synthesis

2 mL of 1 M $FeCl_3$ solution (in 2 M HCl) was mixed with 0.5 mL of 2 M $FeCl_2$ solution (in 2 M HCl). 25 mL of 1 M NH_4OH solution was added dropwise while stirring inside a sonication bath. After stirring for 30 minutes, the nanoparticles were separated from the supernatant with a permanent magnet and washed multiple times until the pH was near neutral. 10 mL of washed MNPs was added into 100 mL of PAH solution (10 mg/mL) and the mixture was sonicated for 15 minutes to coat the MNPs with the polymer. These MNPs were centrifuged at 10,000 g for 15 minutes at 20^oC, the supernatant removed and the solids redispersed. This was repeated three times to remove all excess polymer coating before testing was perfomed. Poly(allylamine hydrochloride, MW ~17,500), or PAH, were used as stabilizing polymer while maintaining their intrinsic chemical properties. PAH was selected as it was positively charged and hence was attracted to the negatively charged Fe_3O_4 nanoparticle core, providing good binding.

The synthesis of silica-coated iron oxide nanoparticles (ION-SIO2-PAH) was based on past literatures [317], [318] with slight modifications. The previously synthesised Fe_3O_4 nanoparticles (100 mg) were suspended in a mixture of anhydrous ethanol (80 mL) and deionized water (20 mL) and sonicated in a water bath for 5 min. Subsequently, 0.10 mL of TEOS was added under N_2 and vigorous stirring and the dispersion was left under stirring at room temperature. After 10 min, 1.0 mL of NaOH solution (2 M) was added in 0.1 mL portions over a period of 2 h and the mixture was stirred for an additional 6 h at room

temperature. Finally obtained Fe_3O_4 @SiO_2 NPs were separated by an external magnet, washed several times with deionized water and then absolute ethanol until the supernatant was clear and stored in ethanol until required. For polymer coating, the Fe_3O_4 @SiO_2 NPs were dispersed in freshly prepared 5% (v/v) solution of poly(allylamine hydrochloride) (PAH, MW~17,500, Sigma Aldrich) and 1 mM acetic acid (99.7%, Sigma Aldrich) and stirred for 60 min. After reaction, amine modified nanoparticles were separated by centrifugation (4500 rpm, 10 min), washed 5–6 times with acetone and water (1:1). The nanoparticles were then redispersed in water.

In addition to our self-made iron-oxide magnetic nanoparticles, amine functionalized MNPs (diameter 30 nm) were purchased from Sigma Aldrich (item no. 747327) to be used as a comparison. These were biocompatible, efficient, and stable in MFCs, though not very cost-effective.

3.2.5. MNP biocompatibility and coating efficiency

Biocompatibility tests were used to provide a measure of MNP toxicity, i.e., how effective the MNPs were at coating *S. oneidensis* cells without killing them. The efficiency of the MNPs at coating the cells was also calculated. Overnight cultures of *S. oneidensis* were washed in the centrifuge, at a speed of 4000 rpm for 6 minutes and at a temperature of 23^{o}C. The supernatant was discarded after each wash and the cells resuspended in 10 mL of sterile dH_2O in each tube. Upon washing, suspended cells were mixed with different volume of MNPs to gather multiple data points as comparison. The mixture was placed in the 30^{o}C shaking incubator for 20 minutes to ensure the cells were coated. Once removed from the incubator, each tube was positioned next a permanent magnet for 30 minutes to isolate the MNP-functionalized cells. The supernatant was pipetted into a separate tube and the MNP coated cells resuspended in sterile dH_2O. Series dilution for both the resuspended cells and

supernatant was performed for plate counting. These were plated on LB agar and incubated at 30°C for 24 hours. Both cultures were also measured for their OD_{600}. Biocompatibility and efficiency were calculated following Equation 3.1 and 3.2.

$$\%Biocompatibility = \frac{\#\ living\ coated\ cells}{\#\ living\ coated\ cells + \#\ dead\ coated\ cells} \quad \text{Eq. 3.1}$$

$$\%Coating\ efficiency = \frac{\#\ coated\ cells}{\#\ original\ cells\ culture} \quad \text{Eq. 3.2}$$

Biocompatibility was measured as the ratio of living coated cells to total number of coated cells, including the dead ones. The number of living coated cells were obtained from CFU calculation, whereas the total number of coated cells were calculated using the OD_{600} to cell number conversion, corrected by the MNP-only baseline. Coating efficiency was calculated in a similar manner following Equation 3.2. Ideally, a good MNP should have both high biocompatibility and coating efficiency.

3.2.6. Total carbohydrate assay

Total carbohydrate assay was conducted following protocol in literature [319]. Anthron solution was prepared fresh prior to experiment by weighting 0.5 g of anthron and dissolved in 10 mL of absolute ethanol. The solution was then added into 250 mL of 75% H_2SO_4 solution and stirred until fully mixed. 0.5 mL of samples were placed into COD tube, added with 1 mL of 75% H_2SO_4 solution, then capped and vortexed to briefly mix. Then, 2 mL of anthron solution was added into the mixture and re-mixed through vortexing. All mixing was done on ice water. The mixture was put in reflux at 100°C for 15 minutes. After heating, samples were let to cool down to room temperature, then read for its absorbance at 578 nm using light spectrometer. The OD_{578} reading was measured against blank solution as baseline and referenced to standard curves previously constructed with known glucose concentration.

3.2.7. Reactor assembly and setup

Double-compartment MFC reactors with a working volume of 50 mL was used to investigate current production. The selection of smaller reactor size was driven by the fact that larger reactors tend to introduce larger resistance hence losses, which might diminish any positive effects MNPs would have in the MFC system. Using a smaller reactor mitigates these losses by reducing the physical distance between electrodes, allowing for more efficient transfer of protons. The smaller size also reduces the complexity of the reactors, which results in lower resistance. The anode consisted of 1.5 x 1.5 cm^2 carbon cloth (H23, 95 g/m^2, Quintech) – for magnetic anodes, neodymium magnet of diameter 10 mm x 2 mm thickness was used and sandwiched between two layers of carbon cloth. The cathode was carbon cloth with a Pt catalyst (1 mg/cm^2, PtC 60%, 1.5 x 1.5 cm^2; FuelCellStore). Titanium wire was used to connect the electrodes to the outside of the reactors. Nafion© 117 was used as the exchange membrane to separate the two compartments. Reactors were assembled and initially filled with deionised water, then autoclaved to achieve sterility. The water was then replaced with appropriate media; M9 minimal salt with trace minerals and appropriate carbon source for anodic compartment, and phosphate buffer saline (PBS) for cathodic compartment. Fixed resistors (1 kΩ) were used to complete the circuit. The anodic chamber was continuously purged with nitrogen gas to maintain anaerobic conditions, whereas the cathodic compartment was gassed with air.

3.2.8. MFC measurements

Potential difference across the 1 kΩ resistor was measured every 10 minutes using datalogger. Once the potential difference had plateaued (i.e., after 4-5 days of constant resistance operation), resistance was removed to bring the reactors into open-circuit mode. The open-circuit potential (OCP) was measured using potentiostat until the voltage remained

constant (to 5.d.p) for 5 consecutive readings and used as starting point for linear sweep voltammetry (LSV) (scan rate 0.1 mV/s) to construct polarisation curves.

From polarisation curve, the power was calculated as shown in Equation 3.3:

$$P = IV \qquad \text{Eq. 3.3}$$

The peak power output was then normalised to the anode surface area (Equation 3.4), to allow comparison with power generation of different MFC systems.

$$P_{an} = \frac{P}{A_{an}} \qquad \text{Eq. 3.4}$$

2 mL of anodic media were sampled regularly – 1 mL was taken from each chamber and filtered into an LC vial for metabolite analysis, whereas another 1 mL was taken for OD_{600} measurement.

3.2.9. Electrode cell composition quantification

At the end of MFC experiment, the electrode was collected and immersed in 20 mL sterile PBS solution inside 50 mL falcon tube. The tube with its content was vortexed vigorously for 15 min to detach cells from the electrode. 1 mL sample were taken from the solution and series diluted to be plated on both LB and agar plates. 100 µL of aliquot was used for each plate to generate enough colonies (i.e., between 20 – 200) for counting. Each dilution for each system were plated in triplicates. The plates were incubated at 30^{o}C for 24-36 hours and the number of colonies were counted for their CFU measurement. Number of colonies formed on glucose plate would correspond to *E. coli*, whereas the difference between the LB and glucose plates would tell the concentration of MR-1.

3.2.10. MFC Systems

The MFC systems that were experimented in this chapter were given in Table 3.2. Each system was run in triplicates. Overnight cultures of the bacteria were used, and washed 3x with PBS buffer prior to injection to the MFC reactors. Suitable volume was injected to achieve initial OD_{600} of 0.05 for MR-1 and 0.01 for *E. coli*. Equal volume of MNPs (10 mg/mL) was used to either coat MR-1, or as free suspension in the anodic chamber.

Table 3.2: Explanation of the different MFC systems being experimented

System	Comment
Negative controls *NoBac_Glu* *NoBac_For*	Two negative controls: anode chamber containing either only the formate or glucose solution and no bacteria. These controls were intended to prove that electricity generation was due to the electron transfer facilitated by bacteria, rather than the carbon source itself.
Pure cultures *MR-1_For* *E.coli_Glu*	Separate pure culture MFCs of *S. oneidensis* & formate, and *E. coli* DH5α & glucose, were used to corroborate earlier findings from growth experiments and literature. It was expected that *S. oneidensis* could oxidise formate, the metabolic product of *E. coli* in glucose, to generate electricity, while *E. coli* alone could not perform EET.
Co-culture *MR1_E.coli_Glu*	MFCs containing a co-culture were set up to investigate whether this combination of bacteria would yield a more power than either of the pure cultures on their own. It was also used as a control, to compare against the electricity generated when using a co-culture plus MNPs
Co-culture + suspended MNPs *Self_MR1_E.coli_Glu* *Si_MR1_E.coli_Glu* *Sigma_MR1_E.coli_Glu*	The MNPs in this experiment were not used to coat any cells, but were simply suspended in the solution, alongside the cultures. This was done to determine whether the mere presence of MNPs affected the electricity generation, as opposed to the act of coating cells with MNPs. Three different MNPs were experimented: self-made iron oxide nanoparticles with PAH coating (total particle diameter 35 nm), silica-coated ION with 30 nm core, and commercial amine functionalized iron-oxide nanoparticles (core size 30 nm) purchased from Sigma-Aldrich (product code #).
Target *Self_MNP-MR1_E.coli_Glu* *Si_MNP-MR1_E.coli_Glu* *Sigma_MNP-MR1_E.coli_Glu*	MFC containing co-culture of MNP-coated MR-1 and E. coli DH5α to degrade glucose as sole carbon source

3.3. Results and discussion

3.3.1. Growth curve

Shewanella oneidensis MR-1 and *E. coli* DH5*α* were grown in several media (LB, glucose, lactate, acetate, and formate) at two different temperatures: 30ºC and 37ºC. Their OD_{600} for 48-hour period was recorded and shown in Figure 3.1. It can be seen that both strains grew relatively well in LB at both temperatures. Under glucose, only *E. coli* grew whereas MR-1 did not. For lactate utilisation, MR-1 grew better than *E. coli* DH5*α* at 30ºC whereas the opposite was observed at 37ºC. This was expected as both strains grow best at corresponding temperatures. For acetate, both strains grew at 30ºC albeit not significant (Max. OD ~0.4), with *E. coli* DH5*α* grew much better at 37ºC. As expected, neither strain grew in formate at either 30ºC or 37ºC.

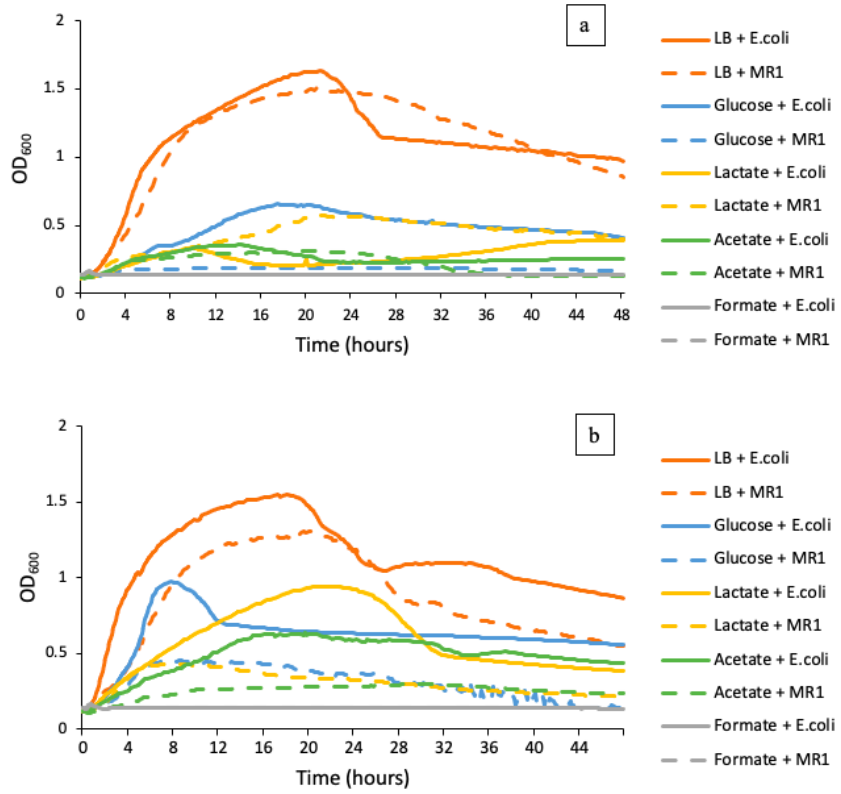

Figure 3.1: Growth curve of *E.coli* and *S.oneidensis* MR-1 in different carbon source (LB, Glucose, Lactate, Acetate and Formate) at a) 30ºC and b) 37ºC. Curves represent the mean value of quadruplicate measurements, error bars not shown for clarity (all standard deviation are within 20% of average)

3.3.2. Anaerobic growth

Both single and co-culture of MR-1 and *E. coli* DH5*α* were cultured in glucose under oxygen-free condition. This was to simulate similar condition in MFC setup when using glucose as sole carbon source, although in this 'tube' experiment, fumarate (instead of an electrode) was used as electron acceptor. The compiled results were given in Table 3.3. As expected, *MR-1_Glu_Fum* did not generate any optical density as the bacteria was unable to degrade glucose. Negative control *MR1_EColi_Fum* also did not show any significant growth as there was no carbon source present. The small OD_{600} of 0.005 ± 0.002 generated from this system was expected to rise from consumption of amino acid present in the media – as supported by previous study [320]. *EColi_Glu_Fum* generated OD_{600} of 0.303 ± 0.060 indicating growth, whereas *MR-1_EColi_Glu_Fum* generated highest OD_{600} of 0.570 ± 0.108. Plate count experiment on LB and glucose plates indicated *E. coli* CFU to be 2.33 ± 0.22 x 10^8/mL, and MR-1 was ~2.80 x 10^7/mL (~12% of total cell numbers). This was somewhat as expected as the anaerobic metabolic product of glucose by *E. coli* DH5*α* mainly consist of formate as confirmed by HPLC result (data not shown), which cannot be utilised by MR-1 for growth hence the dominance of *E. coli* in the culture.

Table 3.3: Anaerobic growth result of single strain and co-culture of *E. coli* and *S. oneidensis* MR-1, with glucose and fumarate as carbon source and electron acceptor, respectively. Cultures were incubated at 30°C for 24 hr prior to OD measurement. Numbers in bracket represent standard deviation from triplicate measurement

Sample	**OD_{600}**	**CFU on agar plate**	**CFU on glucose plate**
MR1_Glu_Fum	0.000	$5.10x10^4$ (0.20)	N/A
MR1_Ecoli_Fum	0.005 (0.002)	~$8x10^5$	~$8x10^5$
Ecoli_Glu_Fum	0.303 (0.060)	$1.38x10^8$ (0.16)	N/A
MR1_Ecoli_Glu_Fum	0.570 (0.108)	$2.33x10^8$ (0.22)	$2.05x10^8$ (0.27)

It was also interesting to see that upon inclusion of MR-1, the growth of *E. coli* DH5*α* has somehow boosted by almost 50%. Further experiment with dead MR-1 cells also showed an increase in *E. coli* growth (data not shown). This has shown the presence of MR-1 and its biological matter was able to increase *E. coli* metabolism, although by the time of this writing, its explanation remains unknown.

3.3.3. Biosynthesis of Iron MNP via iron reduction

Upon incubation at 200 rpm, 30ºC for 12 hours, the two target systems *Target* and *Target_2* indicated successful reduction of iron to form black nanoparticles on the cells surface, as can be seen in Figure 3.2.

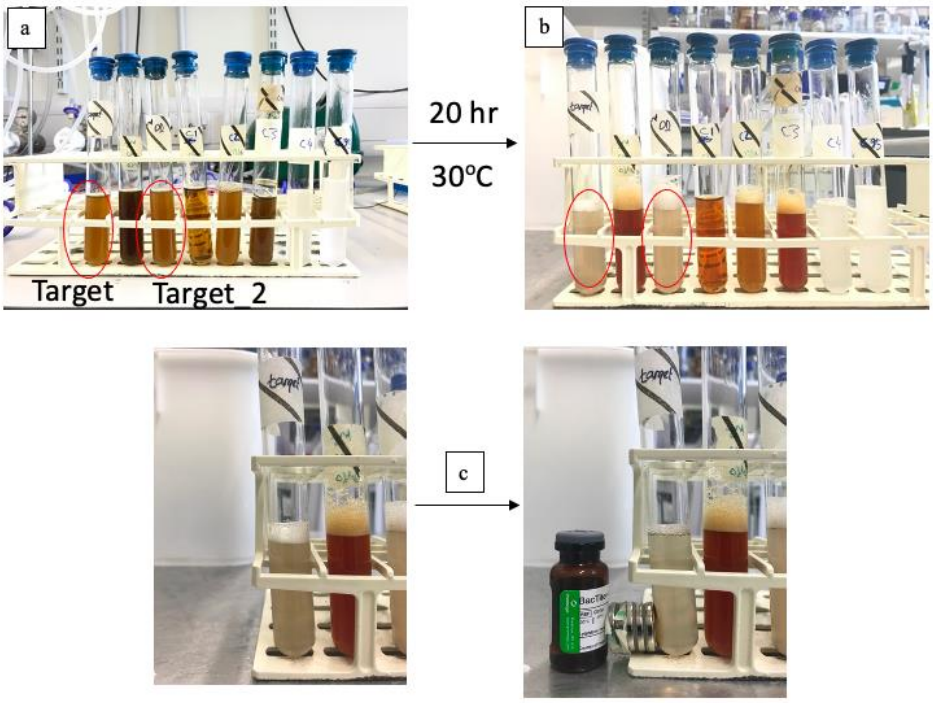

Figure 3.2: Bioproduction of iron-oxide magnetic nanoparticles via iron reduction with *S. oneidensis* MR-1; a) two target systems and 5 negative controls in anaerobic tube, incubated for 20 hour at 30ºC; b) after incubation, the Target systems (in red circles) have turned colour and produced black particles; c) collection of the MNP-coated cells using permanent magnet

The controls C1-C5 did not produce any nanoparticles as expected. Plate count analysis showed that ~15% of *Target's* cells were coated by the produced nanoparticles while

maintaining viability. Furthermore, it was observed that the *Target* system has produced ~10X more cells than in any of the controls (C1 – C5; Figure 3.3), confirming that bacterial metabolism was only possible when both electron donors and electron acceptors were present.

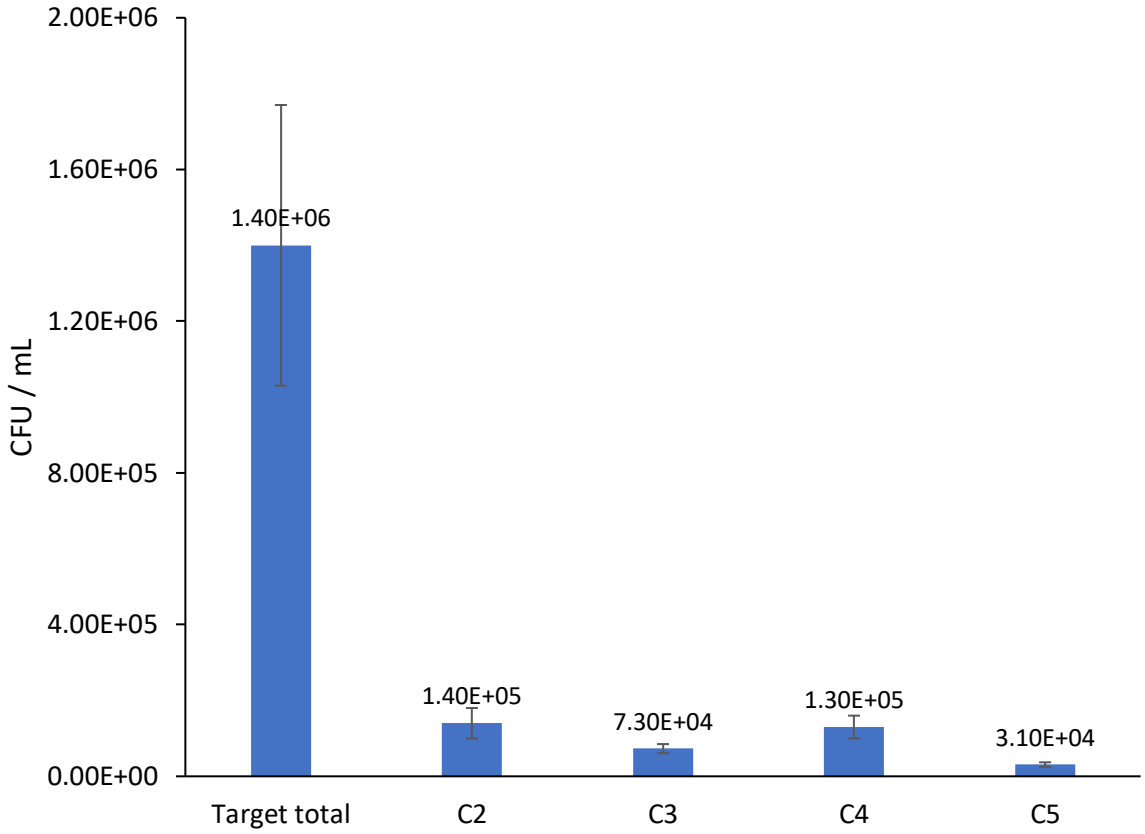

Figure 3.3: Colony forming unit (CFU) of the target system and negative controls of the iron reduction experiment; target system produced ~10x more CFU than any of the controls, showing the significance of both electron donor (lactate) and acceptors (Iron (III) NTA) for growth; error bars represent standard deviation of triplicate measurement

SEM imaging confirmed the present of the iron particles (Figure 3.4).

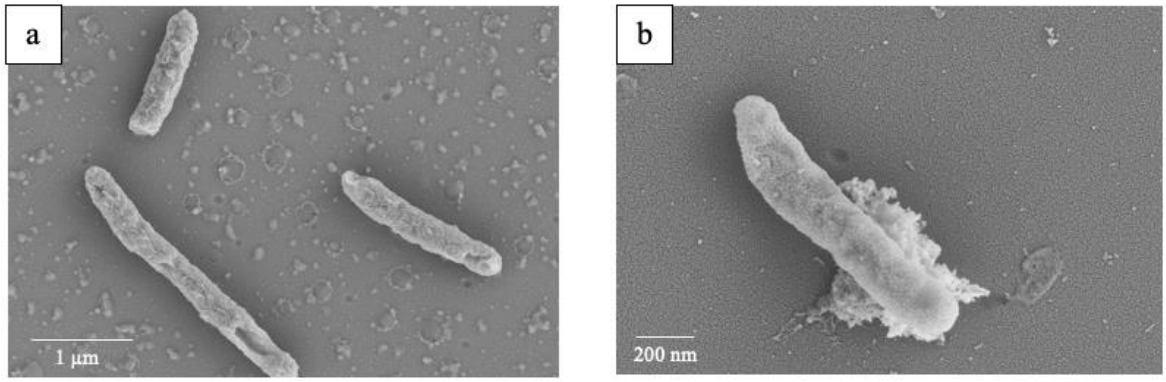

Figure 3.4: SEM images of MR-1; a) MR-1 in free suspensions; b) MR-1 with self-produced iron-oxide nanoparticles clumped on its cell wall.

Further experiment was done with different Iron concentrations (20, 25, 30, 35, 40 and 100 mM). Cell density of 0.8 was selected for MR-1 cells with lactate concentration of 20 mM. Upon incubation, visual observation (Figure 3.5) indicated production of MNP for iron concentration of 20, 25 and 30 mM. From 35 mM onwards, no iron MNP particles were observed in the anaerobic tube.

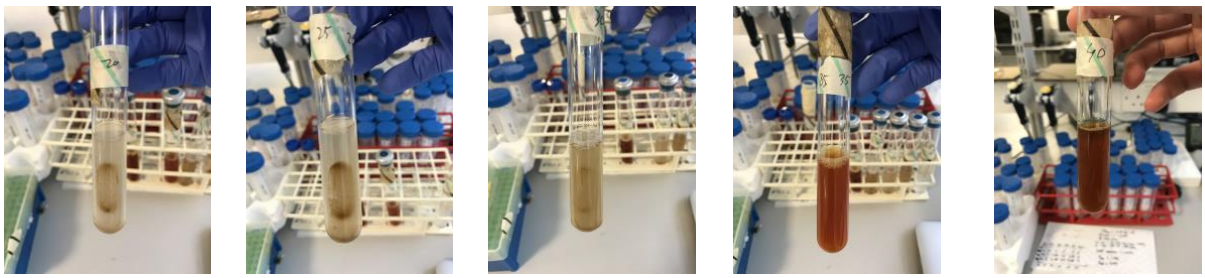

Figure 3.5: Iron reduction experiment with iron (III) concentration of 20, 25, 30, 35 and 40 mM (from left to right). Nanoparticles were shown to form at concentration 20, 25 and 30, whereas 35 and 40 mM did not produce nanoparticles.

Plate counting indicated linear increase of CFU from 20 mM up to 35 mM (Figure 3.6), indicating that iron was the limiting factor for growth when its concentration was below 40 mM. This finding was interesting as this indicated a 1:2 stoichiometric ratio between lactate and iron (for every lactate molecule that was oxidised, two iron irons were reduced). No cells were able to survive when concentration reached 100 mM. Combined with visual

observation, these results showed that although cell was able to survive in relatively large range of iron concentration, the production of iron MNP happened at a narrower range. 25 mM of iron seemed to be the optimum concentration for iron reduction, as can be seen from the thicker 'black' nanoparticles formed on the side of the anaerobic tube.

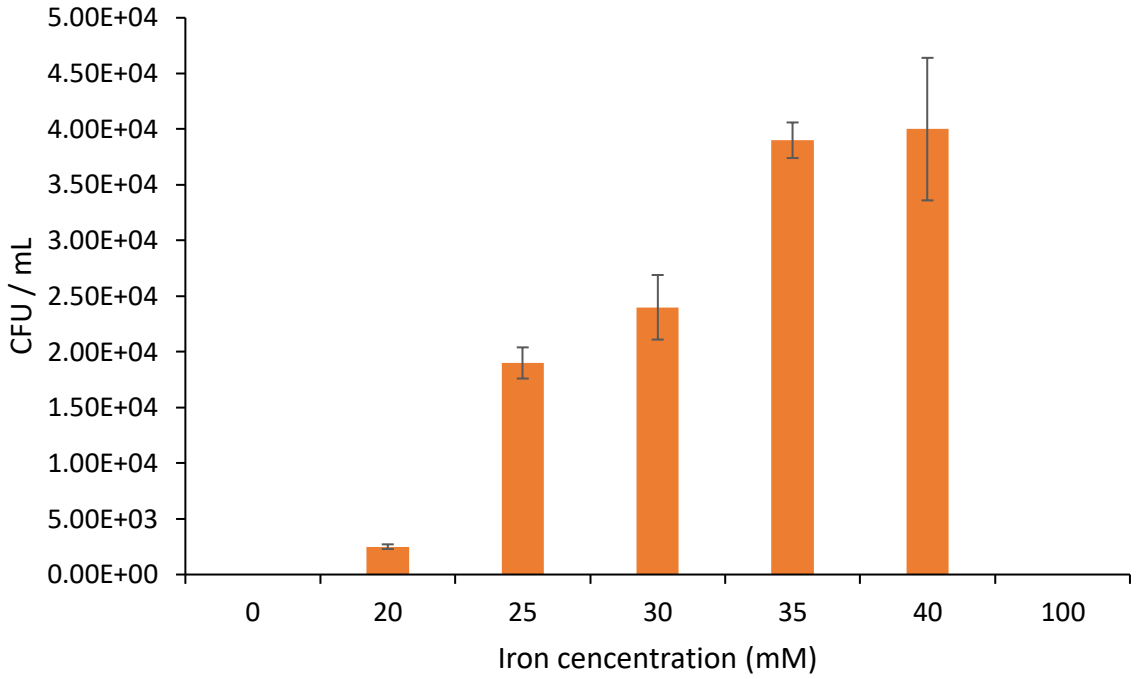

Figure 3.6: CFU of bacterial cells at varying concentration of Iron (III) NTA for iron reduction experiment. Increasing CFU between 20 – 35 mM indicated iron being the limiting factor in cell growth; 1:2 stoichiometric ratio was achieved when iron concentration was 40 mM. No cells survived at iron concentration of 100 mM. Error bars represent standard deviation of triplicate measurements

3.3.4. MNP chemical synthesis

3.3.4.1. PAH-coated Iron Oxide Nanoparticles (ION)

The average size of the PAH-coated ION was analysed via Zetasizer and found to be 35 nm with zeta potential of 56.8 mV (Figure 3.7a). Poly(allylamine hydrochloride, MW ~17,500), or PAH, were used as stabilizing polymer while maintaining their intrinsic chemical properties. Coating efficiency was found to be 99.71% through plate counting (Table 3.4). When compared to uncoated bacteria as control, the MNP was confirmed to be fully biocompatible as there is no significant difference between the coated and uncoated cell

population. Cell functionality was also tested overtime using ATP-based assay and showed that cells remained equally active even after 5 days post-coating (Figure 3.7b).

Table 3.4: Plate count result of *S. oneindensis* coated with PAH-coated ION; CFU of MNP-MR1 was almost identical to those of the control, indicating full biocompatibility. Coating efficiency of 99.71% was achieved when comparing MNP-MR1 CFU with its supernatant. Numbers in bracket represent standard deviation from triplicate measurement

	MR1 – control (10^{-6} dilution)	**MNP-MR1 (10^{-6} dilution)**	**Supernatant (10^{-3} dilution)**
Plate 1	34	46	120
Plate 2	46	30	71
Plate 3	37	38	118
CFU/ml	3.9×10^8 (0.6)	3.8×10^8 (0.8)	1.0×10^6 (0.3)

The coating efficiency was also tested for low bacterial cell concentration. Cell culture containing 100 cells/ml and 10 cells/ml were coated with MNP for different time-period (15 min, 60 min and 24 hrs). It was found that with coating time of 15 min, MNP was able to recover 4.2 ± 1.1% of cells in 100 cells/ml culture and 3.4 ± 1.8% of 10 cells/ml culture (Figure 3.7c). At 60 min, the coating efficiency rather stayed the same, and if left for 24 hrs, 17.8 ± 4.4% cells were able to be functionalised for 100 cells/ml and 9.1 ± 3.2% for 10 cells/ml. This finding could be of significant as other applications of MNP include biosensor and bioremediation. Being able to coat cells where there are not many presents, bring huge opportunity for MNP to be used in bio-sensory system.

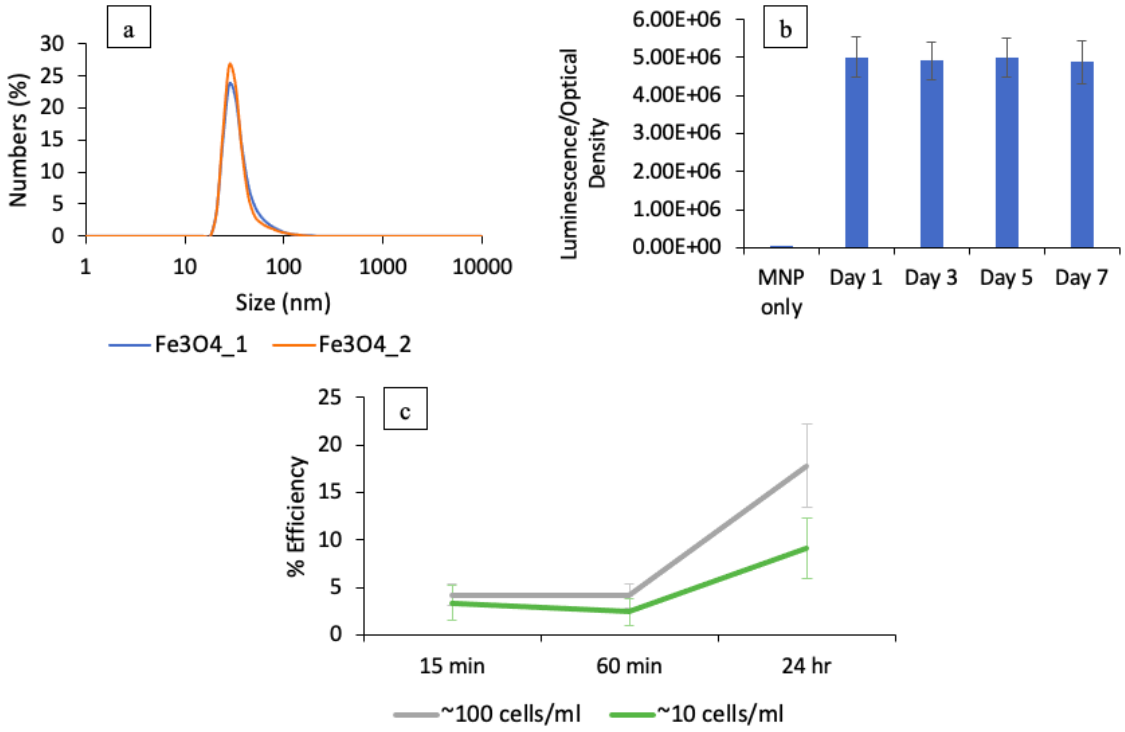

Figure 3.7: a) Size distribution of PAH-coated ION; Measured in duplicates (blue and red) through zetasizer. Average size **34.6 ± 14.6 nm** (zeta potential 56.8 ± 4.4 mV); b) Luminescence per OD via bacterial ATP assay; three negative controls (water, minimal media (MM) and MNPs used as baseline. Luminesce of MNP-MR1 samples was measured for 7 days with no noticeable change in activity, indicating longevity in viability post MNP-coating; c) Coating efficiency of PAH-coated ION for low cell concentration of 100 cells/mL (blue) and 10 cells/mL (orange) at time of 15 min, 60 min and 24 hr. Error bars represent standard deviation of triplicate measurements

3.3.4.2. PAH-SiO_2-ION

Another different type of Iron MNP was synthesized, this time with silica coating sandwiched between the iron core and the PAH shell. A core size of 30 nm was synthesized with TEM images given in Figure 3.8a. Coating efficiency and biocompatibility of the particles were found to be ~74% and ~92% respectively, showing good indicator for its usage in MFC setup. FTIR analysis confirmed N-H bond (Figure 3.8b), which in turn confirmed the presence of PAH coating.

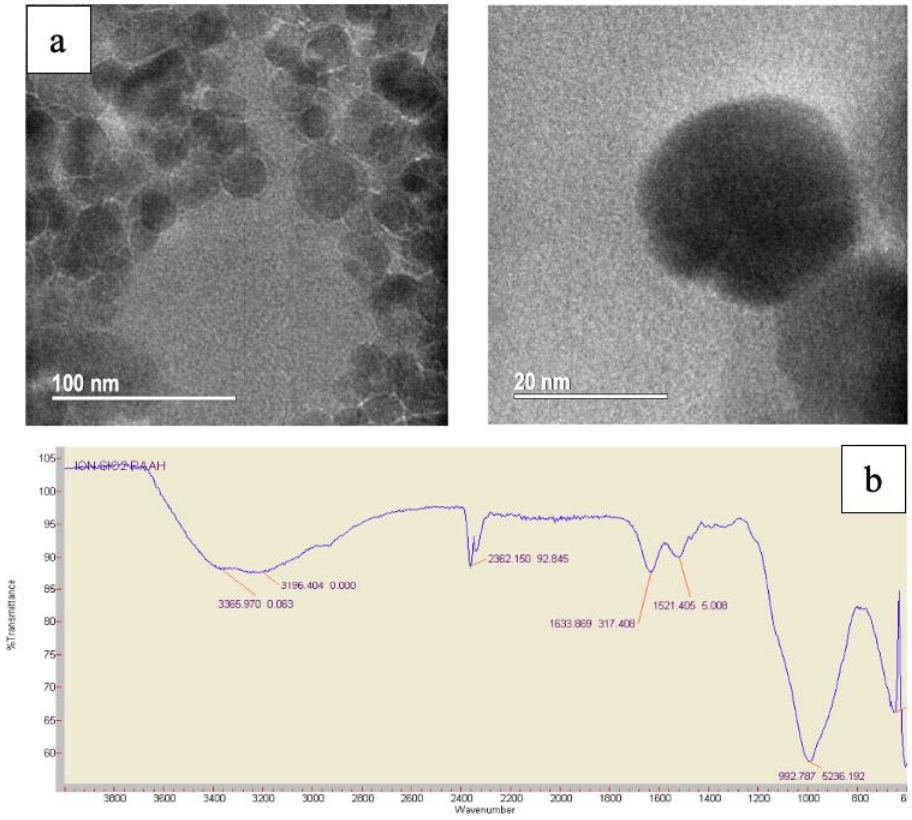

Figure 3.8: a) TEM images of PAH-SiO2-ION; images were taken using JOEL TEM 2100, with 200 kV beam; b) FT-IR spectrum of PAH-SIO2-ION; bands indicate the presence of N-H bonds of PAH polymers; Frontier FT-IR bench top spectrometer, scan range of 600 – 4000 cm^{-1}

3.3.5. Microbial fuel cells

All microbial fuel cell reactors were conducted in triplicate. Of all MFC systems that were experimented, negative controls *NoBac_Glu* and *NoBac_For* did not generate any electricity as expected (data not shown). Furthermore, single culture *E.coli_Glu* also did not generate any meaningful voltage, confirming its inability to undergo extracellular electron transfer (EET) to produce electrical current in MFC systems. The voltage of the other systems for a 5-day period was given in Figure 3.9a. As can be seen, the positive controls *MR1_E.coli_Glu* and *MR1_For* stabilised at ~40 mV, which was contributed by the bio-oxidation of formate by MR-1 in the culture. MFC with PAH-SiO_2-ION, both when used as cell coating (*Si_MNP-MR1_E.coli_Glu*) and free suspension (*Si_MR1_E.coli_Glu*), reached the same voltage level although the former took longer to reach steady-state. The initial peak of *MR1_E.coli_Glu*

(72.5 ± 8.8 mV) could be attributed to intermediate production of longer chain organic acids (i.e. lactate), that would generate higher voltage when utilised by MR-1.

On the other hand, MFC that were equipped with self-synthesized ION and amine-functionalized ION from Sigma failed to reach the same voltage level. *Sigma_MNP-MR1_E.coli_Glu* was able to reach a peak votage of 47.3 ± 6.9 mV, before dropping down to nearly zero. It seems that the presence of ION in these systems actually compete with the electrode as electron acceptors, hence reducing the electrical current being generated. This was supported by positive redox potential of such reaction as given in Equation 3.5, with such effect could potentially be more severe in our system with relatively high internal resistance caused by the simplified reactor setup. This result has shown that the presence of silica-coating on the ION core was essential to preserve its redox inertness, so it would not interfere with the electron transfers from the bacteria to the electrode.

$$Fe^{3+} + e^{-} \rightarrow Fe^{2+} \quad E^{0} = +0.77\,V \qquad \text{Eq. 3.5}$$

Polarization curve construction of the MFC provided more insights into their performance. The polarisation and power curve of *Si_MNP-MR1_E.coli_Glu* and *Self_MNP-MR1_E.coli_Glu* were compared in Figure 3.9b and c. The maximum attainable power of *Si_MNP-MR1_E.coli_Glu* reached 39.8 ± 2.4 mW/m^2, whereas the *Self_MNP-MR1_E.coli_Glu* was only able to reach 7.4 ± 1.1 mW/m^2.

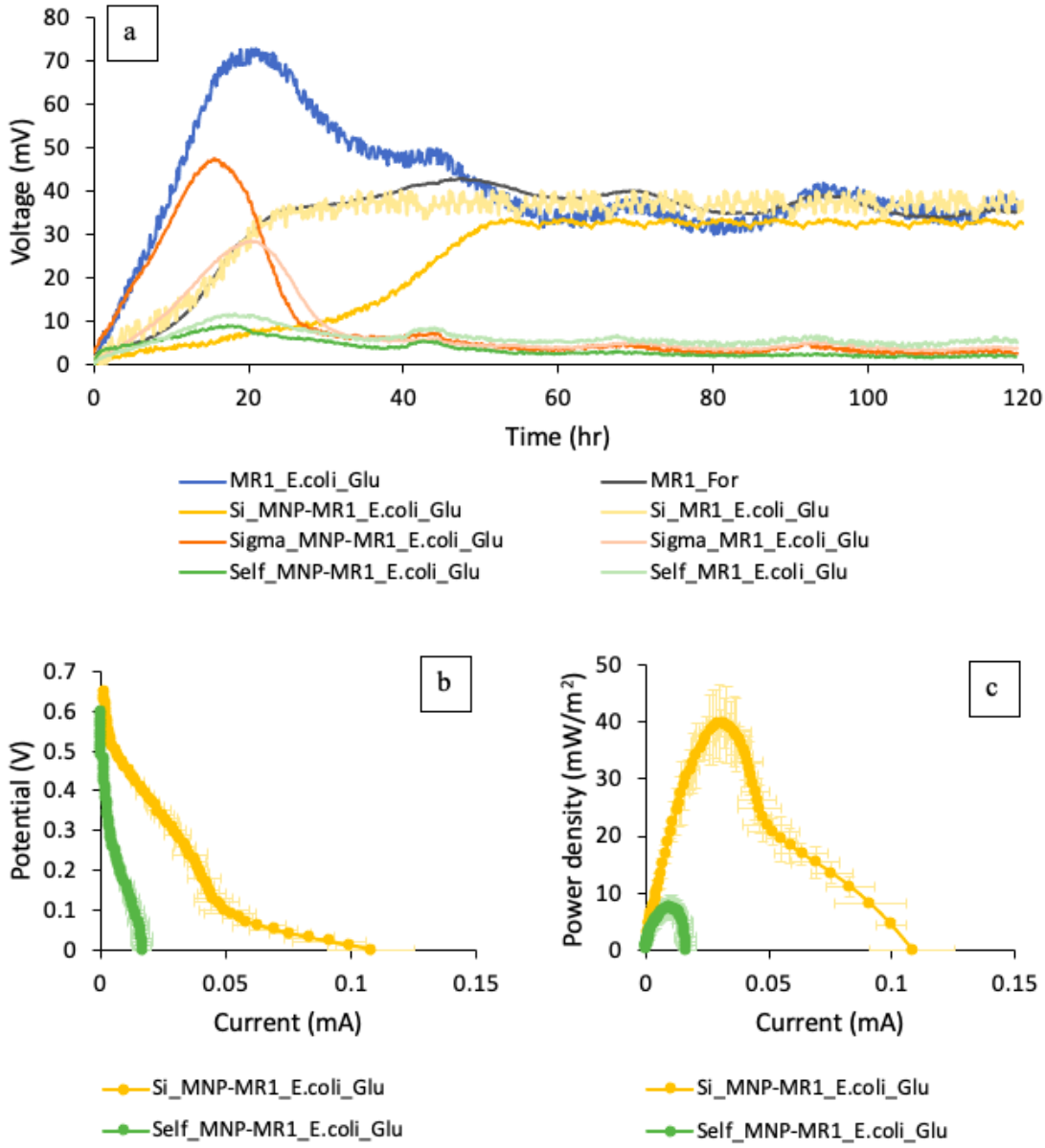

Figure 3.9: a) Voltage of MFC systems across 1 kΩ resistor for 5 days; Positive controls *MR1_E.coli_Glu* (blue) and *MR1_For* (grey), and both MFC with PAH-SIO2-ION (yellow and light yellow) all reach steady state voltage of ~40 mV. Other MFCs dropped to ~5 mV. Data shown were the mean value of triplicate measurements; Negative controls and error bars were not shown for simplicity; b) Polarisation curve and c) power curve of *Si_MNP-MR1_E.coli_Glu* (yellow, P_{max} = 39.8 ± 2.4 mW/m^2) and *Self_MNP-MR1_E.coli_Glu* (green; P_{max} = 7.4 ± 1.1 mW/m^2); error bars represent standard deviation from triplicate measurements

The glucose consumption and cell growth inside the reactors were also compared between the positive control *MR1_E.coli_Glu* and the two MFC working with silica-coated ION (Figure 3.10a). Among the three systems, the positive control actually utilised the least amount of

glucose (16.6 ± 0.7 mM), despite generating highest cell density (~OD_{600} 0.625). This indicated higher efficiency of glucose assimilation for cell growth, deprioritizing its usage for electricity generation.

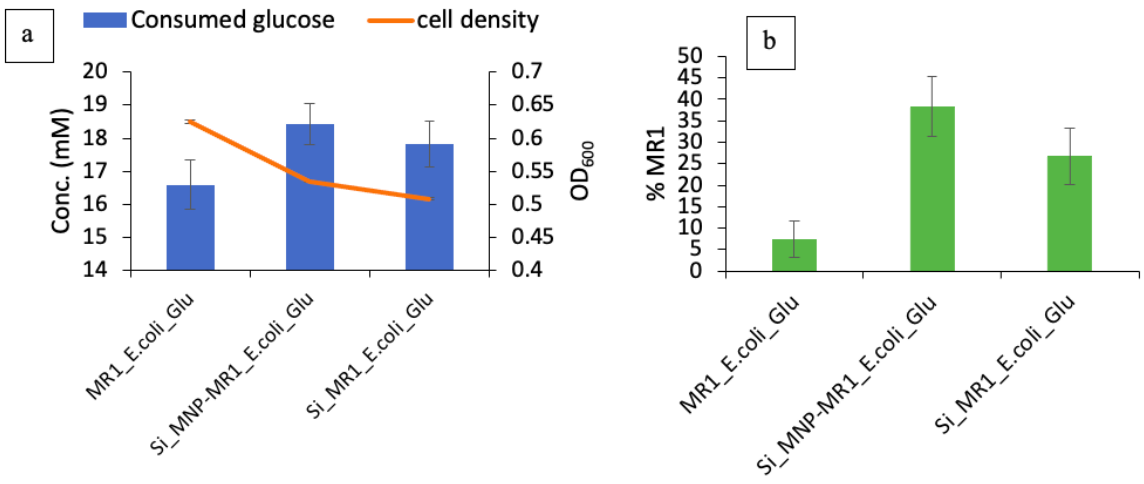

Figure 3.10: a) Concentration of glucose consumed (blue bar) and cell density of anodic culture (orange line) of different MFC systems; error bars represent standard deviation of triplicate measurements; b) %occupancy of MR1 cells on electrode surface of MFC anodes; measurement was taken at the end of MFC experiment (day 5); error bars represent standard deviation of triplicate measurements

Plate count of the bacterial community on the electrode surface post-MFC measurement revealed that only 7.4 ± 4.2% of surface was covered by MR-1 in the conventional *MR1_E.coli_Glu* MFC (Figure 3.10b). In system where silica-coated ION was added in suspension (*Si_MR1-E.coli_Glu*), this proportion was increased to 26.7 ± 6.6%, and further up to 38.3 ± 7.0% for *Si_MNP-MR1_E.coli_Glu*. This result was consistent with our hypothesis that by coating MR-1 with biocompatible ION, we were able to engineer community distribution on the electrode to favour the electrigens to increase electrode usage efficiency.

3.4. Conclusion

The intention of this work was to test the ability of nanoparticles to isolate electrogenic bacteria from wastewater consortium for higher efficiency of electrode usage. A mixture of *S. oneidensis* MR-1 and *E. coli* DH5*α* was used to degrade glucose to represent the organic matter present in typical wastewater. The selection of nanoparticles played crucial role in the final MFC output – misselecting the MNP type could result in lower electricity generation, due to its competing nature with electrode as electron acceptors.

Of all MNPs that were trialled in this work, only PAH-SiO_2-ION generated comparable electrical current (~40 mV across 1 kΩ) when compared to positive control, while the other MNPs affected electricity generation negatively. Although initially unexpected, this might have been caused by two reasons – mainly 1) inhibitory effect of nanoparticles on biofilm growth, and/or 2) competing redox effect of Fe^{3+} as electron acceptors. On potential reason no 1) – supporting evidence include a study on mixed consortia of MFC which showed that cell viability was promoted by a small amount of iron sulfide nanoparticles but inhibited by thick nanoparticle "shell" covered on the bacterial cells [281]. Another study was done on *Candida albicans* biofilm –where it was shown that the MNPs had a significant inhibitory effect on biofilm formation, which reduced biofilm formation of up to 88% [321].

For reason no 2) – reactiveness of the iron core (the Fe^{3+} ions to be specific) can be explained by the positive redox potential of its reduction reaction (Equation 3.5). Hence, shielding with Silica layer might introduce physical barrier which reduce the reactiveness of the core – allowing for the electrons to be transferred to the electrode. However, although improving the redox and colloidal stability of iron oxide nanoparticles [317], [322], [323], it is also worth noting that previous studies have suggested that increasing level of Silica may reduce the conductivity and magnetic properties of MNPs [324], [325]. It is also known that biofilms that are too thick (~100-200 um) can suffer from electron and mass-transfer limitation, with

less-dense biofilm suffers the worst from this phenomenon [326]–[328]. Adding additional layers of Silica-coated MNPs on cell surface may just create more spaces between the cells within the biofilm, resulting in less dense biofilm and lower electron and mass transfer. Hence, a thin layer of Silica is preferable to minimize the effect on magnetic and conductivity dilution as well as the additional mass transfer resistances. Unfortunately, optimization of silica layer thickness was not conducted in this project.

Nonetheless, we did observe ~5X occupancy improvement of MR-1 biofilm on the electrode surface, with magnetized system able to produce biofilm with MR-1 occupying 38.3 ± 7.0% electrode area, versus only 7.4 ± 4.2% in WT control. In system where direct electron transfer (DET) plays the major role in electricity generation such as with *Geobacter*, this could bring crucial and significant contribution. However, when this study was conducted – our choice of *Shewanella* as our subject strain was driven by the hypothesis that DET was the most significant mechanism in its electricity generation. However, our subsequent experiment showed that 70% of electricity generated by *Shewanella oneidensis* MR-1 in MFC system was contributed by mediated electron transfer through riboflavin [329]. This would mean that its biofilm attachment enhancement only affected the minority of power generation, which might explain why we did not see significant improvement in electricity production. This could also explain the slower progression of voltage of *Si_MNP-MR1_E.coli_Glu*, as significantly more MR-1 was immediately attached on the electrode, forcing the bacteria to use direct electron transfer mechanism in higher proportion. Nonetheless, this work has shown promising result that the use of ION MNP, shielded with Silica coating was indeed feasible in MFC system to promote biofilm attachment.

Chapter 4: Genetic engineering biofilms *in situ* using ultrasound-mediated DNA delivery

4.1. Introduction

Microbial biofilms are amongst the most widely distributed and successful modes of life on Earth, where they drive vital biogeochemical cycling processes of most elements in water, soil, sediments and subsurface environments [330]. In the right place, biofilms are fantastically useful and have long been exploited in bioengineered applications including the degradation of wastewater and solids applied to the filtration of potable water [331], [332]. Their high cell densities, intrinsic robustness, self-renewal and stable process rates compared to cells in suspension are stimulating growing interest for exploitation in bioreactors and microbial fuel cells (MFC) to achieve biosynthesis of high-value chemicals and biofuels [333], [334]. A key feature of most biofilms is that they are composed of diverse communities that perform functions that are difficult or impossible for individual species to perform on their own [335], [336]. Thus, there is a division of labour, each population undertaking their specialist task with their metabolites acting as substrates for populations further down the metabolic cascade [337].

The effective harnessing of microbial community functionality and robustness over operationally useful timescales remains a key challenge for the deployment of multispecies biofilms in industrial applications [338], [339]. Engineers and biotechnologists are limited in what they can do when systems are performing sub-optimally or moving towards failure. Furthermore, if poor management leads to biofilms becoming detached and dispersed (e.g. by toxic shock from a sudden influx of heavy metals into a municipal water treatment plant), they take a long time to re-establish resulting in significant downtime and economic loss [340]. While biofilm-based technologies, such as microbial fuel cells (MFCs), are promising

and sustainable in the long run, critical bottlenecks inherent to biofilm physiology such as vulnerable to toxic shock, slow adaption to potential changing conditions and slow biofilm growth remain to be addressed before their widespread applications in industrial settings [339], [340].

The introduction of plasmids into bacterial cells holds great promise in terms of modifying the fate and functioning of a biofilm, while addressing many of the bottlenecks associated to biofilms-based technologies. These small DNA molecules are physically separated from the main chromosomal DNA of the cell and can replicate independently, often endowing the cell with self-maintaining genes which enable new functionalities and allow the cell to deal with changing conditions [341]. Bacteria have been engineered via plasmid or other forms of nucleic acids to perform various activities, ranging from treating radioactive waste [342]–[344], generating bioelectricity [164], [167], [182]–[184], removing heavy metals from industrial effluent [345]–[347], and even visualizing the gut microbiome in bees [348]. However, these applications require inoculation of engineered strains into respective environments where many times the engineered strains may be unable to compete with native strains or existing biofilm communities and hence fail to effectively colonise the environment and perform their intended functions [349]. What is required is *in-situ* microbiome engineering methods that enable manipulation of mature established multi-species biofilms in their native context. However, there is no viable method to date that can introduce desired genes into complex and niche biofilm communities (e.g. activated sludge, gut microbiome), which mainly comprises of non-competent and/or nonculturable cells.

To accomplish our goal, more direct and immediate ways of augmenting biofilms central to the functioning of many engineering systems (e.g. bioreactor) has been developed. In previous study done by our research group, we reported on the successful applications of low frequency 40 kHz ultrasound for transferring plasmids into three different bacterial species in

their planktonic states and achieved a high rate ($9.8 \pm 2.3 \times 10^{-6}$ per mg) of gene uptake [350]. This was one of the first literatures that suggested application of low frequency ultrasound to deliver gene into bacteria. In that study, 40 kHz ultrasound bath was used to successfully transfer plasmid pBBR1MCS2 into *Pseudomonas putida* UWC1, *E.coli* DH5α and *Pseudomonas fluorescens* SBW25. The optimum transformation efficiency at that time was ~12^-5 transformants per cell – nevertheless this was already 9X more efficient than conjugation, and 4X more efficient than electroporation [350]. The gene transfer mechanism was primarily driven by cavitational effect, which physically generates reversible porosity in the cell membrane [351], [352]. Fast forward to 2022, ultrasound-induced gene transfer has commonly been experimented for bacteria-based tumor therapy. Recent study demonstrated the ability to engineer an ultrasound-responsive bacterium (URB) which can induce the expression of exogenous genes in an ultrasound-controllable manner [353]. Cytokine interferon-γ (IFN-γ), an important immune regulatory that plays a significant role in tumor immunotherapy, was successfully expressed via brief hyperthermia induced by focused ultrasound – improving anti-tumor efficacy of URB in vitro and in vivo [353]. Our aim for this study is to determine the potential of ultrasound-based DNA delivery (UDD) for biofilms in MFCs, while demonstrating the scalability of this technology.

4.2. Materials and Methods

4.2.1. Bacterial strain, plasmid and media preparation

List of *Shewanella* strains and plasmids used in the experiment, along with their description are given in table 4.1.

Table 4.1: List of strains and plasmid used in this experiment

Strain or Plasmid	Description	Source
Shewanella oneidensis MR-1 wild type (WT)	Wild type strain of MR-1. Not naturally competent.	[354]
MR-1 Δbfe	Δbfe mutant of MR-1. Loss of ability to transport the FAD into the periplasm, reduced extracellular flavins available for electron transfer.	[163]
MR-1/YYDT-C5	*S. oneidensis* MR-1: pYYDT-C5	This study
Plasmids		
pYYDT-C5	Plasmid with entire flavin biosynthesis gene cluster ribADEHC cloned from *Bacillus subtilis*, Kan^R	[164]

4.2.1.1. Strain Construction

pYYDT-C5 plasmid was inserted into *S. oneidensis* by conjugation via pYYDT-C5 – transformed *E.coli* WM3064. WM3064 strain is a Diaminopimelate (DAP) auxotroph as a result of a mutation in *dapA*, and consequently cannot grow in the absence of DAP, which is required for cell wall synthesis and is also an intermediate of lysine biosynthesis. Transformation of WM3064 strain was achieved via electroporation. 200 uL overnight culture of WM3064 cells was inoculated in 50 mL LB + 100 ug/mL DAP in a 250 mL flask until OD_{600} of 0.4 – 0.5 was reached. The flask was transferred immediately to ice and swirl occasionally to facilitate even cooling. The cells were spun down at 5,000 g for 15 min at

4ºC, and resuspended in 25 mL ice-cold 10% v/v glycerol solution. The washing process was repeated twice before reaching a final resuspension in 1 mL. 100 uL aliquots were transferred into ice-cold Eppendorf tubes and stored at -80ºC until needed. 1 uL of pYYDT-C5 plasmid was added to an aliquot of electrocompetent WM3064 cells on ice. The mixture was mixed by gentle flicking and then transferred to an ice-cold 2-mm gap electroporation cuvette. The electroporation was performed at 2.5 kV and the cells were immediately recovered in 1 mL LB with DAP at 37ºC for 1 hour at 200 rpm. The cells were then inoculated on LB+DAP agar plate supplemented with 50 ug/mL kanamycin antibiotics at 37ºC. Colonies of transformed cells appeared after overnight incubation. Conjugation of pYYDT-C5 plasmid from WM3064 to *S. oneidensis* was achieved by mixing 250 uL overnight culture of both strains on LB+DAP agar plate (without antibiotics) and incubate at 30ºC. When preparing overnight culture of transformed WM3064, the culture needed to be washed with fresh LB before mixing to remove antibiotics. After overnight incubation, a large swab of cells was taken using inoculation loop and resuspended in 1 mL sterile PBS. The suspension was washed once in the same volume of PBS and a serial dilution to 10^{-6} was established. 100 ul aliquot of each dilution was plated on LB agar supplemented with kanamycin (no DAP to restrict WM3064 growth). After overnight incubation, single colonies of MR1-pYYDT-C5 appeared, from which a single clonal re-streak was performed. Overnight culture was established to perform plasmid extraction to assess the success of conjugation via gel electrophoresis.

4.2.1.2. Plasmid extraction

pYYDT-C5 (10450 Bp), containing entire flavin biosynthesis gene cluster ribADEHC, was employed as delivery DNA for S. oneidensis MR-1 WT. Briefly, plasmid DNA were extracted and purified from bacterial cultures at their respective mid-exponential phase using

a QIAprep Spin Miniprep kit (QIAGEN, Germany). DNA concentration was determined using a NanoQuant Plate™ and Spark microplate reader (TECAN, Switzerland).

4.2.1.3. Media preparation

M9 medium supplemented with trace elements was prepared as previously described, but with riboflavin omitted from the vitamin stock. For media containing 20 mM Lactate as carbon source, 20 mL of 1M Sodium DL-Lactate stock was added via sterile filtration to 1L of the M9 medium. PBS solution was prepared as previously described. Cathodic media was 1x concentration phosphate buffer saline (PBS).

4.2.2. MFC reactor setup

Dual-compartment MFC reactors with a working volume of 300 mL per compartment were used to investigate bioelectrical current production. The anode was made of 3.0 x 3.0 cm^2 carbon cloth (H23, 95 g/m^2, Quintech). The cathode was carbon cloth containing a Pt catalyst (1 mg/ cm^2, PtC 60%, 2.5 x 4.0 cm^2; FuelCellStore). Titanium wire was used to connect the electrodes to the outside of the reactors. Nafion© 117 was used as the exchange membrane to separate the two compartments. Reactors were assembled and initially filled with deionised water, then autoclaved to achieve sterility. The water was then replaced with appropriate media; standard M9 minimal salt, supplemented with trace minerals, amino acids and vitamins was chosen as the anodic compartment media and prepared according to past literature [355] with slight modifications. The list of chemicals and their corresponding concentrations in each stock are given in Supplementary Tables S1, S2, and S3. The M9 salt solution was autoclaved before the trace elements were added in 1:100 dilution from their stocks via 20 um pore-size membrane sterile filtration. The final medium was supplemented with 20 mM sodium DL-lactate and 0.75 mM IPTG as pYYDT-C5 plasmid inducer.

Cathodic compartment media was phosphate buffer saline (PBS), prepared by dissolving two 500 mg PBS tablets in 1L deionised water, then autoclaved to achieve sterility. Fixed resistors of 1 kΩ were used to complete the circuit. Keithley Instrument Datalogger 2701 was used to measure the voltage across the resistor every 10 minutes. Before bacterial injection, the anodic compartment was bubbled with nitrogen for 15 minutes to create anaerobic condition. Throughout the experiment, the anodic and cathodic compartments was continuously gassed with nitrogen and air, respectively. Three independent replicate reactors were run for each different system.

4.2.3. Polarisation and power density curve construction

The power production of wild-type *S. oneidensis* MR-1 and its flavin deficient/enhancement mutant counterparts was measured via polarisation curve construction. A potentiostat (PalmSens 4-channel Multi EmStat^{3+}) was used to perform linear sweep voltametry (LSV) on the MFC reactors, with the voltage varied between the theoretical open-circuit potential to zero. (E_{begin} = 0.8V, E_{end} = 0.0V, E_{step} = 0.1V, scan rate = 0.1 mV/s). The power density curve was then constructed using values derived from multiplying the applied voltage and the corresponding measured bioelectrical current, yielding the total electric power in accordance with Ohm's law:

$$P = IV \qquad \text{Eq. 4.1}$$

Here P is total electrical power, I is bioelectrical current, and V is the applied voltage. The total power measured in this manner was then normalised by the anode surface area, yielding the power density.

4.2.4. Planktonic and biofilm cell quantification

The concentration of planktonic cells in the reactor was determined by its optical density (more commonly known as optical absorbance) using a light spectrometer (UV-1800 Shimadzu) to measure light absorption at a wavelength of 600 nm. A cuvette length of 1 cm with sample size of 1 mL was employed, with fresh anodic media as a blank to exclude background reading.

Biofilm cell concentration was measured using a crystal violet assay. The anode was immersed in 20 mL of 0.1% crystal violet solution, then washed twice with 20 mL sterile deionised water. Finally, the cell bound crystal violet was dissolved in 20 mL of 70% isopropanol. The absorbance at 595 nm of four independent 100 µL replicates of the final solution was measured and normalised with background reading of crystal violet originating from a cell-free anode. The OD_{595} value is proportional to the number of cells attached on the biofilm, with the OD-to-cell number conversion was calculated using standard curve of known cell density.

4.2.5. Metabolites quantification

The amount of remaining lactate and produced metabolites within the reactors were quantified via high-performance liquid chromatography (HPLC) equipped with acid column Hi Plex – H (250 x 4.6 mm, particle size 8 µm, Agilent). The eluent was 0.005 M H_2SO_4 with flow rate of 0.6 mL/min, and signal was detected using UV detector at 210 nm and 55^{o}C. One mL of reactor medium was sampled and filtered using a 0.2 µm membrane filter to remove cells before being measured for its chemical concentration. Prior to the MFC experiment, standard curves of lactate and possible metabolites (acetate, pyruvate, formate, and succinate) were constructed.

4.2.6. In-situ plasmid transfer into S. oneidensis MR-1 in MFC

The effect of pYYDT-C5 plasmid transfer into *S. oneidensis* MR-1 via ultrasound was investigated in terms of the bioelectrical current production in an MFC system. Late-stationary phase culture of MR-1 was injected into the reactor to achieve an initial OD of 0.01. After reaching stable bioelectrical current generation across 1 kΩ resistor, 0.1 μg/mL of the plasmid was injected into appropriate reactors (*WT_P_US)*. Ultrasound was then performed for 30s at a frequency 42 kHz (± 6%) to transfer the plasmid into the cell, and bioelectrical current production was monitored. As controls, reactors with wild-type (*WT_US*) and MR-1/YYDT-C5 strain (*MR-1/YYDT-C5_US*) without further addition of plasmid were also experimented as controls. Another control of WT strain with plasmid addition, but without ultrasound treatment, was also measured to exclude the effect of such treatment (*WT_P*). Three independent replicate reactors were run for each system. Injection of kanamycin and lactate was done using sterile syringe and needle through one of the ports on the side of the reactor. Kanamycin was added from 50 mg/mL stock to achieve the desired final concentration in the reactor. Lactate was added from its 1 M stock, pre-filter sterilised to achieve sterility.

4.2.7. Ultrasound apparatus

A standard 42-kHz (± 6%) ultrasonic cleaning bath (Model 3510E-DTH, Branson Ultrasonics Corp., Danbury, CT, USA) with a maximum output power of 100 W was used in this study. The ultrasonic sound field was measured with a hydrophone (Type 8103, Bruel & Kjaer, Denmark) and consisted of bursts with a modulation period of 10 ms and a modulation depth of about 90%. The sound field amplitude spectrum displayed a strong peak at 42 kHz with harmonics extending up to almost 500 kHz. These harmonics were all between -23 dB and -60 dB relative to the primary peak and could be have been caused by nonlinearity in the

acoustic driver and cavitation noise in the waterbath. The pulse-average root-mean-square acoustic pressure was 170 kPa, corresponding to a pulse-average acoustic intensity of 1.9 W/cm^2. The mean and standard deviation of five measured waveforms was employed to estimate the peak-positve acoustic pressure of the pulse, which was 398 ± 62 kPa and the measured peak-negative acoustic pressure was 362 ± 41 kPa.

For each experiment, the bath was filled to the same level with type-1 water at laboratory temperature (order 20ºC) and local atmospheric pressure (order 1 bar). The dissolved air content was not controlled and was believed to vary from 85% to 95% of saturation. The biofilm sample holders used in each experiment (either a microfluidic flow cell or a microbial fuel cell) were submerged to the same depth and same lateral location within the bath. No exogenous cavitation-promoting particles, drops, or microbubbles (i.e., cavitation nuclei) were employed in the study.

4.2.8. Flavin quantification

Fluorescence spectroscopy was used to detect and quantify riboflavin and flavin mononucleotide (FMN) secreted by *S. oneidensis* in the MFC reactor. 100 μL of the cell-free supernatant of anodic media was transferred to a clear 96-well plate and read at 440 nm excitation and 525 nm emission. Four independent replicate aliquots were run for each reactor, and the background fluorescence was corrected by using fresh anodic media as the blank. Flavin concentration was determined using standard curves previously constructed with known concentrations of FMN (concentration range: 1 mg-mL^{-1} to 1 ng-mL^{-1}).

4.2.9. Plasmid sequencing and verification

At the end of MFC experiment, the anodic biofilm was collected and centrifuged to obtain cell pellets. Plasmid extraction protocol using a Monarch Plasmid Miniprep Kit was

performed, and the obtained plasmid was quantified using NanoDrop and a plate reader. The primers *PRTac-SF3_for* and *ribC-02_R8_rev* (Supplementary Materials) was used to sequence and identify the necessary plasmid fragment to confirm successful transfer of pYYDT-C5 plasmid into *S. oneidensis*.

4.2.10. Statistical Analysis

For all measurements involving replication, nested mixed-factor ANOVA tests followed by Tukey's HSD post hoc tests were performed to determine the significance between different treatment groups. A *P* value of less than 0.05 denotes a statistically significant difference between the conditions of interest.

4.3. Results and discussion

4.3.1. Flavin-mediated electron shuttling is the dominant mechanism of extracellular electron transfer in Shewanella oneidensis MR-1

Microbial fuel cells (MFCs) produce electricity using a bacterial biofilm deposited on an electrode to oxidise organic matter [20]. In this experiment biofilms of *S. oneidensis* MR-1 wild type (WT), MR-1 Δbfe [knockout of *bfe* gene for bacterial flavin adenine dinucleotide [FAD] exporter [163] and MR-1/YYDT-C5 [MR-1 with plasmid pYYDT-C5 containing the entire flavin biosynthesis gene cluster *rib*ADEHC cloned from *Bacillus subtilis* [164], [171] were established in the microbial fuel cell (MFC) system.

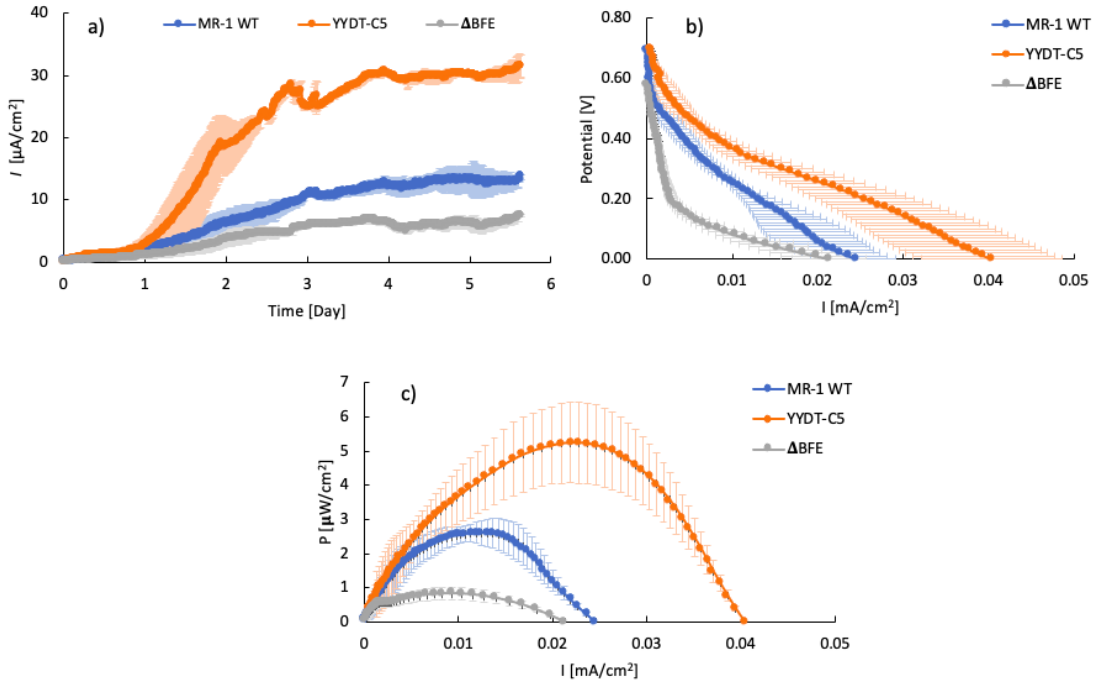

Figure 4.1: a) Electric current density *I* versus elapsed time, **b)** polarisation curve (current density vs. potential) and **c)** power density curve of MFC reactors with *S. oneidensis* MR-1 WT (blue), MR-1/YYDT-C5 mutant (orange) and MR-1 Δ*bfe* strains (grey) with 20 mM sodium lactate as sole carbon source. Measurements were conducted via Linear Sweep Voltammetry, as described above. Error bars represent the standard deviation of triplicate measurements.

The steady-state bioelectrical current density generated by the MR-1 WT reached 13.7 ± 0.3 µA/cm^2, compared to 7.6 ± 0.1 µA/cm^2 for the MR-1 Δbfe and 31.5 ± 1.8 µA/cm^2 for the

MR-1/YYDT-C5 mutant (p<0.05) (Fig. 4.1a; Table 4.2). After about 6 days of operation, MR-1/YYDT-C5 exhibited the highest bioelectrical current density vs. potential, compared to MR-1 WT and MR-1 Δbfe (Fig. 4.1b). The maximum output power density of the MR-1 WT was 2.61 ± 0.35 μW/cm^2, compared to 0.83 ± 0.19 μW/cm^2 from the MR-1 Δbfe, whilst MR-1/YYDT-C5 reached 5.25 ± 1.18 μW/cm^2 (p<0.05) (Fig. 4.1c and Table 4.2).

Table 4.2. The steady-state bioelectrical current density and maximum output power density (power per unit electrode surface area) of the MFC running with MR-1 wild-type and mutants.

	Current Density [μA/cm^2]	Max. Power Density [μW/cm^2]
MR-1 WT	13.7 ± 0.3	2.61 ± 0.35
MR-1 Δbfe	7.6 ± 0.1	0.83 ± 0.19
MR-1/YYDT-C5	31.5 ± 1.8	5.25 ± 1.18

The OD_{600} of anodic culture in the MR-1 WT reactors reached 0.129 ± 0.005, whilst that of MR-1/YYDT-C5 and MR-1 Δbfe peaked at a density of 0.098 ± 0.005 and 0.114 ± 0.005 respectively (Fig. 4.2a). The OD_{595} of cell-bound crystal violet solution from anodic biofilm cells of the MR-1 WT was found to be 0.411 ± 0.030, and 0.267 ± 0.031 for MR-1/YYDT-C5 and 0.458 ± 0.030 for MR-1 Δbfe (Fig. 4.2b). This translated into the number of attached cells in the biofilm as (2.74 ± 0.18) x 10^5 /cm^2 for MR-1 WT, (1.78 ± 0.24) x 10^5 /cm^2 for MR-1/YYDT-C5 and (3.05 ± 0.20) x 10^5 /cm^2 for MR-1 Δbfe. Consumption of lactate in MR-1 WT, MR-1/YYDT-C5 and MR-1 Δbfe were measured to be 12.0 ± 0.6 mM, 9.5 ± 0.7 mM and 11.6 ± 0.6 mM respectively (Fig. 4.2c). The reduction of flavin by *bfe* gene knockout in MR-1 Δbfe only produced 31% power, whilst the increase of flavin by overexpression of ribADEHC in MR-1/YYDT-C5 boosted power generation by 2-fold, in comparison with MR-1 WT (Table 4.2). These results demonstrate that flavin-enabled electron shuttling was the dominant mechanism of MFC-based bioelectricity generation in *S.*

oneidensis MR-1 – contributing towards ~70% of power generation, which is in-agreement with previous study [163]. It also suggests that the introduction of gene cluster encoding flavin biosynthesis (e.g. pYYDT-C5) into the bacteria of MFCs has the potential to significantly enhance electricity production performance.

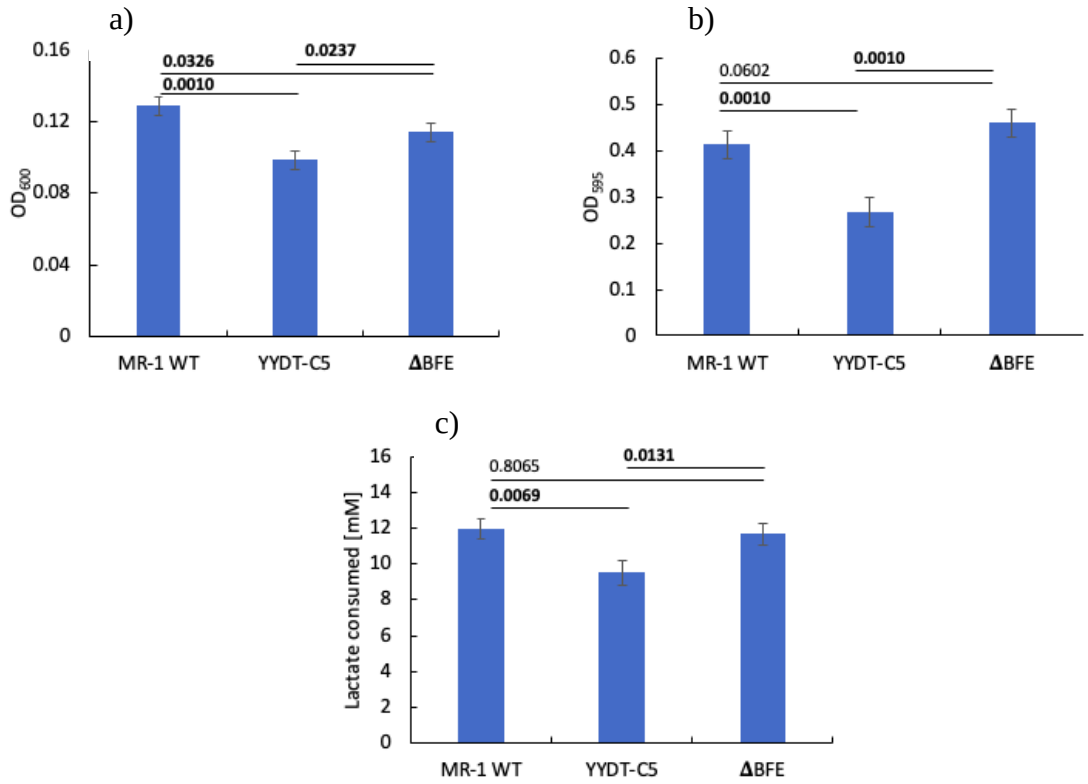

Fig. 4.2: **a)** Measured optical density at 600nm (OD_{600}) of anodic culture of MFC reactors utilising *S. oneidensis* MR-1 WT, MR-1/YYDT-C5 mutant and MR-1 Δ*bfe* strains with 20 mM sodium lactate as sole carbon source. Measurement were done using 1 cm cuvette (1 mL sample size). **b)** Biofilm quantification using crystal violet assay: optical density at 595nm (OD_{595}) of cell-bound crystal violet solution from anodic biofilm cells of the MFC reactors. **c)** The amount of lactate consumed by each reactor. Produced metabolites were mainly acetate, with succinate and pyruvate in trace amounts (data not shown). Measurements in Figure d), e) and f) were done at the end of MFC experiment (day 13). Error bars represent standard deviation of triplicate measurements. *P* values on top of the bars denote differences between sample pairs based on nested mixed-factor ANOVA test followed by Tukey's HSD post hoc test. *P* values showing statistically significant ($p < 0.05$) differences are presented in bold.

4.3.2. Ultrasound-mediated DNA delivery (UDD) to biofilms in microbial fuel cells (MFCs)

The transfer of pYYDT-C5 plasmid into MR-1 WT biofilms via UDD in an MFC was performed employing the setup shown in Figure 4.3, where the acoustic parameters and water bath properties are the same as in the previous study [350]. The effect of pYYDT-C5 on bioelectricity generation in established biofilms was investigated in a double-compartment MFC setup. The MFC system with plasmid transfer via UDD (WT_P_US) was compared to several controls: a positive control with MR-1/YYDT-C5 strain (MR-1/YYDT-C5_US), and two negative controls: the addition of plasmid without ultrasound (WT_P) and ultrasound treatment without plasmid (WT_US).

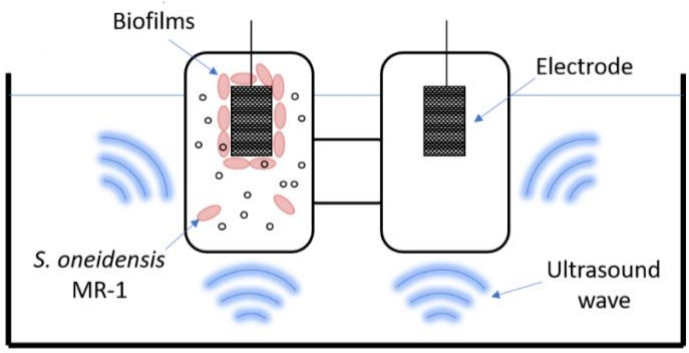

Fig 4.3. Schematic diagram of ultrasound-based DNA delivery (UDD) into bacterial cells of mature biofilms established in microbial fuel cell (MFC). Ultrasound treatments were applied in a commercially available 42 kHz ultrasound cleaning bath. Diagram is not drawn to scale.

Consistent with the previous experiment, the electricity generation of MR-1/YYDT-C5 positive control (28.0 ± 3.3 μA/cm^2) was significantly higher than the WT systems throughout the experiment (Fig. 4.4a). Once the bioelectrical current generation reached steady state after approximately 4 days, the addition of plasmid and/or ultrasound treatment was conducted between day 5 and 6. Bioelectrical current production in all treated MFC systems dropped immediately after ultrasound treatment was performed, which might have been caused by shock disturbance and stress, but it fully recovered after approximately 24 hrs

(Fig. 4.4a). This observation indicates that ultrasound treatment can result in temporary disturbance of the MFC system, possibly due to the physical disruption of the biofilm structure by acoustic cavitation and/or mechanical stress. However, cells in the biofilm were able to restructure themselves and fully recover with no permanent detriment afterwards. It is important to note that the nature and extent of ultrasound physical effects depend critically on a number of acoustic parameters. These effects, which were primarily mechanical and thermal in nature, can serve to both disrupt biofilms and promote gene transfer. We believe that, for a given system, there will exist optimum sets of acoustic parameters and exposure protocols that minimize biofilm disruption and cell death while enhancing gene delivery. This subject lies beyond the scope of the current work and is a topic of ongoing study.

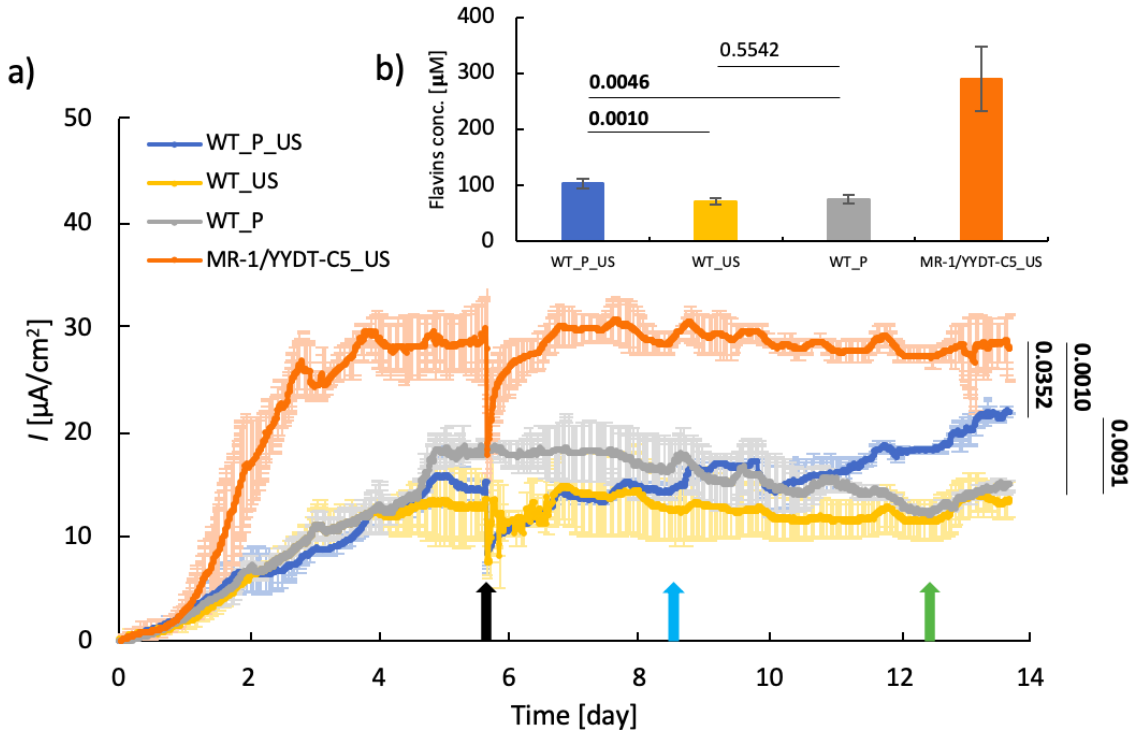

Fig. 4.4. **a)** Electric current density *I* of double-compartment MFC reactors running at 1kΩ load with 20 mM initial concentration of sodium lactate; **b)** extracellular flavins concentration of MFC reactors after 14 days of operation. Four different type of reactors: MR-1/YYDT-C5 strain (MR-1/YYDT-C5_US, orange), MR-1 WT with addition of plasmid and ultrasound treatment (WT_P_US, blue), MR-1 WT with only ultrasound treatment (WT_US, yellow), and WT with only addition of plasmid (WT_P, grey). Ultrasound was performed for 30s on day 6 (black arrow) for appropriate MFC setups. On day 9, kanamycin (10 μg/mL) and 10 mM of additional lactate was added into each reactor (light blue arrow). On day 13, additional kanamycin was added to reach final concentration of 50 μg/mL

(green arrow). Shaded regions represent standard deviations of triplicate measurements. *P* values on top of the bars were calculated for the last day of measurement and denote differences between sample pairs based on nested mixed-factor ANOVA test followed by Tukey's HSD post hoc test. *P* values showing statistically significant ($p < 0.05$) differences are presented in bold.

Forty-eight hours after plasmid transfer using ultrasound treatment, the WT_P_US system started generating higher bioelectrical current than that of WT_US and WT_P. At the end of the experiment, the WT_P_US system generated a bioelectrical current of 21.9 ± 1.2 μA/cm^2, 61% higher (p<0.05) than that of the WT_US system (13.6 ± 1.6 μA/cm^2) (Fig. 4.4a; Table 4.3). The application of UDD to treat the biofilms established within the MFC resulted in the increased production of flavins by the WT_P_US system over time. The WT_P system produced similar bioelectrical current to WT_US (14.9 ± 0.6 μA/cm^2), indicating that bacterial transformation only occurred in treatments in which plasmids were introduced in the presence of ultrasound.

Three days after ultrasound treatment, kanamycin (10 μg/mL) and lactate (10 mM) were added to all reactors to induce selection pressure for transformed cell growth and to maintain high electron donor concentration, respectively (Fig. 4.4a, light blue arrow). A three-day time gap was selected to enable the transformed bacterial cells, which were maintained at room temperature, to produce the necessary proteins in low-growth minimum media to resist the antibiotics. Additional kanamycin (40 μg/mL) was added on day 13 (Fig. 4.4a, green arrow). The addition of antibiotics on the separate occasions had no detectable effect on the bioelectrical current produced by the controls, since the mode of action of kanamycin did not initiate immediate killing of cells but instead interferes with protein synthesis and prevents cell replication [349]. This indicated that the established cell density in those reactors had reached optimum concentration before the antibiotics was added and that the whole process was not catalyst-limited. Injection of additional lactate on day 9 also had no detectable effect

of improving performance on bioelectricity production, indicating that the reaction was not substrate-limited either (Fig. 4.4a, light blue arrow).

The quantity of flavin electron shuttles secreted by the *Shewanella* strain played a significant role in influencing bioelectrical current generation in the MFC system [164]. After 14 days of operation, the amount of extracellular flavins in each MFC reactor was quantified. The WT_P_US system produced an approximately 50% higher concentration ($p<0.05$) of extracellular flavins (103.3 ± 8.3 µM) compared to the WT_US and WT_P systems (70.9 ± 5.9 µM, and 74.8 ± 7.3 µM respectively) (Fig. 4.4b, Table 4.3). Enhanced flavin production in the WT_P_US system was attributed to the additional synthesis pathway encoded in pYYDT-C5 plasmid, which was introduced into the *S. oneidensis* biofilm via UDD. This quantitative analysis of flavin confirmed that the transfer of the plasmid was achieved via ultrasound. The MR-1/YYDT-C5 positive control system contained the greatest concentration of flavin (289.7 ± 57.7 µM), which is consistent with the bioelectrical current generation result.

The extraction and sequencing of plasmids from transformed cells in the WT_P_US MFC system (see the Supplementary Materials) provided additional evidence for the successful transfer of the pYYDT-C5 plasmid into a *S. oneidensis* MFC biofilm. These results combined provide strong evidence of the ability of UDD to deliver desired genes *in situ* into bacterial biofilm. This demonstrates that UDD is able to enhance biofilm-based bioelectrochemical performance in MFCs *in-situ* without the need of restarting the bioreactor and re-building the biofilm, which is highly desirable for large-scale industrial applications involving continuous bioreactors.

Table 4.3. Final electric current density (current per unit electrode surface area) and extracellular flavin concentrations of UDD-treated MFC systems (measurement done in triplicate)

	Current density [μA/cm^2]	Flavins concentrations [μM]
WT_P_US	21.9 ± 1.2	103.3 ± 8.3
WT_US *(-ve control*)	13.6 ± 1.6	70.9 ± 5.9
WT_P *(-ve control*)	14.9 ± 0.6	74.8 ± 7.3
MR-1/YYDT-C5_US *(+ve control*)	28.0 ±3.3	289.7 ± 57.7

4.4. Conclusion

4.4.1. UDD induced in-situ bacterial transformation in MFC

The double-compartment MFC reactor employed in this study allowed reliable evaluation of the impact of UDD on bioelectricity output by MR-1 strains exhibiting varying flavin production and bioelectricity generation capabilities. MR-1 was selected as a model organism due to its unique extracellular electron transfer ability [146] and the fact that it is not naturally competent. The pYYDT-C5 plasmid was chosen as delivery DNA into *S. oneidensis* MR-1 WT biofilms as the plasmid contains the entire flavin biosynthesis gene cluster ribADEHC cloned from *Bacillus subtilis*, which has previously been shown to improve the bioelectricity generation of the transformed MR-1 as compared to the MR-1 WT [164]. Although not tested in this study, it is known that flavin concentrations are directly related to electricity production, although such relationship is not linear [163].

We have demonstrated that applying low frequency ultrasound (42 kHz) to *S. oneidensis* biofilms growing on electrodes in the presence of plasmids results in the *in-situ* uptake of pYYDT-C5 plasmid by bacterial cells, which generated almost twice as much bioelectricity in the MFC after 8 days of incubation as compared to negative controls. The low frequency

of 42 kHz was selected to maintain consistency of operating parameter with previous study [350], also due to apparatus standardization (most sonication baths come as 40-42 kHz frequency). The pYYDT-C5 plasmid used here is a relatively large plasmid (10450 Bp). While it is well recognised that transformation efficiency decreases with increasing plasmid size [350], [356], our results showed that the UDD technology is not limited to the delivery of small plasmids but is also effective for delivering relatively large plasmids as well. By selecting the proper acoustic parameters (primarily frequency and acoustic pressure amplitude), it may even be possible to achieve bacterial transformation via UDD involving the uptake of mega plasmids and genomic DNA fragments [357].

There have not been many studies conducted on UDD application on bacteria, as the technology is very novel. The proposed cavitation mechanism for the UDD is in fact a novel finding through studies conducted in our research group, for which we are currently filing for a patent (a scientific paper will be published once patent is filed). Nonetheless, ultrasound applications on mammalian cells have been extensively studied [358]–[363], from which some comparisons might be drawn. A study conducted on 3T3 mouse cell suspensions [358] have indicated that a low frequency range of 20-100 kHz encouraged uptake of calcein, with cell viability observed to increase as higher frequency was used, for the same applied energy density. Across all applied frequency, the energy density corresponding to maximum calcein delivery increased with increasing frequency, suggesting higher energy requirement to reach maximum delivery when higher frequency is used. Interestingly, the maximum fraction of cells that were reversibly permeabilized (6-8%) is nearly independent of the frequency, suggesting that the uptake efficiency is mostly driven by applied energy density, and not so much on frequency selection. Another study conducted on human triple negative breast cancer MDA-MB-231 cells [364], low frequency ultrasound of 40 kHz was also employed to sonoporate the cells and introduce FD4 staining chemical into the cells. Three different

parameters were varied to study the effect of each on sonoporation frequency – mainly energy density, time of irradiations and microbubble concentration. The study suggested that all three parameters have an optimum point – at which the sonoporation efficiency was peaked. In the setup used in this particular study, a maximum efficiency was achieved when 300 mW/cm^2 of energy was applied (~14%) compared to 1% at 230 mW/cm^2 and 11% at 370 mw/cm^2. Irradiation time have slightly smaller effect, with 10% efficiency achieved in 2 min, compared to 7% in 1 min and 9% in 3 min.

UDD-treated biofilms in MFC were only able to match around 70% of the level of bioelectricity generated by MR-1/YYDT-C5 positive control system by day 14 (Fig. 4.4a). It is evident that bacterial transformation efficiency can be a limiting factor preventing treated biofilms from achieving the maximum theoretical productivity. To alleviate this limitation, the appropriate use of selection pressure can amplify the effects of UDD treatment on the biofilm to exhibit high productivity. In bacteria, plasmids facilitate rapid adaptation by shuttling a vast variety of advantageous traits across microbial communities. However, under non-selective conditions, maintaining plasmid often becomes a costly activity for host cell. In this study, we used antibiotics as a selection pressure mechanism to limit the growth of non-transformed cells, allowing the transformed cells to thrive. Besides this, our system also allowed for a natural plasmid preservation – through biofilm formation. Previous studies have suggested that biofilms can act as a spatiotemporal reserve for plasmids, enabling them to persist under non-selective conditions [365]–[367].

It has been previously suggested that the mechanism of transdermal protein delivery using low frequency ultrasound, such as 20 kHz, is attributed mainly to acoustic cavitation physical effects [368]–[370]. It is possible that the mechanism of UDD in biofilms is similarly via acoustic cavitation where microbubbles, formed on the surface of or within biofilms, are

made to volumetrically oscillate under periodic acoustic forcing. Associated with this behaviour is a host of physical effects that include fluid microstreaming, shock wave production, localized viscous heating, and the formation of re-entrant liquid jets due to asymmetric bubble collapse [371], [372]. Potential bioeffects on cells stemming from these physical effects of acoustic cavitation have been reviewed in the literature [373], [374]. For example, microstreaming breaks down boundary layers and promotes the convection of plasmids proximal to the cell surface. Jetting pokes small holes in the cell, leading to transient enhancement of cell membrane porosity. The biofilm matrix contains extracellular polymeric substances such as lipids, polypeptides and polysaccharides of diverse chemical charges [355], [375]–[377], and is an ideal adsorption material for extracellular DNA or plasmids to be introduced to the biofilms. The high cell density in the biofilms [378], potentially coupled with proximity between the bacteria and plasmids of interest in the biofilm matrix, provides a suitable environment for ultrasound-mediated horizontal gene transfer to take place within non-competent bacterial biofilm communities. While ultrasound treatment and its associated physical effects can aid gene transformation in biofilm, the very same effects can also disrupt the biofilm structure and stability. At present, the mechanistic details of UDD remains elusive and further studies are required to optimize acoustic parameters and exposure protocol, such as ultrasound intensity, duration, duty cycle, types of transducer, temperature and ambient pressure etc., for more efficient and reproducible gene transfer.

4.4.2. Scaling up UDD in biofilms for industrial applications

The goal of this study was to introduce new functionalities into non-competent established biofilms in bioreactors of different scales via *in-situ* UDD. Current conventional gene transfer techniques (such as electroporation, heat shock and conjugation) are optimised for small scale laboratory use, typically < 2 mL [379], [380], but all have limitations that make them unsuitable for larger scale, *in-situ* applications. Electroporation requires salt-free conditions and typically kills >90% cells with transformation usually limited to specific strains. Heat shock requires a rapid and drastic change in temperature (>30 °C) of the cells and their liquid medium. Conjugation requires direct physical contact between donor and recipient strains. Theoretically, ultrasound-mediated DNA delivery (UDD) is capable of engineering bacterial culture and biofilms *in-situ* without these inherent limitations at larger scale. In this study, UDD-induced gene transfer on non-competent biofilms grown in microbial fuel cell (MFC) systems was successfully demonstrated, with working volumes of 300 cm^3, achieving a significant scale-up in operating volume using the same acoustic exposure system. To the best of our knowledge, there has not been any technique designed to enable bacterial transformation within biofilms *in-situ* and/or in operating volumes larger than 2 mL.

These results provide solid evidence that UDD-based techniques hold promise in terms of achieving efficient bacterial transformation at industrial scales. DNA fragments containing genes of interest may be introduced *in-situ* into established biofilms cultured in bioreactors, reducing downtime and ensuring continuous operations. It may also be possible to influence gut microbiome of animals and human beings for agricultural or medical purposes respectively using this approach. Thus, the ability to alter the phenotype of established biofilms creates new possibilities for influencing their behaviour in environmental, industrial, and medical settings. While UDD technology clearly has huge potential, further research into its physical mechanisms is required for optimisation and/or industrial scale exploitation.

As suggested in previous studies [381], [382], effective scale ups may be achieved by ensuring uniform cavitational activity distribution throughout the processing volume, as non-homogenous and dynamic behaviour of such activities often create problems in scale up strategies. Although it was indicated that sonication time played little to no effects for scaling up – maintaining constant energy density is deemed to be key in scaling up UDD process. Furthermore, although not necessarily for UDD in bacteria, other studies have explored novel reactor designs [383]–[386] to ensure constant cavitational distributions for larger volumes in different ultrasound applications i.e., emulsification, chemical extractions.

Nonetheless, by demonstrating that *in-situ* gene transfer in biofilms via UDD is possible for a bioelectrochemical system such as MFC, this exciting proof-of-concept opens the door to opportunities for the exploitation of this novel technology to enhance the controllability and efficiency of biofilm-based processes in the environmental, industrial, and medical contexts.

Chapter 5: Current generation in microbial fuel cells by *Shewanella oneidensis* MR-1 via assimilation of acetate

5.1. Introduction

Electricity generation from organic compounds via microbial fuel cell (MFC) has been intensely studied, using a variety of compounds and bacterial strains. The technology relies on the ability of some bacteria to degrade organic matter and transfer the released electrons to extracellular insoluble electron acceptors (i.e. electrode) that are then harvested as electric current. Such bacteria are called exo-electrogens and several mechanisms have been proposed for this extracellular electron transfer (EET): 1) via direct contact using outer membrane (OM) multi-heme c-type cytochromes; 2) outer membrane extensions referred to as *nanowires;* and 3) non direct-contact via electron shuttles. Different exo-electrogens utilise distinct mechanisms, and some have been shown to utilise all three [140], [156] whereas the others are only capable of employing one or two of the proposed mechanisms [145], [387]. Furthermore, certain exo-electrogenic bacteria have the capability to utilise organic compounds that others cannot, due to different metabolic and respiratory pathways, some of which are yet to be fully understood [388]–[390].

Two of the most extensively studied exo-electrogenic bacteria for bio-electrochemical systems are members of the genus *Shewanella* spp. and *Geobacter* spp [276], [391]–[396]. They are dissimilatory metal-reducing bacteria (DMRB), able to couple metal reduction with their metabolism. *Shewanella oneidensis* MR-1 is a Gram-negative facultative anaerobic bacterium, notable for its ability to reduce metal ions via EET. One of its most significant properties that distinguishes it from that of *Geobacter* spp. is that it does not require direct contact with its substrates for electron transfer. This key feature is due to its ability to

produce extracellular electron shuttles such as riboflavin, which *Geobacter* spp. do not possess [397], [398]. This ability is potentially very beneficial in microbial fuel cell where direct contact to electrodes is often difficult to achieve [163].

Due to its interesting and robust feature, *Shewanella oneidensis* MR-1 has been extensively studied for multiple real-life applications: such as development of gene editing tools [399]–[401], environmental bioremediations of toxic metals and electro-fermentations [401]–[404] as well as its applications in bioelectrochemical system (BES) [405]–[409]. It is able to generate energy by coupling the oxidation of organic compounds such as lactate, pyruvate and hydrogen to the reduction of a wide range of electron acceptors including O_2, fumarate and Fe(III) [406], [409]. Figures S1 [320] provide the typical metabolic pathway for *Shewanella* showing multiple carbon sources which the bacteria can use as electron donors. Lactate was one of the most favourable carbon sources for anaerobic respirations of MR-1 [410]–[412]. The lactate metabolism continues with oxidation to pyruvate, acetyl-CoA, acetyl-phosphate formation and acetate generation to produce 1 ATP per lactate molecule [410].

One interesting possible electron donor is acetate – which have raised certain opposing views among researchers as to whether *Shewanella* can utilize it under anaerobic conditions. Although many literatures have suggested that acetate utilization by *Shewanella* is limited only under oxygen-rich condition [405], [410], [412], [413], such inablility has not been fully understood and explained, especially since *Shewanella* spp. have a complete tricarboxylic acid (TCA) cycle and are able to oxidize acetate to CO_2 under aerobic conditions utilising acetate kinase SO2915 and phosphate acetyltransferase SO2916 enzymes [320], [410]. Previous studies have only gone so far to *suggest* that such inability *might be caused* by insufficient energetic requirements by the interruption of the TCA cycle under anaerobic conditions [412], or the bacteria's inability to re-oxidize NADH that it was only possible to

utilize such organic compounds if the generated NAD(P)H from its catabolism does not exceed the needs of anabolism under anaerobic conditions [410], [414].

In terms of experimental setup, one of the earlier studies that claimed *Shewanella's* inability to utilize acetate anaerobically [413] – which was cited by many other literatures that follow – only attempted to couple acetate oxidation with reduction of Iron (III) and Manganese (IV) – but not with other oxidising metals nor under bioelectrochemical (BES) setup with electrode as electron acceptor. A more recent study which suggested the same observation did use MFC setup to run the wild-type strain with acetate as sole carbon source [412] – however ferricyanide $[Fe(CN)_6]^{3-}$ was used as the final electron acceptors in the cathodic chamber instead of the usual air purging / exposure. This could be the reason why acetate was not utilized in this setup – as the selection of electron acceptors would play major role as to whether acetate would be utilized under anaerobic condition. This hypothesis was supported by a study conducted by *Yoon et al*., where acetate was utilized by *Shewanella* spp. under nitric reducing environment, but not with ferric iron or fumarate reduction [415].

The first study which suggested potential utilization of acetate under oxygen-free condition by *Shewanella* MR-1 was actually done in 2001 – where the strain was grown under H_2-acetate environment with nitrate as the electron acceptor, resulting in growth yield of 9.4 gr cell/M of substrate [416]. Fast forward in 2013, study conducted by *Yoon et al.* reported similar observation which is the utilization of acetate as electron donor by *Shewanella spp.* under nitric reducing environment, but not ferric iron or fumarate reduction [415]. Another, more recent study has shown degradation of acetate by *Shewanella* under anaerobic conditions with concomitant implementation of EET via external mediators such as riboflavin, AQDS and hexacyanoferrate [417]. This was the first reported case of utilization of acetate as electron donor on *Shewanella* anodes in bioelectrochemical setup, despite only able to achive 6% carbon utilization to support biomass (5%) and current generation (1%).

Another study conducted by *Dai et al.* in 2020 has shown successful degradation of acetate from bamboo fermentation effluent by *Shewanella oneidensis* MR-1 in an MFC setup – achieving 98% utilization after 8 days of operation [418]. Finally, a study done by *Calderon et al.* has also shown acetate consumption by *Shewanella spp.* isolated from *Odentesthes regia* via double compartment MFC, achiving 0.11 mA cm^{-2} steady current after 72 hrs with 65% coulombic efficiency under anaerobic conditions [419]. These studies have provided boosts of optimisms for *Shewanella's* application in microbial fuel cell, as acetate has often been considered as valuable by-products whose chemical energy is relatively easy to recover due to their simple VFA structure, which often present in waste of many industrial processes and wastewaters such as anaerobic digesters [420]–[422]. Hence, integrating MFC with anaerobic digester to utilise the unwanted acetate would optimise the overall carbon and energy efficiency. To date, most studies of acetate utilisation as electron donor in MFC systems have relied on bacterial communities, usually present in anaerobic sludges [139], [423], [424]. However, these systems are difficult to engineer and optimise, because of the complexity and uncertainty regarding bacterial community composition, interactions and metabolic activities of different bacterial species present in the consortium [425]. Hence, it would be of significant advantage to have a well-studied bacterial strain capable of utilising acetate to generate electric current, preferably via both direct contact and electron shuttles mechanisms.

In this study, lactate-fed MFC composed of pure culture of *Shewanella oneidensis* MR-1 was investigated for its electrical current generation in batch mode. As lactate had been completely depleted, the bacteria were forced to switch its metabolism to assimilate the produced acetate to survive, generating additional electricity at a lower potential. As previously reported, *Shewanella* strain will first utilize lactate, followed by pyruvate and acetate [417]. To confirm utilisation of acetate by *S. oneidensis,* separate studies of acetate-

fed MFC with digestate from Anaerobic Digester (AD) were established. The results confirm that *S. oneidensis* was able to utilise acetate under anaerobic conditions producing electric current in MFC system. To the best of our knowledge, no reported study has yet to utilize direct AD liquor as carbon source and electron donor to drive EET on pure *Shewanella* anodes. This study thus expands our understanding of *Shewanella* ecophysiology and its potential applications in bioelectrochemical systems.

5.2. Materials and Methods

5.2.1. Bacterial strain and media preparation

The strains used in this study is listed in Table 5.1.

Shewanella oneidensis MR-1 wild-type strain was inoculated on LB plate from a -80^{o}C stock. The plate was incubated at 30^{o}C for 24 hr until single colonies were formed, from which a single clonal re-streak was obtained. A single colony was inoculated in 10 mL LB broth overnight (~18 hr) to reach late stationary phase. The culture was washed with PBS three times and diluted accordingly before being injected into MFC reactors. Standard M9 minimal salt, supplemented with trace minerals, amino acids and vitamins was chosen as the anodic media and prepared based on *Cao et al*. [355] with slight modifications. The list of chemicals and their corresponding concentrations in each stock are given in Supplementary Materials (Table S1, S2 and S3).

The M9 salt solution was autoclaved before the trace elements were added in 1:100 dilution from their stocks via 20 um pore-size membrane sterile filtration. The final medium was supplemented with sterile carbon source (sodium DL-Lactate or sodium acetate; also via filtration) to reach a final concentration of 20 mM. The cathodic media employed was PBS solution, prepared by dissolving two 500 mg PBS tablets in 1L deionised water, then autoclaved to achieve sterility.

Anaerobic digester (AD) liquor was obtained from a high-rate hydrolyser using maize silage as feedstock. The liquor was centrifuged at 10,000 g for 15 minutes to remove solid particulates and filtered through 0.2 µm pore to achieve sterility.

5.2.2. Reactor Assembly and Setup

Double-compartment MFC reactors with a working volume of 300 mL was used to investigate current production. The anode consisted of 3.0 x 3.0 cm^2 carbon cloth (H23, 95 g/m^2, Quintech). The cathode was carbon cloth with a Pt catalyst (1 mg/cm^2, PtC 60%, 2.5 x 4.0 cm^2; FuelCellStore). Titanium wire was used to connect the electrodes to the outside of the reactors. Nafion© 117 was used as the exchange membrane to separate the two compartments. Reactors were assembled and initially filled with deionised water, then autoclaved to achieve sterility. The water was then replaced with appropriate media; M9 minimal salt with trace elements and appropriate carbon source for anodic compartment, and phosphate buffer saline (PBS) for cathodic compartment. Fixed resistors (1 kΩ – 10 MΩ) were used to complete the circuit. The anodic chamber was continuously purged with nitrogen gas to maintain anaerobic conditions, whereas the cathodic compartment was gassed with air.

5.2.3. Performance evaluation of MFC reactors

S. oneidensis MR-1 (*MR1_Lac*) was investigated for its current production ability and checked against a negative control that was lacking the bacteria (*NoMR1_Lac*). Late-stationary phase culture of MR-1 was injected into the reactors to achieve an initial OD of 0.01. Variable resistance experiment was conducted to construct the polarisation curve of the MFC system. At the initiation of the experiment, external resistor of 1 kΩ was used for 8 days to start bacterial build-up. After reaching stable electricity generation, the resistance was

gradually stepped up to 10 MΩ. The voltage across the external resistor was measured every ten minutes with Keithley 2701 Dataloggers instrument. All systems were conducted in triplicate and the reactors were run for a total of 60 days.

At different resistance, the produced electric current could be calculated from the measured voltage using Ohm's Law:

$$I = \frac{V}{R} \qquad \text{Eq. 5.1}$$

And generated power density (W/m^2):

$$P = \frac{IV}{A} = \frac{V^2}{AR} \qquad \text{Eq. 5.2}$$

The current was then plotted against the corresponding voltage and power density to identify the maximum deliverable power output.

To confirm the utilisation of acetate in bioreactors by *S. oneidensis*, acetate-fed MFC systems were investigated. Sodium acetate (20 mM) was used as the sole carbon source, and the bioreactors (*MR1_Ac)* were measured for their current production ability. Two negative controls, each lacking either the bacteria or the carbon source (*NoMR1_Ac* and *MR1_NoAc*, respectively) were also investigated. In reactors where bacteria were supposed to be present, late-stationary phase culture of MR-1 was injected into the reactors to achieve an initial OD of 0.005. All bioreactor systems were triplicated. 1 kΩ resistor was used to represent load for 6 days, before the resistor was switched to 10 kΩ and was let to run for additional 45 days. Polarisation curves were constructed using PalmStens 4+ Potentiostat, with E_{begin} = 0.7 V, E_{end} = 0.0V and scan rate 0.1 mV/s.

For MFC experiment running with AD liquor, 1.1 mL of sterile liquor (C_{Ac} = ~8 g/L) was injected into the anodic chamber to achieve initial acetate concentration of 30 mg/L inside the

reactor. Trace elements of amino acid, vitamin and minerals were added to stimulate growth. Three different bacterial strains were used: wild-type, pYYDT-C5 and ΔBFE mutants. One kΩ resistor was used to represent load for 5 days, and the voltage across it was measured every 10 minutes.

5.2.4. Chemical Analysis and Coulombic Efficiency

The concentration of the remaining lactate (or acetate) and the produced metabolites in the reactors was determined via High Performance Liquid Chromatography (HPLC), with acid column Hi Plex – H from Agilent. The eluent was 0.005 M H_2SO_4 with flow rate of 0.6 mL/min, and signal was detected via UV 210 nm at 55ºC. One mL of reactors' medium was sampled regularly for the concentration analysis. The sample was filtered using 0.2 ul pore-size membrane filter to remove cells before being measured for its chemical concentration. Prior to the MFC experiment, standard curves of lactate and possible metabolites (acetate, pyruvate, formate, and succinate) were constructed.

VFAs content of AD liquor-fed MFC was analysed using gas chromatography (Shimadzu GC-2010, Japan) equipped with a flame ionisation detector (GC-FID) and a 30 m × 0.25 mm × 0.25 µm fused silica capillary column (ZB-FFAP). The temperatures of the detector and injector were 350 °C and 250 °C, respectively. The oven temperatures were set at 100 °C for 2 min and then increased at a rate of 8 °C/min. Helium was used as the carrier gas at a flow rate of 5.53 ml/min. Sample volume of 1.5 ml was inserted into GC vial and acidified with 3% (v/v) formic acid. Prior to the start of the experiment, standards containing 7 different type of VFAs (acetic acid, propionic acid, isobutyric acid, n-butyric acid, isovaleric acid, n-valeric acid and n-hexanoic acid) with known concentrations were used to construct standard curve. The retention time for each detectable VFAs are 3.83 min, 4.76 min, 5.07 min, 5.85 min, 6.36 min, 7.27 min and 8.65 min respectively.

Coulombic efficiency indicated the portion of charge generated by the oxidation of the carbon source that was successfully converted into useful current. The amount of useful charge was calculated via integration of produced current with respect to time:

$Q = \int_0^t idt$; Eq. 5.3

Whereas the total charge released by oxidation of acetate was calculated using Faraday's Law of Electrolysis:

$Q_{tot} = zF(V\Delta C)$; Eq. 5.4

Where z = 8 for the oxidation of acetate to CO_2; see equation 5.5.

$CH_3COO^- + 2\ H_2O \rightarrow 2CO_2 + 7\ H^+ + 8\ e^-$ Eq. 5.5

F = 96485 Cmol^{-1}; V is working volume of the reactor and ΔC is change in carbon source concentration. Coulombic efficiency was then calculated as:

$\varepsilon = \frac{Q}{Q_{tot}}$; Eq. 5.6

5.2.5. Bacterial cell quantification

One mL of samples from the anodic compartment of the reactors was taken regularly to determine the Optical Density via 600 nm light spectrometer (OD_{600}) of cultures. This measurement provided a direct correlation with cell concentrations in the medium, which was proportional to the number of planktonic cells in the anode. Plate counting was also conducted to quantify the number of colonies forming unit (CFU) of anode culture. One mL of anodic media was sampled and diluted in series up to 10^{-5} dilution. A 100 ul aliquot of each dilution was plated in triplicate for CFU count.

5.2.6. Carbon and mass balance

Mass balance was calculated under several assumptions [426], [427]. Bacterial cell's empirical formula is taken as $CH_{1.77}O_{0.49}N_{0.24}$, and that OD-to-cell dry weight conversion of

0.39 g/L per OD_{600}. From OD measurement, empirical moles of bacterial cell were calculated and compared to the amount of acetate consumed to deduce the portion of carbon source used for cell growth.

5.2.7. Microscope (SEM) imaging

At the removal from the anodic compartment, the anode samples were immediately sliced by a sterilized bistoury and fixed by phosphate buffer saline (PBS) with 2.5% glutaraldehyde (pH 7.2–7.4) for 1 hour. The samples were then washed 3x with the same buffer and dehydrated stepwise with a series of ethanol solutions (30, 50, 70, 80, 90 and 100%). The electrode samples were finally critical-point dried with tertbutyl-ethanol and sputter coated with a thin layer of gold. The biofilm was observed in high vacuum using Zeiss Merlin Compact Field Emission Gun – Scanning Electron Microscope (FEG – SEM). Electron high tension voltage of 2.00 kV was used with a working distance of 6.2 mm to optimise image resolutions.

5.3. Results and discussion

5.3.1. Electricity generation and metabolites quantification of Lactate-Fed MFC

The lactate-fed MFC (named as MR1_Lac) was operated in a dual-chamber reactor with working volume of 300 mL using a pure culture of *Shewanella oneidensis* MR-1. In the anode chamber, 20 mM sodium D-lactate was used as the sole carbon source, supplemented by trace elements to support growth [355] (Table S1 – S3). A negative control without bacteria was also investigated. A fixed resistor of 1 kΩ was used to start the experiment and the voltage across it reached stability at 0.10 ± 0.02 V after ~3 days (Fig. 5.1a). The external resistance was increased step-by-step to establish polarisation curve (Fig. 5.1b). Maximum attainable power was measured to be 2.39 ± 0.61 $\mu W/cm^2$. The negative control did not

produce any detectable current at any applied resistance, demonstrating that oxidation of lactate was only possible via biocatalysis by bacteria.

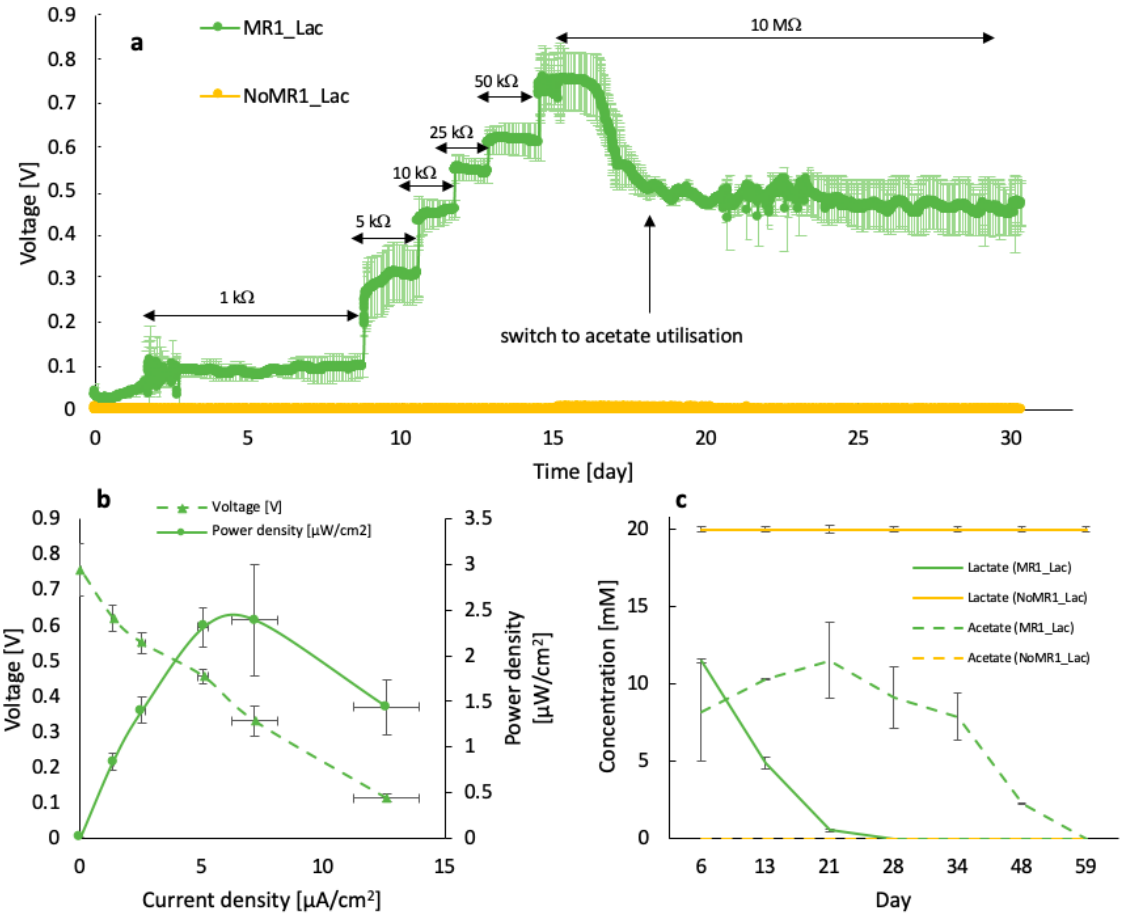

Fig. 5.1: a) Voltage of Lactate-fed MFC across 1 kΩ resistor over time; the resistance was increased gradually to establish a polarisation curve. *MR1_Lac* system (green) showed a step increase in voltage each time the resistance was increased, whereas *NoMR1_Lac* system did not generate any current; b) Polarisation curves of *MR1_Lac* system showing a maximum attainable power of 2.39 ± 0.61 µW/cm^2; c) Concentration of lactate (solid) and acetate (dash) over time in *MR1_Lac* (green) and *NoMR1_Lac* (yellow) systems. Error bars/region represent the standard error of triplicate measurements.

Around day 20, the generated voltage across the 10 MΩ dropped from 0.75 ± 0.08 V to 0.48 ± 0.04 V (Fig. 5.1a), and HPLC analysis indicated complete depletion of lactate (Fig. 5.1c). Interestingly, a substantial amount of voltage remained, suggesting that further utilisation of metabolites (in this case acetate) could have been responsible for the additional production of electric current. Acetate, pyruvate, and succinate were identified as metabolites of lactate

oxidation (Supplementary Fig. S2). Acetate was generated from lactate oxidation which reached a peak concentration of 11.5 ± 2.4 mM after 21 days before decreasing (Fig. 5.1c), which was consumed in the process to enable further electricity generation. All acetate was depleted after around 60 days. The control *NoMR1_Lac* exhibited no change in concentrations as expected. Pyruvate was detected at the initial stage of the operation (<15 days), reaching a concentration of 0.25 ± 0.03 mM. Small quantities of succinate were also produced (0.26 ± 0.08 mM) (Fig. S2).

5.3.2. Confirmation of Acetate Utilisation in Acetate-Fed MFC

The ability of acetate utilisation in *S. oneidensis* to produce electric current was further confirmed in the acetate-fed MFC experiment. In these reactors, 20 mM sodium acetate was used as the sole carbon source (named as *MR1_Ac*) and the MFC was operated under a constant external resistance of 1 kΩ. A triplicate of acetate-fed MFC reactors was run alongside two negative controls, each lacking the bacterial cells or the carbon source (named as *NoMR1_Ac* and *MR1_NoAc*, respectively).

Voltage generation of *MR1_Ac* initially increased within the first 9 hours, before approaching steady state at 0.032 ± 0.011 V after 2 days (Fig. 5.2a). The maximum attainable power was 0.12 ± 0.01 μW/cm^2 (Fig. 5.2b). *MR1_NoAc* initially generated a small voltage of up to 0.008 ± 0.002 V, but eventually decayed to zero. This negligible level of electricity generation was attributed to the oxidation of trace amino acids present in the media, as it has been reported that *S. oneidensis* MR-1 was able to utilise them as carbon source [320]. *NoMR1_Ac* did not generate any voltage at any point during the study as was expected.

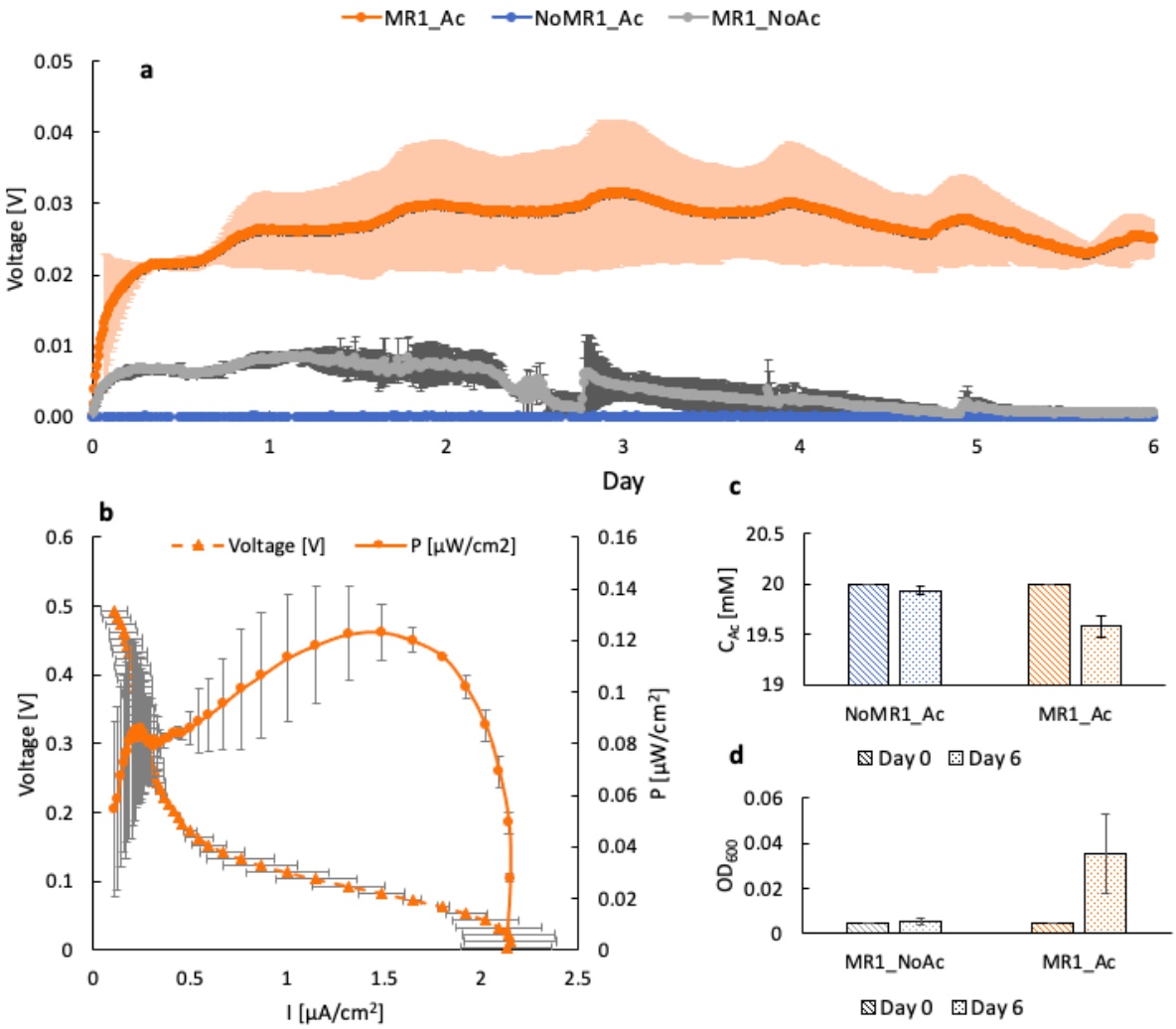

Fig. 5.2: a) Voltage of Acetate-Fed MFC systems over time across 1kΩ resistor for 6 days, *MR1_Ac* (orange) and *NoMR1_Ac* (blue) was fed with 20 mM acetate whereas *MR1_NoAc* (grey) has no carbon source; b) Polarisation curve of *MR1_Ac* established on day 6 with potentiostat showing maximum power output of 0.12 ± 0.01 µW/cm^2; c) Concentration of acetate in the anodic compartments of *MR1_Ac* (orange) and *NoMR1_Ac* (blue) on day 0 (stripes) and day 6 (dots); d) Optical density at 600 nm wavelength (OD_{600}) of anodic culture of *MR1_Ac* (orange) and *MR1_NoAc* (grey) on day 0 (stripes) dan day 6 (dots). Error bars/region represent standard error of triplicate measurements.

HPLC analysis indicated that 0.42 ± 0.11 mM of acetate was consumed within the first 6 days of operation in *MR1_Ac* (Fig. 5.2c). The concentration of acetate in the *NoMR1_Ac* system remained unchanged after 6 days, evidence that the consumption of acetate only took place in the presence of bacteria. No soluble metabolites were detected throughout the experiment, suggesting that carbon dioxide may have been the final oxidation product. After

being left running for 50 days, the concentration of acetate remaining in the *MR1_Ac* reactor was 1.72 ± 0.22 mM (data not shown).

OD_{600} of *MFC_Ac* anodic consortium reached 0.036 ± 0.018 by day 6 (Fig. 5.2d). Plate counts of the planktonic cells at this stage generated of 4.1 ± 1.0 x 10^5 CFU/ml. Maximum OD was reached after 35 days (0.153 ± 0.007; data not shown). *MR1_NoAc* system did not show any detectable increase in OD_{600} over 6 days, indicating that there was no bacterial growth in the absence of acetate.

Carbon – mass balance analysis further confirmed acetate utilisation both as a carbon and energy source in anaerobic conditions. Assuming the empirical formula for a bacterial cell to be $CH_{1.77}O_{0.49}N_{0.24}$ [426], and that OD-to-cell dry weight conversion of 0.39 g/L per OD_{600} [427], it can be estimated that 67.5 ± 11.2 % of the acetate was used for cell replication. The energy balance based on chemical-to-electrical energy conversion indicated a coulombic efficiency of 14.1 ± 1.8%, which represented 81.6 ± 13.0% of the known carbon usage. Low coulombic efficiencies have been previously reported with MFCs running with acetate as sole carbon source [139], [428]–[430]. The remaining undetected carbon could be attributed to energy and/or mass losses to the surrounding and/or cathodic chamber as acetate is quite volatile by nature (as observed in the negative control that the acetate concentration slightly dropped; Fig. 5.2c). Furthermore, some studies have suggested the ability of bacteria to store acetate within the cell [431], hence is not detected in the media, although no specific evidence that this occurred for *Shewanella* strains in this study.

5.3.3. Microbial fuel cell acetate utilisation from anaerobic digester liquor

One of the key sources of acetate in industrial sector is anaerobic digester by-products. In this study, industrial sample of anaerobic digester liquor, obtained from a high-rate hydrolyser using maize silage as feedstock, was used as carbon source in microbial fuel cell. AD liquor

containing ~8 g/L acetate (along with ~4 g/L propionate (C3), ~3g/L of butyrate (C4), <1 g/L valerate (C5) and <1 g/L caproate (C6)) was sterile-filtered and fed into 300 mL dual-chamber MFC reactor to achieve initial acetate concentration of 30 mg/L with *S. oneidensis* as single culture biocatalyst (remaining volume filled with M9 minimal media). Three different *Shewanella oneidensis* strains: wild-type (WT), *pYYDT-C5* and ΔBFE were examined and compared. The comparison between different strains can be seen in Table 5.1.

Table 5.1: Bacterial strains and plasmids used in this study

Bacterial strain or plasmid	Genotype, description	Reference or source
Strains		
Shewanella oneidensis MR-1 wild type (WT)	Wild type strain of MR-1	[354]
MR-1 ΔBFE	ΔBFE mutant of MR-1. Loss of ability to transport the FAD into the periplasm, reduced extracellular flavins available for electron transfer	[163]
MR-1/YYDT-C5	*S. oneidensis* MR-1: pYYDT-C5	[329]
Plasmid		
pYYDT-C5	Plasmid with entire flavin biosynthesis gene cluster ribADEHC cloned from *Bacillus subtilis*, Kan^R	[164]

A voltage of over 1 kΩ resistor was immediately observed with the MFC which gradually increased in the first 20 days, before it dropped off due to acetate depletion. The pYYDT-C5 strain generated the highest voltage at 0.044 ± 0.003 V, with the WT came second with 0.033 ± 0.002 V and ΔBFE producing the lowest voltage at 0.019 ± 0.003 V (Fig. 5.3a). This indicates that the deletion of FAD transport gene in ΔBFE mutant – disabling the flavin excretion for EET, has resulted in drop of voltage generation by ~42%. The consumption of acetate in the liquor was confirmed by gas chromatography. After 5 days, 13.0 ± 2.8 mg/L of acetate had been consumed by pYYDT-C5, 16.2 ± 4.1 mg/L by WT and 23.3 ± 2.9 mg/L by ΔBFE respectively (Fig. 5.3b). Changes in concentration of other VFAs present in the liquor

were too small to be detected. The optical density of the anodic culture in the MFC systems were also measured. The ΔBFE MFC had the highest biomass (Day 5; OD_{600} 0.042 ± 0.009) vs. 0.019 ± 0.006 for pYYDT-C5 and 0.022 ± 0.003 for WT, despite generating less electricity (Fig. 5.3c).

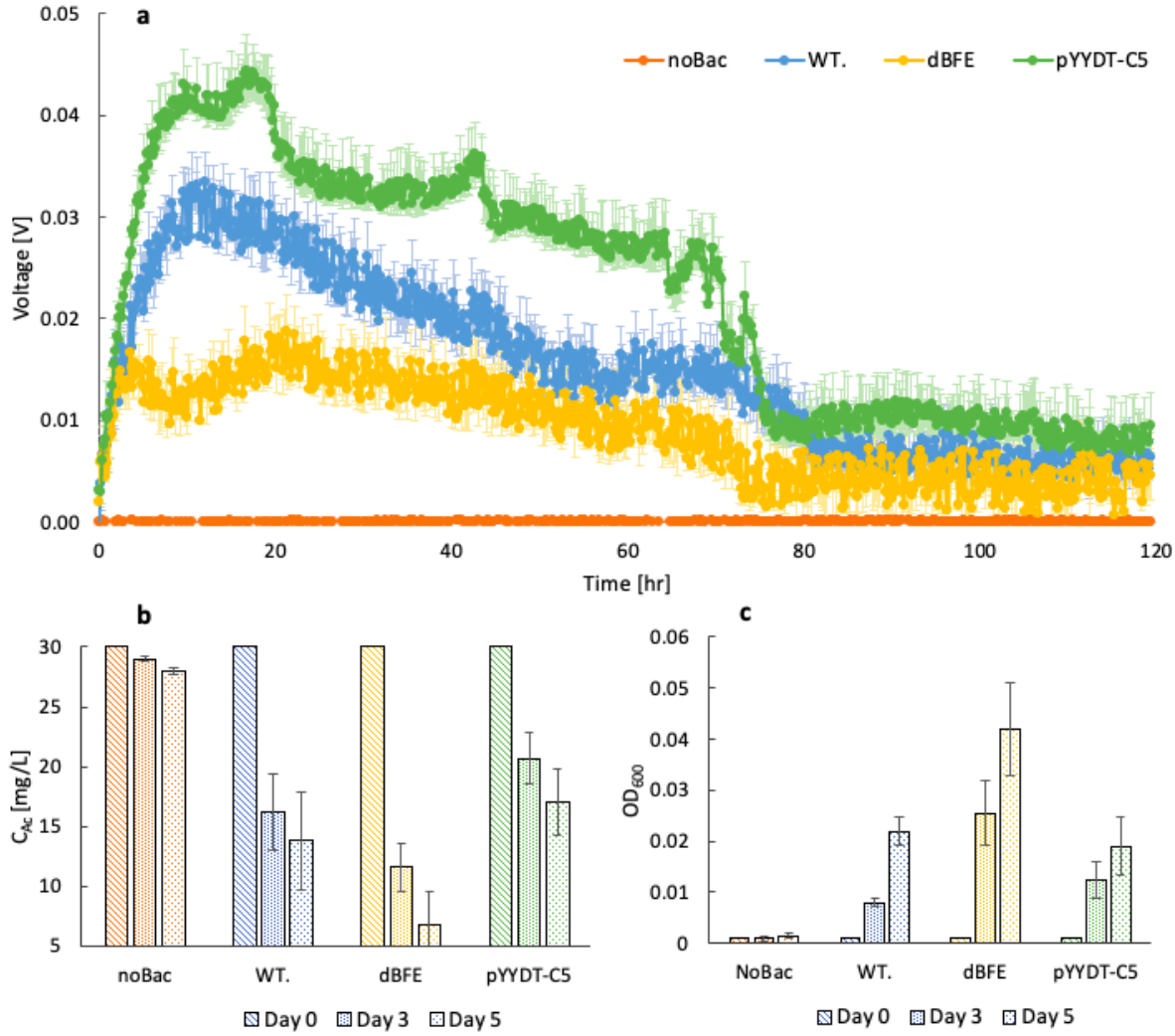

Fig. 5.3: a) Voltage of MFC systems fed with AD liquor across 1kΩ resistor for 5 days, all systems were injected with 1.1 mL AD liquor to achieve initial acetate concentration of 30 mg/L inside the reactors. Wild-type strain (blue) reached a voltage of 0.033 ± 0.002 V, consistent with acetate-fed MFC result (fig. 4.2); *pYYDT-C5* strain (green), *dBFE* (yellow) and negative control *No Bac* (orange); b) Concentration of acetate inside MFC reactors at day 0, 3 and 5. Acetate concentration in *no Bac* reactors remained unchanged; c) optical density of anodic culture at day 0, 3 and 5. dBFE gave the highest cell growth of (OD_{600} 0.042 ± 0.009). This showed that in strain lacking capabilities to produce electron carriers, acetate was predominantly used for cell growth over electricity production. Error bars/region represent standard error of triplicate measurements.

As ΔBFE is unable to pump out riboflavin to produce electricity, the energy was predominately used for biomass. This indicates that more carbon source was used for cell replication and less for electricity generation by *Shewanella oneidensis* MR1. This observation further emphasises the need of electron transporter genes in *Shewanella* spp. for electricity production optimisation. The resulting coulombic efficiencies were 10.7% for WT, 19.7% for pYYDT-C5 and 4.4% for ΔBFE. This result is consistent to our recent report [329], where riboflavin was demonstrated to enhance electricity production in *Shewanella oneidensis* MR1.

5.3.4. SEM Images

At the end of the experiment, the anodic electrode was collected, and the images were taken using Scanning Electron Microscope (SEM). The bacterial cells were seen attached on the carbon fibres of the anode (Fig. 5.4a), with thick biofilm found at some areas of the electrode surface (Fig. 5.4b). The image of planktonic *S.oneidensis* MR-1 is shown in Fig. 5.4c.

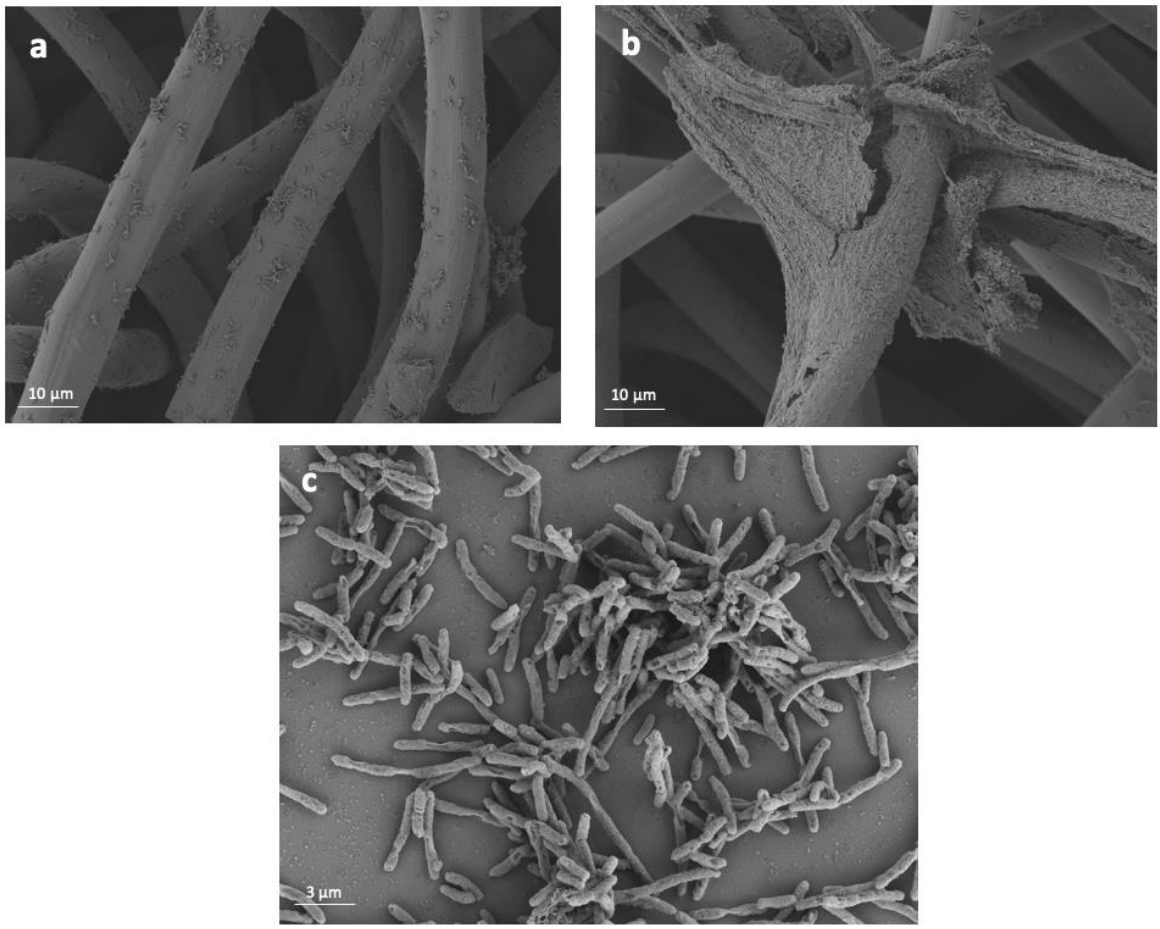

Fig. 5.4: a) Scanning Electron Microscope (SEM) image of *Shewanella oneidensis* MR-1 biofilm on carbon cloth electrode; b) thick biofilm was found at some parts of the electrode surface; c) planktonic *S. oneidensis* isolated from the anodic media.

5.4. Conclusion

This is the first reported case of acetate utilisation to generate electric current in lactate-fed microbial fuel cell (MFC) and anaerobic digester (AD) liquor using pure cultures of *Shewanella oneidensis* MR-1. Double-compartment MFCs were used in this study with carbon cloth acting as electrode materials. Sodium lactate 20 mM was fed into the reactors in batch mode, and the polarisation curve through variable resistance experiment was constructed. Towards the end of lactate utilisation, the reaction taking place inside the anodic chamber switched to acetate oxidation, resulting in lower voltage generation. Acetate consumption was confirmed by detection of breakdown metabolites using High Performance

Liquid Chromatography (HPLC). SEM images were also taken to confirm the formation of biofilm in the MFC reactors.

To confirm utilisation of acetate by the MR-1 strain, subsequent MFC system experiments were performed with acetate as the sole carbon source. Here, 20 mM sodium acetate was fed in batch mode into fresh MFC reactors and inoculated with MR-1 strain sampled from the lactate-fed MFC at its end-stage. A voltage of 0.032 ± 0.011 V was achieved via acetate oxidation after two days when 1 kΩ resistor was used to represent the load. The performance of the acetate-fed MFC was investigated and compared to two negative controls, neither of which generated any significant current. The optical density (OD_{600}) of the media in anodic compartment also increased throughout the experiment, indicating growth of bacterial cells. These observations confirmed that the oxidation of acetate by *S. oneidensis* and supported cell growth under anaerobic condition resulting in the generation of current.

The study was further pushed towards a more realistic industrial application. Real anaerobic digester liquor, which contained mostly acetate (C_{Ac} = 30 mg/L) with other volatile acids in trace amount, was used to generate electricity in the same MFC setup. A current density of 3.67 ± 0.22 μA/cm^2 was generated with pure-culture *S. oneidensis* MR-1 as the biocatalyst, with its pYYDT-C5 mutant strain counterpart delivering 4.89 ± 0.34 μA/cm^2 (33% higher). Energy and mass balance confirmed the utilisation of acetate in the AD liquor as both carbon and energy source for *S. oneidensis* in a microbial fuel cell setup. The obtained coulombic efficiencies were 10.7% for WT, 19.7% for pYYDT-C5 and 4.4% for ΔBFE respectively. To the best of our knowledge, this is the first reported study of AD liquor utilization by pure culture *S. oneidensis* to degrade the acetate content within the liquor for electricity generation.

Further studies such as operation of fuel cell in potentiostatic mode would enable a more controlled experiment and internal resistance determination via electrochemical impedance

spectroscopy (EIS) might provide further insights into source of losses and the bottleneck of optimisation effort. Nonetheless, this study has opened the possibility of new carbon source options for electricity generation using *S. oneidensis* in microbial fuel cell. Historically, despite of all of its advantages, one key limitation of *S. oneidensis* that prevents its vast application in industrial applications was its "pickiness" of carbon sources that it can utilize under anaerobic condition. Through this study, we have pushed further the on-going research of acetate utilization by pure culture *S. oneidensis* – using real AD effluent as source of acetate for electricity generation. Moreover, we have also successfully demonstrated the ability of increasing electricity generations capability of *S. oneidensis* via genetic modification. Moving forward, this study can act as a foundation of more studies on pure culture *S. oneindeisis* to degrade acetate-based real industrial wastewater, enabling more straightforward optimization efforts compared to using mixed-culture that is naturally available in the wastewater e.g., activated sludge, whose exact biology and mechanisms are still poorly understood till this day.

Chapter 6: Conclusion, limitations, and future directions

6.1. Conclusion

The research undertaken in this study has expanded the understanding and application of microbial fuel cell as wastewater treatment technology as well as one for energy generation. The following conclusions can be drawn from this DPhil thesis:

- Determination of flavin-mediated electron transfer as the most dominant Extracellular Electron Transfer (EET) mechanism for *S. oneidensis* MR-1. The results of this research confirm that electron transfer via mediator contributed towards 70% of power output, and genetic engineering of cells to include additional flavin-production gene from *B. subtilis* increased the power output by over two-fold.
- First reported case of the transfer of flavin-overexpression genes into the cell using ultrasound in microbial fuel cell setup. This study has also demonstrated a significant scale-up to ultrasound gene transfer technology – with working volume of 300 mL, providing ~150X scale-up than those previously reported elsewhere [379], [380].
- Demonstration of the ability of *S. oneidensis* MR-1 to utilise acetate as sole carbon and energy source in an MFC setup. A voltage of 0.032 ± 0.011 V was generated across 1kΩ resistor with 20 mM sodium acetate as the sole carbon source, with maximum power output that reached 1.2 ± 0.1 mW/m^2.
- Utilisation of anaerobic digester (AD) liquor as source of acetate for electricity generation by *S. oneidensis* – with 16.2 ± 4.1 mg/L of acetate content consumed within 5 days, resulting in ~11% coulombic efficiency.
- Selective biofilm formation on anode surface favouring *electrigen* species *S. oneindensis* in MFC system containing *E. coli* – *S. oneindensis* consortium, via

deployment of silica-coated iron-oxide nanoparticles (ION). The biofilm composition was found to have shifted towards a community predominated by MR-1 strains, reaching 38.3 ± 7.0% of MR-1 population, compared to 7.4 ± 4.2% in the control where the nanoparticles were not present. A voltage of ~40 mV was achieved using *E. coli* – *S. oneindensis* MR-1 consortium to degrade glucose, with maximum power production of 39.8 ± 2.4 mW/m^2.

6.2. Limitations

The research presented in this thesis makes significant contributions to several fields in fuel cells, gene modification and delivery, biofilm and nanotechnology. Despite these achievements, there were several limitations to the study which had been contributed by several factors, both methodological and circumstantial – one interlinked with another. Methodological limitations were mainly driven by the unavailability of necessary equipment to conduct complementary analysis such as 1) EDX spectroscopy to confirm the presence of iron core NPs which was bio-synthesised by *S. oneidensis*; 2) electrochemical impedance spectroscopy (EIS) to measure the internal resistance of MFC reactors; and 3) confocal laser scanning microscope (CLSM) to allow for 3D imaging (z-stack) and thickness measurement of biofilms. This set of equipment might have been available at different research groups; however, scheduling challenges and lack of suitable operators prevented us from proceeding with renting such equipment. These challenges were made worse by COVID-19 pandemic, where most labs were closed for a prolonged period in 2020. Even when re-opened, lab access was fairly restricted which added further unexpected challenges and delays to our research. Works that involved people collaboration (e.g., using shared equipment at other departments) were made impossible, as health and safety of personnel must be put as priority.

Nonetheless, despite the unprecedented challenges, these results have provided a substantial foundation for future projects and continuation of the works in the field.

6.3. Future directions

In the future, we believe that the application of MFC would not only be limited to wastewater treatment but become integrated with other technologies such as biosensory systems, anaerobic digester as well as energy storage and chemical productions. Moving forward, we see more of such studies to be conducted – which are made possible through better understanding of the science and underlying mechanisms. It is well known that the biggest opportunities for improvements for MFC lie within the advancement of electrode materials towards cheaper, more biocompatible and higher effective surface area which promote better biofilm attachment [432]–[434], and further understanding of the biology within bacteria consortium that is often very complex [56], [435] – coupled with genetic engineering and modifications to implement capabilities across multi species for complex substrate degradation and enhanced electricity generation capabilities [117], [230], [436]. This study has contributed to some of these areas, although further studies and development are still required to reach our target end-state.

The successful demonstration of *in-situ* gene transfer via ultrasound achieved in this study has opened new windows of opportunities for genetic engineering in MFC systems. Previously, any genetic modifications were done prior to operations, which create almost impossible hurdles when it comes to applying to real wastewater treatment plants. With the possibility of *in-situ* modifications, the situation has been completely changed. In order to make sure that this could be done in industrial cases, the results of our findings need to be further validated in larger scale experiments – towards reactor sizes in the order of litres. Furthermore, further studies on the effect of ultrasound parameters, such as frequency, power

and selection pressure would be crucial for optimization efforts – to enhance key performance outputs such as plasmid transfer / transformation efficiency and transformed cell viability. Use of different genes and bacterial species such as *Geobacter* would also be important to expand the current application. *Geobacter*, being one of the most efficient known wild-type electrigens [437], [438], require direct contact with electrode in order to pass electrons. The addition of genes responsible for stronger / more enriched biofilm formation, could potentially enhance its capabilities to generate more energy in MFC systems. An example of such genes are Plasmid pYedQ2, encodes *yedQ* gene from *E.coli* which is responsible for the formation of c-di-GMP [169]. The insertion of this plasmid can increase the production of cytoplasmic c-di-GMP, resulting in increased biofilm formation.

Although the study on the utilisation of acetate in AD liquor by pure culture *S. oneidensis* MR-1 to generate electricity has generated new optimism in respect to the technology, we are also aware that further validations are required. Moving forward, it would beneficial to test similar systems using different electron acceptors in the cathodic chamber (other than oxygen / air) – not only to validate whether selection of final electron acceptors is the source of contradictive findings by different researchers, but also to expand our understanding on the implications of electron acceptor selections towards overall acetate-fed MFC performance. Furthermore, more studies on different acetate sources from other industrial / municipal wastes would also be important to understand the full potential of *S. oneidensis* MFC in industrial applications – considering the abundance of acetate in industrial wastewaters. Finally, comparison with other pure culture electrigens on acetate utilisation from AD liquor would also be beneficial, to further understand its comparative performance and what further optimisations are required to allow for maximum potential to be achieved.

Moving forwards, we will see nanotechnology being the “go-to” solutions to many real-life challenges, including medical, energy and climate change. We have shown the use of Iron-

Oxide Nanoparticles (ION) as viable solutions to engineer biofilm formation, but other nanoparticles also need to be trialled as comparisons. Possible nanoparticles to be trialled include gold-based [439], silver-based [440], or other iron-based species (e.g., $NaFeO_2$ core) [441]. Furthermore, use of different bacterial strains, and preferably in a larger scale, would further validate its importance and significance in bringing real improvement to MFC system. Our findings of silica coating as protective layer to prevent iron core reductions also need to be further tested and optimized. Its effect on mass transfer and electrical conductivity of the system needs to be further understood – through testing of different thickness and/or Si:Fe ratio. This would enable better optimization efforts – to find the optimum thickness and/or structure for best trade-off between iron core reduction prevention and minimizing any negative effects on implied conductivity and mass transfer kinetics.

References

[1] IBISWorld, “Sewage in the UK - Market Research Report 2022,” *https://www.ibisworld.com/united-kingdom/market-research-reports/sewerage-industry/*, Mar. 30, 2022.

[2] M. Gandiglio, A. Lanzini, A. Soto, P. Leone, and M. Santarelli, “Enhancing the energy efficiency of wastewater treatment plants through co-digestion and fuel cell systems,” *Front Environ Sci*, vol. 5, p. 70, 2017.

[3] M. Maktabifard, E. Zaborowska, and J. Makinia, “Achieving energy neutrality in wastewater treatment plants through energy savings and enhancing renewable energy production,” *Rev Environ Sci Biotechnol*, vol. 17, no. 4, pp. 655–689, 2018.

[4] H. Gao, Y. D. Scherson, and G. F. Wells, “Towards energy neutral wastewater treatment: methodology and state of the art,” *Environ Sci Process Impacts*, vol. 16, no. 6, pp. 1223–1246, 2014.

[5] A. Whiting and A. Azapagic, “Life cycle environmental impacts of generating electricity and heat from biogas produced by anaerobic digestion,” *Energy*, vol. 70, pp. 181–193, 2014.

[6] N. Bachmann, J. la Cour Jansen, G. Bochmann, and N. Montpart, *Sustainable biogas production in municipal wastewater treatment plants*. IEA Bioenergy Massongex, Switzerland, 2015.

[7] S. Lee, I. J. Esfahani, P. Ifaei, W. Moya, and C. Yoo, “Thermo-environ-economic modeling and optimization of an integrated wastewater treatment plant with a combined heat and power generation system,” *Energy Convers Manag*, vol. 142, pp. 385–401, 2017.

[8] G. S. Cerveira, C. P. Borges, and F. de Araujo Kronemberger, “Gas permeation applied to biogas upgrading using cellulose acetate and polydimethylsiloxane membranes,” *J Clean Prod*, vol. 187, pp. 830–838, 2018.

[9] L. Lin, R. Li, Y. Li, J. Xu, and X. Li, “Recovery of organic carbon and phosphorus from wastewater by Fe-enhanced primary sedimentation and sludge fermentation,” *Process Biochemistry*, vol. 54, pp. 135–139, 2017.

[10] L. Lin, R. Li, and X. Li, “Recovery of organic resources from sewage sludge of Al-enhanced primary sedimentation by alkali pretreatment and acidogenic fermentation,” *J Clean Prod*, vol. 172, pp. 3334–3341, 2018.

[11] M. Ayoub, H. Afify, and A. Abdelfattah, “Chemically enhanced primary treatment of sewage using the recovered alum from water treatment sludge in a model of hydraulic clari-flocculator,” *Journal of Water Process Engineering*, vol. 19, pp. 133–138, 2017.

[12] G. Kooijman, M. K. de Kreuk, and J. B. van Lier, “Influence of chemically enhanced primary treatment on anaerobic digestion and dewaterability of waste sludge,” *Water Science and Technology*, vol. 76, no. 7, pp. 1629–1639, 2017.

[13] W. P. F. Barber, “Thermal hydrolysis for sewage treatment: a critical review,” *Water Res*, vol. 104, pp. 53–71, 2016.

[14] W. Wei *et al.*, “Free nitrous acid pre-treatment of waste activated sludge enhances volatile solids destruction and improves sludge dewaterability in continuous anaerobic digestion,” *Water Res*, vol. 130, pp. 13–19, 2018.

[15] M. C. Potter, “Electrical effects accompanying the decomposition of organic compounds,” *Proceedings of the royal society of London. Series b, containing papers of a biological character*, vol. 84, no. 571, pp. 260–276, 1911.

[16] B. Cohen, “The bacterial culture as an electrical half-cell,” *J. Bacteriol*, vol. 21, no. 1, pp. 18–19, 1931.

[17] I. Karube, T. Matsunaga, S. Tsuru, and S. Suzuki, “Continous hydrogen production by immobilized whole cells of Clostridium butyricum,” *Biochimica et Biophysica Acta (BBA)-General Subjects*, vol. 444, no. 2, pp. 338–343, 1976.
[18] H. P. Bennetto, “Electricity generation by microorganisms,” *Biotechnology education*, vol. 1, no. 4, pp. 163–168, 1990.
[19] N. Mokhtarian, M. Ghasemi, W. R. Wan Daud, M. Ismail, G. Najafpour, and J. Alam, “Improvement of microbial fuel cell performance by using nafion polyaniline composite membranes as a separator,” *J Fuel Cell Sci Technol*, vol. 10, no. 4, 2013.
[20] B. E. Logan *et al.*, “Microbial fuel cells: methodology and technology,” *Environ Sci Technol*, vol. 40, no. 17, pp. 5181–5192, 2006.
[21] S. J. Cooper, A. G. Gunner, G. Hoogers, and D. Thompsett, “Reformate tolerance in proton exchange membrane fuel cells: electrocatalyst solutions,” 1997.
[22] Q. Lu, X. Zou, and Y. Bu, “Introduction to Zinc–Air Batteries,” *Zinc-Air Batteries: Introduction, Design Principles, and Emerging Technologies*, 2022.
[23] S. Cheng, H. Liu, and B. E. Logan, “Increased power generation in a continuous flow MFC with advective flow through the porous anode and reduced electrode spacing,” *Environ Sci Technol*, vol. 40, no. 7, pp. 2426–2432, 2006.
[24] P.-Y. Zhang and Z.-L. Liu, “Experimental study of the microbial fuel cell internal resistance,” *J Power Sources*, vol. 195, no. 24, pp. 8013–8018, 2010.
[25] B. E. Logan *et al.*, “Impact of ohmic resistance on measured electrode potentials and maximum power production in microbial fuel cells,” *Environ Sci Technol*, vol. 52, no. 15, pp. 8977–8985, 2018.
[26] T. Mbarire, O. Aloys, and B. Chaka, “Investigating the ohmic behavior of mediator-less microbial fuel cells using sewerage water as the bio-anode,” *Cogent Eng*, vol. 9, no. 1, p. 2079222, 2022.
[27] B. G. Lusk, I. Peraza, G. Albal, A. K. Marcus, S. C. Popat, and C. I. Torres, “pH dependency in anode biofilms of Thermincola ferriacetica suggests a proton-dependent electrochemical response,” *J Am Chem Soc*, vol. 140, no. 16, pp. 5527–5534, 2018.
[28] Z. Du, H. Li, and T. Gu, “A state of the art review on microbial fuel cells: a promising technology for wastewater treatment and bioenergy,” *Biotechnol Adv*, vol. 25, no. 5, pp. 464–482, 2007.
[29] H. Rismani-Yazdi, S. M. Carver, A. D. Christy, and O. H. Tuovinen, “Cathodic limitations in microbial fuel cells: an overview,” *J Power Sources*, vol. 180, no. 2, pp. 683–694, 2008.
[30] M. M. Ghangrekar, A. Dhanda, S. M. Sathe, and I. Chakraborty, “Enhancing microbial fuel cell performance by carbon nitride-based nanocomposites,” in *Nanostructured Carbon Nitrides for Sustainable Energy and Environmental Applications*, Elsevier, 2022, pp. 63–79.
[31] K.-W. Park and S.-E. Oh, “Measurement of activation and ohmic losses using a current interruption technique in a microbial fuel cell,” *Journal of Korean Society of Environmental Engineers*, vol. 32, no. 4, pp. 357–362, 2010.
[32] M. Sabri, N. A. Shamsuddin, M. F. A. Alias, H. A. Tajaruddin, and M. M. Z. Makhtar, “Assessment of Power Generation from Dewatered Sludge using Membrane-Less Microbial Fuel Cell,” in *IOP Conference Series: Earth and Environmental Science*, 2021, vol. 765, no. 1, p. 012060.
[33] S. Oh, B. Min, and B. E. Logan, “Cathode performance as a factor in electricity generation in microbial fuel cells,” *Environ Sci Technol*, vol. 38, no. 18, pp. 4900–4904, 2004.
[34] L. Rago *et al.*, “Influences of dissolved oxygen concentration on biocathodic microbial communities in microbial fuel cells,” *Bioelectrochemistry*, vol. 116, pp. 39–51, 2017.

[35] S. Mateo, M. Rodrigo, L. P. Fonseca, P. Cañizares, and F. J. Fernandez-Morales, "Oxygen availability effect on the performance of air-breathing cathode microbial fuel cell," *Biotechnol Prog*, vol. 31, no. 4, pp. 900–907, 2015.
[36] I. Ieropoulos, J. Winfield, and J. Greenman, "Effects of flow-rate, inoculum and time on the internal resistance of microbial fuel cells," *Bioresour Technol*, vol. 101, no. 10, pp. 3520–3525, 2010.
[37] S. Potrykus, S. Mateo, J. Nieznański, and F. J. Fernández-Morales, "The Influent Effects of Flow Rate Profile on the Performance of Microbial Fuel Cells Model," *Energies (Basel)*, vol. 13, no. 18, p. 4735, 2020.
[38] L. Tang, X. Li, Y. Zhao, F. Fu, Y. Ren, and X. Wang, "Effect of stirring rates in anodic area of sediment microbial fuel cell on its power generation," *Energy Sources, Part A: Recovery, Utilization, and Environmental Effects*, vol. 39, no. 1, pp. 23–28, 2017.
[39] Q. Feng *et al.*, "Enhancing the anode performance of microbial fuel cells in the treatment of oil-based drill sludge by adjusting the stirring rate and supplementing oil-based drill cuttings," *Sustain Energy Fuels*, vol. 5, no. 22, pp. 5773–5788, 2021.
[40] U. Schröder, "Anodic electron transfer mechanisms in microbial fuel cells and their energy efficiency," *Physical Chemistry Chemical Physics*, vol. 9, no. 21, pp. 2619–2629, 2007.
[41] H. Lin, S. Wu, and J. Zhu, "Modeling power generation and energy efficiencies in air-cathode microbial fuel cells based on Freter equations," *Applied Sciences*, vol. 8, no. 10, p. 1983, 2018.
[42] L. Alvarez-Benítez, S. Silva-Martínez, A. Hernandez-Perez, S. K. Kamaraj, S. Z. Abbas, and A. Alvarez-Gallegos, "Quantification of Internal Resistance Contributions of Sediment Microbial Fuel Cells Using Petroleum-Contaminated Sediment Enriched with Kerosene," *Catalysts*, vol. 12, no. 8, p. 871, 2022.
[43] V. F. Passos, S. Aquino Neto, A. R. de Andrade, and V. Reginatto, "Energy generation in a Microbial Fuel Cell using anaerobic sludge from a wastewater treatment plant," *Sci Agric*, vol. 73, pp. 424–428, 2016.
[44] W. Chen, Z. Liu, Y. Li, X. Xing, Q. Liao, and X. Zhu, "Improved electricity generation, coulombic efficiency and microbial community structure of microbial fuel cells using sodium citrate as an effective additive," *J Power Sources*, vol. 482, p. 228947, 2021.
[45] A. Parkash, "Microbial fuel cells: a source of bioenergy," *J Microb Biochem Technol*, vol. 8, no. 3, pp. 247–255, 2016.
[46] M. Chen *et al.*, "Facilitated extracellular electron transfer of Geobacter sulfurreducens biofilm with in situ formed gold nanoparticles," *Biosens Bioelectron*, vol. 108, pp. 20–26, 2018.
[47] Y.-J. Qiao, Y. Qiao, L. Zou, X.-S. Wu, and J.-H. Liu, "Biofilm promoted current generation of Pseudomonas aeruginosa microbial fuel cell via improving the interfacial redox reaction of phenazines," *Bioelectrochemistry*, vol. 117, pp. 34–39, 2017.
[48] I. Ulusoy and A. Dimoglo, "Electricity generation in microbial fuel cell systems with Thiobacillus ferrooxidans as the cathode microorganism," *Int J Hydrogen Energy*, vol. 43, no. 2, pp. 1171–1178, 2018.
[49] L.-X. You *et al.*, "Flavins mediate extracellular electron transfer in Gram-positive Bacillus megaterium strain LLD-1," *Bioelectrochemistry*, vol. 119, pp. 196–202, 2018.
[50] H. Liu, R. Ramnarayanan, and B. E. Logan, "Production of electricity during wastewater treatment using a single chamber microbial fuel cell," *Environ Sci Technol*, vol. 38, no. 7, pp. 2281–2285, 2004.

[51] H. Liu and B. E. Logan, “Electricity generation using an air-cathode single chamber microbial fuel cell in the presence and absence of a proton exchange membrane,” *Environ Sci Technol*, vol. 38, no. 14, pp. 4040–4046, 2004.
[52] S. Ou, Y. Zhao, D. S. Aaron, J. M. Regan, and M. M. Mench, “Modeling and validation of single-chamber microbial fuel cell cathode biofilm growth and response to oxidant gas composition,” *J Power Sources*, vol. 328, pp. 385–396, 2016.
[53] C. Sato, N. E. Paucar, S. Chiu, M. Z. I. M. Mahmud, and J. Dudgeon, “Single-Chamber Microbial Fuel Cell with Multiple Plates of Bamboo Charcoal Anode: Performance Evaluation,” *Processes*, vol. 9, no. 12, p. 2194, 2021.
[54] N. Saravanan and M. Karthikeyan, “Study of single chamber and double chamber efficiency and losses of wastewater treatment,” *Int Res J Eng Technol*, vol. 5, pp. 1225–1230, 2018.
[55] R. Jinisha, J. J. Regin, and J. Maheswaran, “A review on the emergence of single-chamber microbial fuel cell on wastewater treatment,” in *IOP Conference Series: Materials Science and Engineering*, 2020, vol. 983, no. 1, p. 012002.
[56] M. Li *et al.*, “Microbial fuel cell (MFC) power performance improvement through enhanced microbial electrogenicity,” *Biotechnol Adv*, vol. 36, no. 4, pp. 1316–1327, 2018.
[57] H. E. Braustein, “Microbial tango with Shewanella Oneidensis: Design elements and application of a novel renewable energy source using wastewater containing organic compounds,” *ECS Trans*, vol. 41, no. 31, p. 9, 2012.
[58] D. H. Park and J. G. Zeikus, “Improved fuel cell and electrode designs for producing electricity from microbial degradation,” *Biotechnol Bioeng*, vol. 81, no. 3, pp. 348–355, 2003.
[59] J. K. Jang *et al.*, “Construction and operation of a novel mediator-and membrane-less microbial fuel cell,” *Process biochemistry*, vol. 39, no. 8, pp. 1007–1012, 2004.
[60] S. Narayanasamy and J. Jayaprakash, “Carbon cloth/nickel cobaltite (NiCo2O4)/polyaniline (PANI) composite electrodes: Preparation, characterization, and application in microbial fuel cells,” *Fuel*, vol. 301, p. 121016, 2021.
[61] M. Aghababaie, M. Farhadian, A. Jeihanipour, and D. Biria, “Effective factors on the performance of microbial fuel cells in wastewater treatment–a review,” *Environmental Technology Reviews*, vol. 4, no. 1, pp. 71–89, 2015.
[62] J. V. Boas, V. B. Oliveira, M. Simões, and A. M. F. R. Pinto, “Review on microbial fuel cells applications, developments and costs,” *J Environ Manage*, vol. 307, p. 114525, 2022.
[63] J. M. Sonawane, A. Yadav, P. C. Ghosh, and S. B. Adeloju, “Recent advances in the development and utilization of modern anode materials for high performance microbial fuel cells,” *Biosens Bioelectron*, vol. 90, pp. 558–576, 2017.
[64] Y. Liu, F. Harnisch, K. Fricke, U. Schröder, V. Climent, and J. M. Feliu, “The study of electrochemically active microbial biofilms on different carbon-based anode materials in microbial fuel cells,” *Biosens Bioelectron*, vol. 25, no. 9, pp. 2167–2171, 2010.
[65] J. Wei, P. Liang, and X. Huang, “Recent progress in electrodes for microbial fuel cells,” *Bioresour Technol*, vol. 102, no. 20, pp. 9335–9344, 2011.
[66] S.-J. Huang *et al.*, “Modification of carbon based cathode electrode in a batch-type microbial fuel cells,” *Biomass Bioenergy*, vol. 145, p. 105972, 2021.
[67] P. Gupta, K. Pandey, and N. Verma, “Improved oxygen reduction and simultaneous glyphosate degradation over iron phthalocyanine and reduced graphene oxide–dispersed activated carbon fiber electrodes in a microbial fuel cell,” *J Power Sources*, vol. 514, p. 230592, 2021.

[68] T. Krieg, A. Sydow, U. Schröder, J. Schrader, and D. Holtmann, “Reactor concepts for bioelectrochemical syntheses and energy conversion,” *Trends Biotechnol*, vol. 32, no. 12, pp. 645–655, 2014.
[69] Y. Liang *et al.*, “Enhancement of anodic biofilm formation and current output in microbial fuel cells by composite modification of stainless steel electrodes,” *J Power Sources*, vol. 342, pp. 98–104, 2017.
[70] J. Xia *et al.*, “High-performance anode material based on S and N co-doped graphene/iron carbide nanocomposite for microbial fuel cells,” *J Power Sources*, vol. 512, p. 230482, 2021.
[71] R. C. O. Tang *et al.*, “Review on design factors of microbial fuel cells using Buckingham’s Pi Theorem,” *Renewable and Sustainable Energy Reviews*, vol. 130, p. 109878, 2020.
[72] L. Yang, A. Wang, Q. Wen, and Y. Chen, “Modified cobalt-manganese oxide-coated carbon felt anodes: an available method to improve the performance of microbial fuel cells,” *Bioprocess Biosyst Eng*, vol. 44, no. 12, pp. 2615–2625, 2021.
[73] K. Tahir *et al.*, “MnCo2O4 coated carbon felt anode for enhanced microbial fuel cell performance,” *Chemosphere*, vol. 265, p. 129098, 2021.
[74] S. Gadkari, S. Gu, and J. Sadhukhan, “Towards automated design of bioelectrochemical systems: A comprehensive review of mathematical models,” *Chemical Engineering Journal*, vol. 343, pp. 303–316, 2018.
[75] A. A. Yaqoob, M. N. M. Ibrahim, and S. Rodríguez-Couto, “Development and modification of materials to build cost-effective anodes for microbial fuel cells (MFCs): An overview,” *Biochem Eng J*, vol. 164, p. 107779, 2020.
[76] J. E. Darnell, “Molecular cell biology,” 1986.
[77] K. Watanabe, “Recent developments in microbial fuel cell technologies for sustainable bioenergy,” *J Biosci Bioeng*, vol. 106, no. 6, pp. 528–536, 2008.
[78] Z. Wang, C. Cao, Y. Zheng, S. Chen, and F. Zhao, “Abiotic oxygen reduction reaction catalysts used in microbial fuel cells,” *ChemElectroChem*, vol. 1, no. 11, pp. 1813–1821, 2014.
[79] Z. Wang, G. D. Mahadevan, Y. Wu, and F. Zhao, “Progress of air-breathing cathode in microbial fuel cells,” *J Power Sources*, vol. 356, pp. 245–255, 2017.
[80] S. G. Peera *et al.*, “A review on carbon and non-precious metal based cathode catalysts in microbial fuel cells,” *Int J Hydrogen Energy*, vol. 46, no. 4, pp. 3056–3089, 2021.
[81] H. Hiegemann *et al.*, “Performance and inorganic fouling of a submergible 255 L prototype microbial fuel cell module during continuous long-term operation with real municipal wastewater under practical conditions,” *Bioresour Technol*, vol. 294, p. 122227, 2019.
[82] H. Wang and Z. J. Ren, “Bioelectrochemical metal recovery from wastewater: a review,” *Water Res*, vol. 66, pp. 219–232, 2014.
[83] L. Dai, Y. Xue, L. Qu, H.-J. Choi, and J.-B. Baek, “Metal-free catalysts for oxygen reduction reaction,” *Chem Rev*, vol. 115, no. 11, pp. 4823–4892, 2015.
[84] X. Zhang, D. Pant, F. Zhang, J. Liu, W. He, and B. E. Logan, “Long-term performance of chemically and physically modified activated carbons in air cathodes of microbial fuel cells,” *ChemElectroChem*, vol. 1, no. 11, pp. 1859–1866, 2014.
[85] X. Zhang, X. Xia, I. Ivanov, X. Huang, and B. E. Logan, “Enhanced activated carbon cathode performance for microbial fuel cell by blending carbon black,” *Environ Sci Technol*, vol. 48, no. 3, pp. 2075–2081, 2014.
[86] C. Tang and Q. Zhang, “Can metal–nitrogen–carbon catalysts satisfy oxygen electrochemistry?,” *J Mater Chem A Mater*, vol. 4, no. 14, pp. 4998–5001, 2016.

[87] C.-T. Wang, Y.-S. Huang, T. Sangeetha, and W.-M. Yan, “Assessment of recirculation batch mode operation in bufferless bio-cathode microbial fuel cells (MFCs),” *Appl Energy*, vol. 209, pp. 120–126, 2018.
[88] M. Elangovan and S. Dharmalingam, “Application of polysulphone based anion exchange membrane electrolyte for improved electricity generation in microbial fuel cell,” *Mater Chem Phys*, vol. 199, pp. 528–536, 2017.
[89] M. Rahimnejad, A. Adhami, S. Darvari, A. Zirepour, and S.-E. Oh, “Microbial fuel cell as new technology for bioelectricity generation: A review,” *Alexandria Engineering Journal*, vol. 54, no. 3, pp. 745–756, 2015.
[90] M. I. Kerwick, S. M. Reddy, A. H. L. Chamberlain, and D. M. Holt, “Electrochemical disinfection, an environmentally acceptable method of drinking water disinfection?,” *Electrochim Acta*, vol. 50, no. 25–26, pp. 5270–5277, 2005.
[91] R. Goswami and V. K. Mishra, “A review of design, operational conditions and applications of microbial fuel cells,” *Biofuels*, vol. 9, no. 2, pp. 203–220, 2018.
[92] F. J. Hernández-Fernández, A. P. de los Ríos, F. Mateo-Ramírez, M. D. Juarez, L. J. Lozano-Blanco, and C. Godínez, “New application of polymer inclusion membrane based on ionic liquids as proton exchange membrane in microbial fuel cell,” *Sep Purif Technol*, vol. 160, pp. 51–58, 2016.
[93] G. Hernández-Flores *et al.*, “Characteristics of a single chamber microbial fuel cell equipped with a low cost membrane,” *Int J Hydrogen Energy*, vol. 40, no. 48, pp. 17380–17387, 2015.
[94] S. L. Holder, C.-H. Lee, and S. R. Popuri, “Simultaneous wastewater treatment and bioelectricity production in microbial fuel cells using cross-linked chitosan-graphene oxide mixed-matrix membranes,” *Environmental Science and Pollution Research*, vol. 24, no. 15, pp. 13782–13796, 2017.
[95] V. Yousefi, D. Mohebbi-Kalhori, and A. Samimi, “Ceramic-based microbial fuel cells (MFCs): A review,” *Int J Hydrogen Energy*, vol. 42, no. 3, pp. 1672–1690, 2017.
[96] U. S. Jayapiriya and S. Goel, “Influence of cellulose separators in coin-sized 3D printed paper-based microbial fuel cells,” *Sustainable Energy Technologies and Assessments*, vol. 47, p. 101535, 2021.
[97] C. Vilela *et al.*, “Poly (4-styrene sulfonic acid)/bacterial cellulose membranes: Electrochemical performance in a single-chamber microbial fuel cell,” *Bioresour Technol Rep*, vol. 9, p. 100376, 2020.
[98] X. C. Abrevaya, N. J. Sacco, M. C. Bonetto, A. Hilding-Ohlsson, and E. Cortón, “Analytical applications of microbial fuel cells. Part I: Biochemical oxygen demand,” *Biosens Bioelectron*, vol. 63, pp. 580–590, 2015.
[99] M. Rahimnejad, G. Bakeri, G. Najafpour, M. Ghasemi, and S.-E. Oh, “A review on the effect of proton exchange membranes in microbial fuel cells,” *Biofuel Research Journal*, vol. 1, no. 1, pp. 7–15, 2014.
[100] J. X. Leong, W. R. W. Daud, M. Ghasemi, K. ben Liew, and M. Ismail, “Ion exchange membranes as separators in microbial fuel cells for bioenergy conversion: a comprehensive review,” *Renewable and Sustainable Energy Reviews*, vol. 28, pp. 575–587, 2013.
[101] H. Wang, J.-D. Park, and Z. J. Ren, “Practical energy harvesting for microbial fuel cells: a review,” *Environ Sci Technol*, vol. 49, no. 6, pp. 3267–3277, 2015.
[102] L. Liu, D.-J. Lee, A. Wang, N. Ren, A. Su, and J.-Y. Lai, “Isolation of Fe (III)-reducing bacterium, Citrobacter sp. LAR-1, for startup of microbial fuel cell,” *Int J Hydrogen Energy*, vol. 41, no. 7, pp. 4498–4503, 2016.

[103] J. Huang, N. Zhu, Y. Cao, Y. Peng, P. Wu, and W. Dong, “Exoelectrogenic bacterium phylogenetically related to Citrobacter freundii, isolated from anodic biofilm of a microbial fuel cell,” *Appl Biochem Biotechnol*, vol. 175, no. 4, pp. 1879–1891, 2015.
[104] W. Li, “Nano-materials as anode electrocatalysts for microbial fuel cells,” *Adv Mater*, vol. 4, pp. 1–3, 2019.
[105] B. Cao *et al.*, “Silver nanoparticles boost charge-extraction efficiency in Shewanella microbial fuel cells,” *Science (1979)*, vol. 373, no. 6561, pp. 1336–1340, 2021.
[106] S. Zhao *et al.*, “Three-dimensional graphene/Pt nanoparticle composites as freestanding anode for enhancing performance of microbial fuel cells,” *Sci Adv*, vol. 1, no. 10, p. e1500372, 2015.
[107] Y.-Z. Wang, Y. Shen, L. Gao, Z.-H. Liao, J.-Z. Sun, and Y.-C. Yong, “Improving the extracellular electron transfer of Shewanella oneidensis MR-1 for enhanced bioelectricity production from biomass hydrolysate,” *RSC Adv*, vol. 7, no. 48, pp. 30488–30494, 2017.
[108] T. Yamashita and H. Yokoyama, “Molybdenum anode: a novel electrode for enhanced power generation in microbial fuel cells, identified via extensive screening of metal electrodes,” *Biotechnol Biofuels*, vol. 11, no. 1, pp. 1–13, 2018.
[109] D. Xing, Y. Zuo, S. Cheng, J. M. Regan, and B. E. Logan, “Electricity generation by Rhodopseudomonas palustris DX-1,” *Environ Sci Technol*, vol. 42, no. 11, pp. 4146–4151, 2008.
[110] Y. Tao *et al.*, “Hierarchically three-dimensional nanofiber based textile with high conductivity and biocompatibility as a microbial fuel cell anode,” *Environ Sci Technol*, vol. 50, no. 14, pp. 7889–7895, 2016.
[111] Y. Cui, N. Rashid, N. Hu, M. S. U. Rehman, and J.-I. Han, “Electricity generation and microalgae cultivation in microbial fuel cell using microalgae-enriched anode and bio-cathode,” *Energy Convers Manag*, vol. 79, pp. 674–680, 2014.
[112] A. P. Borole *et al.*, “Integrating engineering design improvements with exoelectrogen enrichment process to increase power output from microbial fuel cells,” *J Power Sources*, vol. 191, no. 2, pp. 520–527, 2009.
[113] L. I. U. Zhi-Dan, L. Jing, D. U. Zhu-Wei, and H.-R. Li, “Construction of sugar-based microbial fuel cells by dissimilatory metal reduction bacteria,” *Chin J Biotechnol*, vol. 22, no. 1, pp. 131–137, 2006.
[114] N. Ali, M. Anam, S. Yousaf, S. Maleeha, and Z. Bangash, “Characterization of the electric current generation potential of the pseudomonas aeruginosa using glucose, fructose, and sucrose in double chamber microbial fuel cell,” *Iran J Biotechnol*, vol. 15, no. 4, p. 216, 2017.
[115] L. Deng, F. Li, S. Zhou, D. Huang, and J. Ni, “A study of electron-shuttle mechanism in Klebsiella pneumoniae based-microbial fuel cells,” *Chinese Science Bulletin*, vol. 55, no. 1, pp. 99–104, 2010.
[116] K. S. Aiyer, “Synergistic effects in a microbial fuel cell between co-cultures and a photosynthetic alga Chlorella vulgaris improve performance,” *Heliyon*, vol. 7, no. 1, p. e05935, 2021.
[117] Y. Cao *et al.*, “Electricigens in the anode of microbial fuel cells: pure cultures versus mixed communities,” *Microb Cell Fact*, vol. 18, no. 1, pp. 1–14, 2019.
[118] B. E. Logan, C. Murano, K. Scott, N. D. Gray, and I. M. Head, “Electricity generation from cysteine in a microbial fuel cell,” *Water Res*, vol. 39, no. 5, pp. 942–952, 2005.
[119] Z. Ren, L. M. Steinberg, and J. M. Regan, “Electricity production and microbial biofilm characterization in cellulose-fed microbial fuel cells,” *Water Science and Technology*, vol. 58, no. 3, pp. 617–622, 2008.

[120] T. Catal, K. Li, H. Bermek, and H. Liu, “Electricity production from twelve monosaccharides using microbial fuel cells,” *J Power Sources*, vol. 175, no. 1, pp. 196–200, 2008.
[121] L. di Palmaa *et al.*, “Experimental assessment of a process including microbial fuel cell for nitrogen removal from digestate of anaerobic treatment of livestock manure and agricultural wastes,” *CHEMICAL ENGINEERING*, vol. 43, 2015.
[122] A. Gurung and S.-E. Oh, “Rice straw as a potential biomass for generation of bioelectrical energy using microbial fuel cells (MFCs),” *Energy Sources, Part A: Recovery, Utilization, and Environmental Effects*, vol. 37, no. 24, pp. 2625–2631, 2015.
[123] Y. Yang *et al.*, “Engineering electrode-attached microbial consortia for high-performance xylose-fed microbial fuel cell,” *ACS Catal*, vol. 5, no. 11, pp. 6937–6945, 2015.
[124] Y. Qu, Y. Feng, X. Wang, and B. E. Logan, “Use of a coculture to enable current production by Geobacter sulfurreducens,” *Appl Environ Microbiol*, vol. 78, no. 9, pp. 3484–3487, 2012.
[125] Z. Ren, T. E. Ward, and J. M. Regan, “Electricity production from cellulose in a microbial fuel cell using a defined binary culture,” *Environ Sci Technol*, vol. 41, no. 13, pp. 4781–4786, 2007.
[126] T. Lin *et al.*, “Synthetic Saccharomyces cerevisiae-Shewanella oneidensis consortium enables glucose-fed high-performance microbial fuel cell,” *AIChE Journal*, vol. 63, no. 6, pp. 1830–1838, 2017.
[127] F. Li, C. Yin, L. Sun, Y. Li, X. Guo, and H. Song, “Synthetic Klebsiella pneumoniae-Shewanella oneidensis consortium enables glycerol-fed high-performance microbial fuel cells,” *Biotechnol J*, vol. 13, no. 5, p. 1700491, 2018.
[128] F. Li *et al.*, “Engineering microbial consortia for high-performance cellulosic hydrolyzates-fed microbial fuel cells,” *Front Microbiol*, vol. 10, p. 409, 2019.
[129] V. B. Wang *et al.*, “Metabolite-enabled mutualistic interaction between Shewanella oneidensis and Escherichia coli in a co-culture using an electrode as electron acceptor,” *Sci Rep*, vol. 5, no. 1, pp. 1–11, 2015.
[130] J. Ren, N. Li, M. Du, Y. Zhang, C. Hao, and R. Hu, “Study on the effect of synergy effect between the mixed cultures on the power generation of microbial fuel cells,” *Bioengineered*, vol. 12, no. 1, pp. 844–854, 2021.
[131] H. Moon, I. S. Chang, and B. H. Kim, “Continuous electricity production from artificial wastewater using a mediator-less microbial fuel cell,” *Bioresour Technol*, vol. 97, no. 4, pp. 621–627, 2006.
[132] F. Oveisi, N. Fallah, and B. Nasernejad, “Biodegradation of synthetic wastewater containing styrene in microbial fuel cell: Effect of adaptation of microbial community,” *Fuel*, vol. 305, p. 121382, 2021.
[133] M. Rahimnejad, G. D. Najafpour, A. A. Ghoreyshi, T. Jafari, and F. Haghparast, “Microbial Fuel Cell a Reliable Source for Recovery of Electrical Power from Synthetic Wastewater,” *Linnaeus Eco-Tech*, pp. 627–635, 2010.
[134] D. R. Lovley, “Bug juice: harvesting electricity with microorganisms,” *Nat Rev Microbiol*, vol. 4, no. 7, pp. 497–508, 2006.
[135] N. R. Glasser, S. H. Saunders, and D. K. Newman, “The colorful world of extracellular electron shuttles,” *Annu Rev Microbiol*, vol. 71, p. 731, 2017.
[136] F. Kracke, I. Vassilev, and J. O. Krömer, “Microbial electron transport and energy conservation–the foundation for optimizing bioelectrochemical systems,” *Front Microbiol*, vol. 6, p. 575, 2015.

[137] C. O. Colpan, I. Dincer, and F. Hamdullahpur, “Portable fuel cells–Fundamentals, technologies and applications,” in *Mini-micro fuel cells*, Springer, 2008, pp. 87–101.
[138] P. Mani, V. T. Fidal Kumar, T. Keshavarz, T. S. Chandra, and G. Kyazze, “The role of natural laccase redox mediators in simultaneous dye decolorization and power production in microbial fuel cells,” *Energies (Basel)*, vol. 11, no. 12, p. 3455, 2018.
[139] H. Liu, S. Cheng, and B. E. Logan, “Production of electricity from acetate or butyrate using a single-chamber microbial fuel cell,” *Environ Sci Technol*, vol. 39, no. 2, pp. 658–662, 2005.
[140] E. D. Brutinel and J. A. Gralnick, “Shuttling happens: soluble flavin mediators of extracellular electron transfer in Shewanella,” *Appl Microbiol Biotechnol*, vol. 93, no. 1, pp. 41–48, 2012.
[141] B. Conley and J. Gralnick, “Anaerobic Bacteria: Solving a shuttle mystery,” *Elife*, vol. 8, p. e49831, 2019.
[142] K. P. Nevin and D. R. Lovley, “Mechanisms for accessing insoluble Fe (III) oxide during dissimilatory Fe (III) reduction by Geothrix fermentans,” *Appl Environ Microbiol*, vol. 68, no. 5, pp. 2294–2299, 2002.
[143] K. Rabaey, N. Boon, S. D. Siciliano, M. Verhaege, and W. Verstraete, “Biofuel cells select for microbial consortia that self-mediate electron transfer,” *Appl Environ Microbiol*, vol. 70, no. 9, pp. 5373–5382, 2004.
[144] R. Mahadevan *et al.*, “Characterization of metabolism in the Fe (III)-reducing organism Geobacter sulfurreducens by constraint-based modeling,” *Appl Environ Microbiol*, vol. 72, no. 2, pp. 1558–1568, 2006.
[145] Y. A. Gorby *et al.*, “Electrically conductive bacterial nanowires produced by Shewanella oneidensis strain MR-1 and other microorganisms,” *Proceedings of the National Academy of Sciences*, vol. 103, no. 30, pp. 11358–11363, 2006.
[146] L. Shi, T. C. Squier, J. M. Zachara, and J. K. Fredrickson, “Respiration of metal (hydr) oxides by Shewanella and Geobacter: a key role for multihaem c-type cytochromes,” *Mol Microbiol*, vol. 65, no. 1, pp. 12–20, 2007.
[147] A. E. Franks, K. P. Nevin, R. H. Glaven, and D. R. Lovley, “Microtoming coupled to microarray analysis to evaluate the spatial metabolic status of Geobacter sulfurreducens biofilms,” *ISME J*, vol. 4, no. 4, pp. 509–519, 2010.
[148] K. C. Wrighton *et al.*, “Evidence for direct electron transfer by a Gram-positive bacterium isolated from a microbial fuel cell,” *Appl Environ Microbiol*, vol. 77, no. 21, pp. 7633–7639, 2011.
[149] W. Khawdas, K. Watanabe, H. Karatani, Y. Aso, T. Tanaka, and H. Ohara, “Direct electron transfer of Cellulomonas fimi and microbial fuel cells fueled by cellulose,” *J Biosci Bioeng*, vol. 128, no. 5, pp. 593–598, 2019.
[150] G. Reguera, “Microbial nanowires and electroactive biofilms,” *FEMS Microbiol Ecol*, vol. 94, no. 7, p. fiy086, 2018.
[151] G. W. Chong, A. A. Karbelkar, and M. Y. El-Naggar, “Nature’s conductors: what can microbial multi-heme cytochromes teach us about electron transport and biological energy conversion?,” *Curr Opin Chem Biol*, vol. 47, pp. 7–17, 2018.
[152] S. Sure, M. L. Ackland, A. A. J. Torriero, A. Adholeya, and M. Kochar, “Microbial nanowires: an electrifying tale,” *Microbiology (N Y)*, vol. 162, no. 12, pp. 2017–2028, 2016.
[153] S. Pirbadian *et al.*, “Shewanella oneidensis MR-1 nanowires are outer membrane and periplasmic extensions of the extracellular electron transport components,” *Proceedings of the National Academy of Sciences*, vol. 111, no. 35, pp. 12883–12888, 2014.

[154] M. Ghasemi *et al.*, "Effect of pre-treatment and biofouling of proton exchange membrane on microbial fuel cell performance," *Int J Hydrogen Energy*, vol. 38, no. 13, pp. 5480–5484, 2013.
[155] A. E. Franks and K. P. Nevin, "Microbial fuel cells, a current review," *Energies (Basel)*, vol. 3, no. 5, pp. 899–919, 2010.
[156] X. Jiang *et al.*, "Probing electron transfer mechanisms in Shewanella oneidensis MR-1 using a nanoelectrode platform and single-cell imaging," *Proceedings of the National Academy of Sciences*, vol. 107, no. 39, pp. 16806–16810, 2010.
[157] S. Kato, "Microbial extracellular electron transfer and its relevance to iron corrosion," *Microb Biotechnol*, vol. 9, no. 2, pp. 141–148, 2016.
[158] A. Kouzuma, T. Kasai, A. Hirose, and K. Watanabe, "Catabolic and regulatory systems in Shewanella oneidensis MR-1 involved in electricity generation in microbial fuel cells," *Front Microbiol*, vol. 6, p. 609, 2015.
[159] D. Coursolle and J. A. Gralnick, "Modularity of the Mtr respiratory pathway of Shewanella oneidensis strain MR-1," *Mol Microbiol*, vol. 77, no. 4, pp. 995–1008, 2010.
[160] G. Reguera, K. P. Nevin, J. S. Nicoll, S. F. Covalla, T. L. Woodard, and D. R. Lovley, "Biofilm and nanowire production leads to increased current in Geobacter sulfurreducens fuel cells," *Appl Environ Microbiol*, vol. 72, no. 11, pp. 7345–7348, 2006.
[161] Y. Zhang *et al.*, "Accelerating anodic biofilms formation and electron transfer in microbial fuel cells: role of anionic biosurfactants and mechanism," *Bioelectrochemistry*, vol. 117, pp. 48–56, 2017.
[162] Z. Yang, H. Pei, Q. Hou, L. Jiang, L. Zhang, and C. Nie, "Algal biofilm-assisted microbial fuel cell to enhance domestic wastewater treatment: nutrient, organics removal and bioenergy production," *Chemical Engineering Journal*, vol. 332, pp. 277–285, 2018.
[163] N. J. Kotloski and J. A. Gralnick, "Flavin electron shuttles dominate extracellular electron transfer by Shewanella oneidensis," *mBio*, vol. 4, no. 1, pp. e00553-12, 2013.
[164] Y. Yang *et al.*, "Enhancing bidirectional electron transfer of Shewanella oneidensis by a synthetic flavin pathway," *ACS Synth Biol*, vol. 4, no. 7, pp. 815–823, 2015.
[165] J. Oram and L. J. C. Jeuken, "A re-evaluation of electron-transfer mechanisms in microbial electrochemistry: Shewanella releases iron that mediates extracellular electron transfer," *ChemElectroChem*, vol. 3, no. 5, pp. 829–835, 2016.
[166] C. A. Abbas and A. A. Sibirny, "Genetic control of biosynthesis and transport of riboflavin and flavin nucleotides and construction of robust biotechnological producers," *Microbiology and Molecular Biology Reviews*, vol. 75, no. 2, pp. 321–360, 2011.
[167] D. Min *et al.*, "Enhancing extracellular electron transfer of Shewanella oneidensis MR-1 through coupling improved flavin synthesis and metal-reducing conduit for pollutant degradation," *Environ Sci Technol*, vol. 51, no. 9, pp. 5082–5089, 2017.
[168] D.-G. Ha and G. A. O'Toole, "c-di-GMP and its effects on biofilm formation and dispersion: a Pseudomonas aeruginosa review," *Microbiol Spectr*, vol. 3, no. 2, pp. 2–3, 2015.
[169] V. Sanchez-Torres, H. Hu, and T. K. Wood, "GGDEF proteins YeaI, YedQ, and YfiN reduce early biofilm formation and swimming motility in Escherichia coli," *Appl Microbiol Biotechnol*, vol. 90, no. 2, pp. 651–658, 2011.
[170] A. Kouzuma, X.-Y. Meng, N. Kimura, K. Hashimoto, and K. Watanabe, "Disruption of the putative cell surface polysaccharide biosynthesis gene SO3177 in Shewanella

oneidensis MR-1 enhances adhesion to electrodes and current generation in microbial fuel cells," *Appl Environ Microbiol*, vol. 76, no. 13, pp. 4151–4157, 2010.
[171] T. Liu *et al.*, "Enhanced Shewanella biofilm promotes bioelectricity generation," *Biotechnol Bioeng*, vol. 112, no. 10, pp. 2051–2059, 2015.
[172] X.-Y. Yong *et al.*, "Enhancement of bioelectricity generation by cofactor manipulation in microbial fuel cell," *Biosens Bioelectron*, vol. 56, pp. 19–25, 2014.
[173] H.-B. Shen *et al.*, "Enhanced bioelectricity generation by improving pyocyanin production and membrane permeability through sophorolipid addition in Pseudomonas aeruginosa-inoculated microbial fuel cells," *Bioresour Technol*, vol. 167, pp. 490–494, 2014.
[174] E. A. Abu *et al.*, "Cyclic voltammetric, fluorescence and biological analysis of purified aeruginosin A, a secreted red pigment of Pseudomonas aeruginosa PAO1," *Microbiology (N Y)*, vol. 159, no. Pt_8, pp. 1736–1747, 2013.
[175] J. Liu, Y. Qiao, Z. S. Lu, H. Song, and C. M. Li, "Enhance electron transfer and performance of microbial fuel cells by perforating the cell membrane," *Electrochem commun*, vol. 15, no. 1, pp. 50–53, 2012.
[176] K. C. Costa, N. R. Glasser, S. J. Conway, and D. K. Newman, "Pyocyanin degradation by a tautomerizing demethylase inhibits Pseudomonas aeruginosa biofilms," *Science (1979)*, vol. 355, no. 6321, pp. 170–173, 2017.
[177] X.-Y. Yong *et al.*, "Enhancement of bioelectricity generation by manipulation of the electron shuttles synthesis pathway in microbial fuel cells," *Bioresour Technol*, vol. 152, pp. 220–224, 2014.
[178] Y.-C. Yong, Y.-Y. Yu, C.-M. Li, J.-J. Zhong, and H. Song, "Bioelectricity enhancement via overexpression of quorum sensing system in Pseudomonas aeruginosa-inoculated microbial fuel cells," *Biosens Bioelectron*, vol. 30, no. 1, pp. 87–92, 2011.
[179] J. Förster, I. Famili, P. Fu, B. Ø. Palsson, and J. Nielsen, "Genome-scale reconstruction of the Saccharomyces cerevisiae metabolic network," *Genome Res*, vol. 13, no. 2, pp. 244–253, 2003.
[180] Y.-C. Yong *et al.*, "Increasing intracellular releasable electrons dramatically enhances bioelectricity output in microbial fuel cells," *Electrochem commun*, vol. 19, pp. 13–16, 2012.
[181] S. Han, X. Gao, H. Ying, and C. C. Zhou, "NADH gene manipulation for advancing bioelectricity in Clostridium ljungdahlii microbial fuel cells," *Green Chemistry*, vol. 18, no. 8, pp. 2473–2478, 2016.
[182] Y. Cao, X. Li, F. Li, and H. Song, "CRISPRi–sRNA: transcriptional–translational regulation of extracellular electron transfer in Shewanella oneidensis," *ACS Synth Biol*, vol. 6, no. 9, pp. 1679–1690, 2017.
[183] Y. Cao *et al.*, "A synthetic plasmid toolkit for Shewanella oneidensis MR-1," *Front Microbiol*, vol. 10, p. 410, 2019.
[184] A. Vellingiri *et al.*, "Overexpression of c-type cytochrome, CymA in Shewanella oneidensis MR-1 for enhanced bioelectricity generation and cell growth in a microbial fuel cell," *Journal of Chemical Technology & Biotechnology*, vol. 94, no. 7, pp. 2115–2122, 2019.
[185] F. Li *et al.*, "Modular engineering intracellular NADH regeneration boosts extracellular electron transfer of Shewanella oneidensis MR-1," *ACS Synth Biol*, vol. 7, no. 3, pp. 885–895, 2018.
[186] F. Li *et al.*, "Modular engineering to increase intracellular NAD (H/+) promotes rate of extracellular electron transfer of Shewanella oneidensis," *Nat Commun*, vol. 9, no. 1, pp. 1–13, 2018.

[187] A. R. Burmeister, “Horizontal gene transfer,” *Evol Med Public Health*, vol. 2015, no. 1, p. 193, 2015.
[188] J. E. Cronan, “Escherichia coli as an experimental organism,” *eLS*, 2014.
[189] J. B. Alderliesten, S. J. N. Duxbury, M. P. Zwart, J. de Visser, A. Stegeman, and E. A. J. Fischer, “Effect of donor-recipient relatedness on the plasmid conjugation frequency: a meta-analysis,” *BMC Microbiol*, vol. 20, no. 1, pp. 1–10, 2020.
[190] A.-J. Wang *et al.*, “Electrochemistry-stimulated environmental bioremediation: Development of applicable modular electrode and system scale-up,” *Environmental Science and Ecotechnology*, vol. 3, p. 100050, 2020.
[191] P. Liang, R. Duan, Y. Jiang, X. Zhang, Y. Qiu, and X. Huang, “One-year operation of 1000-L modularized microbial fuel cell for municipal wastewater treatment,” *Water Res*, vol. 141, pp. 1–8, 2018.
[192] Z. Ge and Z. He, “Long-term performance of a 200 liter modularized microbial fuel cell system treating municipal wastewater: treatment, energy, and cost,” *Environ Sci (Camb)*, vol. 2, no. 2, pp. 274–281, 2016.
[193] R. A. Rozendal, H. V. M. Hamelers, K. Rabaey, J. Keller, and C. J. N. Buisman, “Towards practical implementation of bioelectrochemical wastewater treatment,” *Trends Biotechnol*, vol. 26, no. 8, pp. 450–459, 2008.
[194] J. Prasad and R. K. Tripathi, “Scale-up and control the voltage of sediment microbial fuel cell for charging a cell phone,” *Biosens Bioelectron*, vol. 172, p. 112767, 2021.
[195] X. A. Walter, I. Merino-Jiménez, J. Greenman, and I. Ieropoulos, “PEE POWER® urinal II–Urinal scale-up with microbial fuel cell scale-down for improved lighting,” *J Power Sources*, vol. 392, pp. 150–158, 2018.
[196] W. He *et al.*, “Field tests of cubic-meter scale microbial electrochemical system in a municipal wastewater treatment plant,” *Water Res*, vol. 155, pp. 372–380, 2019.
[197] M. Lu *et al.*, “Long-term performance of a 20-L continuous flow microbial fuel cell for treatment of brewery wastewater,” *J Power Sources*, vol. 356, pp. 274–287, 2017.
[198] T. Tommasi and G. Lombardelli, “Energy sustainability of Microbial Fuel Cell (MFC): A case study,” *J Power Sources*, vol. 356, pp. 438–447, 2017.
[199] W. H. Tan *et al.*, “Microbial fuel cell technology—a critical review on scale-up issues,” *Processes*, vol. 9, no. 6, p. 985, 2021.
[200] I. Ieropoulos, J. Greenman, and C. Melhuish, “Microbial fuel cells based on carbon veil electrodes: stack configuration and scalability,” *Int J Energy Res*, vol. 32, no. 13, pp. 1228–1240, 2008.
[201] X. A. Walter, S. Forbes, J. Greenman, and I. A. Ieropoulos, “From single MFC to cascade configuration: the relationship between size, hydraulic retention time and power density,” *Sustainable Energy Technologies and Assessments*, vol. 14, pp. 74–79, 2016.
[202] S. Wu *et al.*, “A novel pilot-scale stacked microbial fuel cell for efficient electricity generation and wastewater treatment,” *Water Res*, vol. 98, pp. 396–403, 2016.
[203] E. B. Estrada-Arriaga *et al.*, “Domestic wastewater treatment and power generation in continuous flow air-cathode stacked microbial fuel cell: Effect of series and parallel configuration,” *J Environ Manage*, vol. 214, pp. 232–241, 2018.
[204] X. A. Walter, C. Santoro, J. Greenman, and I. A. Ieropoulos, “Scalability and stacking of self-stratifying microbial fuel cells treating urine,” *Bioelectrochemistry*, vol. 133, p. 107491, 2020.
[205] A. Vilajeliu-Pons, S. Puig, I. Salcedo-Dávila, M. D. Balaguer, and J. Colprim, “Long-term assessment of six-stacked scaled-up MFCs treating swine manure with different electrode materials,” *Environ Sci (Camb)*, vol. 3, no. 5, pp. 947–959, 2017.

[206] B. Kim, S. V. Mohan, D. Fapyane, and I. S. Chang, “Controlling voltage reversal in microbial fuel cells,” *Trends Biotechnol*, vol. 38, no. 6, pp. 667–678, 2020.
[207] J. An, J. Nam, B. Kim, H.-S. Lee, B. H. Kim, and I. S. Chang, “Performance variation according to anode-embedded orientation in a sediment microbial fuel cell employing a chessboard-like hundred-piece anode,” *Bioresour Technol*, vol. 190, pp. 175–181, 2015.
[208] S. Chen, S. A. Patil, R. K. Brown, and U. Schröder, “Strategies for optimizing the power output of microbial fuel cells: transitioning from fundamental studies to practical implementation,” *Appl Energy*, vol. 233, pp. 15–28, 2019.
[209] M. Blatter, L. Delabays, C. Furrer, G. Huguenin, C. P. Cachelin, and F. Fischer, “Stretched 1000-L microbial fuel cell,” *J Power Sources*, vol. 483, p. 229130, 2021.
[210] H. C. Boghani *et al.*, “Controlling for peak power extraction from microbial fuel cells can increase stack voltage and avoid cell reversal,” *J Power Sources*, vol. 269, pp. 363–369, 2014.
[211] Y. Song, J. An, and K. Chae, “Effect of temperature variation on the performance of microbial fuel cells,” *Energy Technology*, vol. 5, no. 12, pp. 2163–2167, 2017.
[212] P. Kumar and A. K. Mungray, “Microbial fuel cell: optimizing pH of anolyte and catholyte by using taguchi method,” *Environ Prog Sustain Energy*, vol. 36, no. 1, pp. 120–128, 2017.
[213] W. Yang, J. Li, D. Ye, L. Zhang, X. Zhu, and Q. Liao, “A hybrid microbial fuel cell stack based on single and double chamber microbial fuel cells for self-sustaining pH control,” *J Power Sources*, vol. 306, pp. 685–691, 2016.
[214] F. Guo, H. Luo, Z. Shi, Y. Wu, and H. Liu, “Substrate salinity: A critical factor regulating the performance of microbial fuel cells, a review,” *Science of The Total Environment*, vol. 763, p. 143021, 2021.
[215] F. Vicari *et al.*, “Influence of the methodology of inoculation in the performance of air-breathing microbial fuel cells,” *Journal of Electroanalytical Chemistry*, vol. 803, pp. 81–88, 2017.
[216] Y. Ye *et al.*, “Impacts of hydraulic retention time on a continuous flow mode dual-chamber microbial fuel cell for recovering nutrients from municipal wastewater,” *Science of The Total Environment*, vol. 734, p. 139220, 2020.
[217] G. H. Rau, “Electrochemical splitting of calcium carbonate to increase solution alkalinity: Implications for mitigation of carbon dioxide and ocean acidity,” *Environ Sci Technol*, vol. 42, no. 23, pp. 8935–8940, 2008.
[218] M. M. Tlili, M. Benamor, C. Gabrielli, H. Perrot, and B. Tribollet, “Influence of the interfacial pH on electrochemical CaCO3 precipitation,” *J Electrochem Soc*, vol. 150, no. 11, p. C765, 2003.
[219] E. Zhang, F. Wang, Q. Yu, K. Scott, X. Wang, and G. Diao, “Durability and regeneration of activated carbon air-cathodes in long-term operated microbial fuel cells,” *J Power Sources*, vol. 360, pp. 21–27, 2017.
[220] I. A. Moujdin and J. K. Summers, “Promising Techniques for Wastewater Treatment and Water Quality Assessment,” 2021.
[221] S. V. Mohan, A. Pandey, and S. Varjani, *Biomass, biofuels, biochemicals: Microbial electrochemical technology: Sustainable platform for fuels, chemicals and remediation*. Elsevier, 2018.
[222] V. D. Villanueva, J. Font, T. Schwartz, and A. M. Romani, “Biofilm formation at warming temperature: acceleration of microbial colonization and microbial interactive effects,” *Biofouling*, vol. 27, no. 1, pp. 59–71, 2011.

[223] G. Buitrón, I. López-Prieto, I. T. Zúñiga, and A. Vargas, “Reduction of start-up time in a microbial fuel cell through the variation of external resistance,” *Energy Procedia*, vol. 142, pp. 694–699, 2017.
[224] R. Kumar, L. Singh, A. W. Zularisam, and F. I. Hai, “Microbial fuel cell is emerging as a versatile technology: a review on its possible applications, challenges and strategies to improve the performances,” *Int J Energy Res*, vol. 42, no. 2, pp. 369–394, 2018.
[225] K. Senthilkumar, M. Naveenkumar, M. V. Ratnam, and S. Samraj, “A review on scaling-up of microbial fuel cell: Challenges and opportunities,” *Scaling Up of Microbial Electrochemical Systems*, pp. 13–28, 2022.
[226] Y. Hindatu, M. S. M. Annuar, and A. M. Gumel, “Mini-review: Anode modification for improved performance of microbial fuel cell,” *Renewable and Sustainable Energy Reviews*, vol. 73, pp. 236–248, 2017.
[227] A. A. Yaqoob, M. N. M. Ibrahim, and K. Umar, “Electrode material as anode for improving the electrochemical performance of microbial fuel cells,” in *Energy Storage Battery Systems-Fundamentals and Applications*, IntechOpen, 2021.
[228] R. Agrahari, B. Bayar, H. N. Abubackar, B. S. Giri, E. R. Rene, and R. Rani, “Advances in the development of electrodes material for improving reactor kinetics in Microbial Fuel Cells,” *Chemosphere*, p. 133184, 2021.
[229] M. Christwardana, J. Joelianingsih, and L. A. Yoshi, “A novel of 2D-3D combination carbon electrode to improve yeast microbial fuel cell performance,” *J Appl Electrochem*, vol. 52, no. 5, pp. 801–812, 2022.
[230] P. Choudhury, U. S. Prasad Uday, T. K. Bandyopadhyay, R. N. Ray, and B. Bhunia, “Performance improvement of microbial fuel cell (MFC) using suitable electrode and Bioengineered organisms: A review,” *Bioengineered*, vol. 8, no. 5, pp. 471–487, 2017.
[231] D. Wang *et al.*, “Surface modification of Shewanella oneidensis MR-1 with polypyrrole-dopamine coating for improvement of power generation in microbial fuel cells,” *J Power Sources*, vol. 483, p. 229220, 2021.
[232] Y.-J. Jiang, S. Hui, L.-P. Jiang, and J.-J. Zhu, “Functional Nanomaterial-Modified Anodes in Microbial Fuel Cells: Advances and Perspectives,” *Chemistry–A European Journal*, 2022.
[233] K. M. Alarjani, A. M. Almutairi, S. R. F. Raj, J. Rajaselvam, S. W. Chang, and B. Ravindran, “Biofilm producing indigenous bacteria isolated from municipal sludge and their nutrient removal ability in moving bed biofilm reactor from the wastewater,” *Saudi J Biol Sci*, vol. 28, no. 9, pp. 4994–5001, 2021.
[234] V. Sapireddy, K. P. Katuri, A. Muhammad, and P. E. Saikaly, “Competition of two highly specialized and efficient acetoclastic electroactive bacteria for acetate in biofilm anode of microbial electrolysis cell,” *NPJ Biofilms Microbiomes*, vol. 7, no. 1, pp. 1–11, 2021.
[235] S. Rahimi *et al.*, “Co-culturing Bacillus subtilis and wastewater microbial community in a bio-electrochemical system enhances denitrification and butyrate formation,” *Chemical Engineering Journal*, vol. 397, p. 125437, 2020.
[236] S.-G. Park *et al.*, “Methanogenesis stimulation and inhibition for the production of different target electrobiofuels in microbial electrolysis cells through an on-demand control strategy using the coenzyme M and 2-bromoethanesulfonate,” *Environ Int*, vol. 131, p. 105006, 2019.
[237] K. Gurung, W. Z. Tang, and M. Sillanpää, “Unit energy consumption as benchmark to select energy positive retrofitting strategies for Finnish wastewater treatment plants (WWTPs): a case study of Mikkeli WWTP,” *Environmental Processes*, vol. 5, no. 3, pp. 667–681, 2018.

[238] O. Dimou, J. Andresen, V. Feodorovich, I. Goryanin, A. Harper, and D. Simpson, "Optimisation of scale-up of microbial fuel cell for sustainable wastewater treatment with positive net energy generation," *New Biotechnol*, vol. 31, no. supplement, p. S213, 2014.
[239] T. Kim, J. An, J. K. Jang, and I. S. Chang, "Coupling of anaerobic digester and microbial fuel cell for COD removal and ammonia recovery," *Bioresour Technol*, vol. 195, pp. 217–222, 2015.
[240] R. Chung *et al.*, "Development of a consolidated anaerobic digester and microbial fuel cell to produce biomethane and electricity from cellulosic biomass using bovine rumen microorganisms," *J Sustain Bioenergy Syst*, vol. 9, no. 02, p. 17, 2019.
[241] M. Cerrillo, M. Viñas, and A. Bonmatí, "Microbial fuel cells for polishing effluents of anaerobic digesters under inhibition, due to organic and nitrogen overloads," *Journal of Chemical Technology & Biotechnology*, vol. 92, no. 12, pp. 2912–2920, 2017.
[242] Y. Hou *et al.*, "A 3D hybrid of layered MoS 2/nitrogen-doped graphene nanosheet aerogels: an effective catalyst for hydrogen evolution in microbial electrolysis cells," *J Mater Chem A Mater*, vol. 2, no. 34, pp. 13795–13800, 2014.
[243] E. S. Heidrich, S. R. Edwards, J. Dolfing, S. E. Cotterill, and T. P. Curtis, "Performance of a pilot scale microbial electrolysis cell fed on domestic wastewater at ambient temperatures for a 12 month period," *Bioresour Technol*, vol. 173, pp. 87–95, 2014.
[244] Y. Zhang and I. Angelidaki, "Microbial electrolysis cells turning to be versatile technology: recent advances and future challenges," *Water Res*, vol. 56, pp. 11–25, 2014.
[245] D. Aboelela and M. A. Soliman, "Hydrogen production from microbial electrolysis cells powered with microbial fuel cells," *Journal of King Saud University-Engineering Sciences*, 2022.
[246] S. Oh and B. E. Logan, "Hydrogen and electricity production from a food processing wastewater using fermentation and microbial fuel cell technologies," *Water Res*, vol. 39, no. 19, pp. 4673–4682, 2005.
[247] A. Saravanan, S. Karishma, P. S. Kumar, P. R. Yaashikaa, S. Jeevanantham, and B. Gayathri, "Microbial electrolysis cells and microbial fuel cells for biohydrogen production: Current advances and emerging challenges," *Biomass Convers Biorefin*, pp. 1–21, 2020.
[248] R. Xie *et al.*, "Improved energy efficiency in microbial fuel cells by bioethanol and electricity co-generation," *Biotechnology for biofuels and bioproducts*, vol. 15, no. 1, pp. 1–14, 2022.
[249] A. ter Heijne, F. Geppert, T. H. J. A. Sleutels, P. Batlle-Vilanova, D. Liu, and S. Puig, "Mixed culture biocathodes for production of hydrogen, methane, and carboxylates," *Bioelectrosynthesis*, pp. 203–229, 2017.
[250] S. Bajracharya, N. Aryal, H. de Wever, and D. Pant, "Bioelectrochemical syntheses," in *An Economy Based on Carbon Dioxide and Water*, Springer, 2019, pp. 327–358.
[251] S. Saheb-Alam *et al.*, "Effect of start-up strategies and electrode materials on carbon dioxide reduction on biocathodes," *Appl Environ Microbiol*, vol. 84, no. 4, pp. e02242-17, 2018.
[252] B. E. Logan and K. Rabaey, "Conversion of wastes into bioelectricity and chemicals by using microbial electrochemical technologies," *Science (1979)*, vol. 337, no. 6095, pp. 686–690, 2012.
[253] R. Stalder and G. P. Roth, "Preparative microfluidic electrosynthesis of drug metabolites," *ACS Med Chem Lett*, vol. 4, no. 11, pp. 1119–1123, 2013.

[254] H. Hwang *et al.*, "Electro-biocatalytic production of formate from carbon dioxide using an oxygen-stable whole cell biocatalyst," *Bioresour Technol*, vol. 185, pp. 35–39, 2015.
[255] D. R. Lovley and K. P. Nevin, "Electrobiocommodities: powering microbial production of fuels and commodity chemicals from carbon dioxide with electricity," *Curr Opin Biotechnol*, vol. 24, no. 3, pp. 385–390, 2013.
[256] C. Liu *et al.*, "Nanowire–bacteria hybrids for unassisted solar carbon dioxide fixation to value-added chemicals," *Nano Lett*, vol. 15, no. 5, pp. 3634–3639, 2015.
[257] K. P. Nevin *et al.*, "Electrosynthesis of organic compounds from carbon dioxide is catalyzed by a diversity of acetogenic microorganisms," *Appl Environ Microbiol*, vol. 77, no. 9, pp. 2882–2886, 2011.
[258] K. Rabaey and R. A. Rozendal, "Microbial electrosynthesis—revisiting the electrical route for microbial production," *Nat Rev Microbiol*, vol. 8, no. 10, pp. 706–716, 2010.
[259] G. M. Whitesides, "Nanoscience, nanotechnology, and chemistry," *Small*, vol. 1, no. 2, pp. 172–179, 2005.
[260] A. Hervault and N. T. K. Thanh, "Magnetic nanoparticle-based therapeutic agents for thermo-chemotherapy treatment of cancer," *Nanoscale*, vol. 6, no. 20, pp. 11553–11573, 2014.
[261] M. Wu and S. Huang, "Magnetic nanoparticles in cancer diagnosis, drug delivery and treatment," *Mol Clin Oncol*, vol. 7, no. 5, pp. 738–746, 2017.
[262] S. Mukherjee, L. Liang, and O. Veiseh, "Recent advancements of magnetic nanomaterials in cancer therapy," *Pharmaceutics*, vol. 12, no. 2, p. 147, 2020.
[263] E. I. Nosike, Y. Zhang, and A. Wu, "Magnetic hybrid nanoparticles for environmental remediation," in *Magnetic Nanoparticle-Based Hybrid Materials*, Elsevier, 2021, pp. 591–615.
[264] J. Kong, K. Coolahan, and A. Mugweru, "Manganese based magnetic nanoparticles for heavy metal detection and environmental remediation," *Analytical Methods*, vol. 5, no. 19, pp. 5128–5133, 2013.
[265] B. Jiang *et al.*, "Advances of magnetic nanoparticles in environmental application: environmental remediation and (bio) sensors as case studies," *Environmental Science and Pollution Research*, vol. 25, no. 31, pp. 30863–30879, 2018.
[266] Z. Akchiche, A. B. Abba, and S. Saggai, "Magnetic nanoparticles for the Removal of Heavy Metals from industrial wastewater," *Algerian Journal of Chemical Engineering AJCE*, vol. 1, no. 1, pp. 8–15, 2021.
[267] I. Matsui, "Preparation of FePt magnetic nanoparticle film by plasma chemical vapor deposition for ultrahigh density data storage media," *Jpn J Appl Phys*, vol. 45, no. 10S, p. 8302, 2006.
[268] P. Malik, S. Pandya, and V. Katyal, "Synthesis and application of magnetic nanomaterials for memory storage devices," *Int. J. Adv. Res*, vol. 1, no. 1, 2013.
[269] V. Kumari, K. Dey, S. Giri, and A. Bhaumik, "Magnetic memory effect in self-assembled nickel ferrite nanoparticles having mesoscopic void spaces," *RSC Adv*, vol. 6, no. 51, pp. 45701–45707, 2016.
[270] J. Liao, H. Zhang, and C. Lai, "Magnetic nanomaterials for data storage," *Magnetic Nanomaterials: Fundamentals, Synthesis and Applications*, pp. 439–472, 2017.
[271] E. Katz and I. Willner, "Integrated nanoparticle–biomolecule hybrid systems: synthesis, properties, and applications," *Angewandte Chemie International Edition*, vol. 43, no. 45, pp. 6042–6108, 2004.
[272] D. Zhang *et al.*, "Functionalization of whole-cell bacterial reporters with magnetic nanoparticles," *Microb Biotechnol*, vol. 4, no. 1, pp. 89–97, 2011.

[273] C. Noubactep, S. Caré, and R. Crane, “Nanoscale metallic iron for environmental remediation: prospects and limitations,” *Water Air Soil Pollut*, vol. 223, no. 3, pp. 1363–1382, 2012.
[274] D. Zhang *et al.*, “Magnetic nanoparticle-mediated isolation of functional bacteria in a complex microbial community,” *ISME J*, vol. 9, no. 3, pp. 603–614, 2015.
[275] K. Guo *et al.*, “Flame oxidation of stainless steel felt enhances anodic biofilm formation and current output in bioelectrochemical systems,” *Environ Sci Technol*, vol. 48, no. 12, pp. 7151–7156, 2014.
[276] R. Kumar, L. Singh, and A. W. Zularisam, “Exoelectrogens: recent advances in molecular drivers involved in extracellular electron transfer and strategies used to improve it for microbial fuel cell applications,” *Renewable and Sustainable Energy Reviews*, vol. 56, pp. 1322–1336, 2016.
[277] X.-W. Liu *et al.*, “Conductive carbon nanotube hydrogel as a bioanode for enhanced microbial electrocatalysis,” *ACS Appl Mater Interfaces*, vol. 6, no. 11, pp. 8158–8164, 2014.
[278] F. A. Alatraktchi, Y. Zhang, and I. Angelidaki, “Nanomodification of the electrodes in microbial fuel cell: impact of nanoparticle density on electricity production and microbial community,” *Appl Energy*, vol. 116, pp. 216–222, 2014.
[279] Y. Qiao, X.-S. Wu, and C. M. Li, “Interfacial electron transfer of Shewanella putrefaciens enhanced by nanoflaky nickel oxide array in microbial fuel cells,” *J Power Sources*, vol. 266, pp. 226–231, 2014.
[280] X. Jiang *et al.*, “Nanoparticle facilitated extracellular electron transfer in microbial fuel cells,” *Nano Lett*, vol. 14, no. 11, pp. 6737–6742, 2014.
[281] Y. Cui *et al.*, “Biosynthesized iron sulfide nanoparticles by mixed consortia for enhanced extracellular electron transfer in a microbial fuel cell,” *Bioresour Technol*, vol. 318, p. 124095, 2020.
[282] M. Tahernia, M. Mohammadifar, S. Feng, and S. Choi, “Biogenic Palladium Nanoparticles for Improving Bioelectricity Generation in Microbial Fuel Cells,” in *2020 IEEE 33rd International Conference on Micro Electro Mechanical Systems (MEMS)*, 2020, pp. 425–428.
[283] S. Chen *et al.*, “Promoting interspecies electron transfer with biochar,” *Sci Rep*, vol. 4, no. 1, pp. 1–7, 2014.
[284] M. A. Gacitúa, B. González, M. Majone, and F. Aulenta, “Boosting the electrocatalytic activity of Desulfovibrio paquesii biocathodes with magnetite nanoparticles,” *Int J Hydrogen Energy*, vol. 39, no. 27, pp. 14540–14545, 2014.
[285] F. Miran, M. W. Mumtaz, H. Mukhtar, and S. Akram, “Iron oxide–modified carbon electrode and sulfate-reducing bacteria for simultaneous enhanced electricity generation and tannery wastewater treatment,” *Front Bioeng Biotechnol*, vol. 9, 2021.
[286] S. C. D. Sharma *et al.*, “Decolorization of azo dye methyl red by suspended and co-immobilized bacterial cells with mediators anthraquinone-2, 6-disulfonate and Fe3O4 nanoparticles,” *Int Biodeterior Biodegradation*, vol. 112, pp. 88–97, 2016.
[287] I. H. Park, Y. H. Heo, P. Kim, and K. S. Nahm, “Direct electron transfer in E. coli catalyzed MFC with a magnetite/MWCNT modified anode,” *RSC Adv*, vol. 3, no. 37, pp. 16665–16671, 2013.
[288] F. Aulenta, S. Rossetti, S. Amalfitano, M. Majone, and V. Tandoi, “Conductive magnetite nanoparticles accelerate the microbial reductive dechlorination of trichloroethene by promoting interspecies electron transfer processes,” *ChemSusChem*, vol. 6, no. 3, pp. 433–436, 2013.

[289] S. Kato, K. Hashimoto, and K. Watanabe, “Microbial interspecies electron transfer via electric currents through conductive minerals,” *Proceedings of the National Academy of Sciences*, vol. 109, no. 25, pp. 10042–10046, 2012.
[290] M. Shabani, H. Younesi, M. Pontié, A. Rahimpour, M. Rahimnejad, and A. A. Zinatizadeh, “A critical review on recent proton exchange membranes applied in microbial fuel cells for renewable energy recovery,” *J Clean Prod*, vol. 264, p. 121446, 2020.
[291] A. Nawaz *et al.*, “Microbial fuel cells: Insight into simultaneous wastewater treatment and bioelectricity generation,” *Process Safety and Environmental Protection*, vol. 161, pp. 357–373, 2022.
[292] G. Bhargavi, V. Venu, and S. Renganathan, “Microbial fuel cells: recent developments in design and materials,” in *IOP Conference Series: Materials Science and Engineering*, 2018, vol. 330, no. 1, p. 012034.
[293] R. Rossi and B. E. Logan, “Impact of reactor configuration on pilot-scale microbial fuel cell performance,” *Water Res*, p. 119179, 2022.
[294] X. Song, C. Jo, L. Han, and M. Zhou, “Recent advance in microbial fuel cell reactor configuration and coupling technologies for removal of antibiotic pollutants,” *Curr Opin Electrochem*, vol. 31, p. 100833, 2022.
[295] S. Xin *et al.*, “High electricity generation and COD removal from cattle wastewater in microbial fuel cells with 3D air cathode employed non-precious Cu2O/reduced graphene oxide as cathode catalyst,” *Energy*, vol. 196, p. 117123, 2020.
[296] Z. Ren *et al.*, “Accelerated start-up and improved performance of wastewater microbial fuel cells in four circuit modes: Role of anodic potential,” *J Power Sources*, vol. 535, p. 231403, 2022.
[297] M. S. Hamed, H. S. Majdi, and B. O. Hasan, “Effect of electrode material and hydrodynamics on the produced current in double chamber microbial fuel cells,” *ACS Omega*, vol. 5, no. 18, pp. 10339–10348, 2020.
[298] M. J. Angelaalincy, R. Navanietha Krishnaraj, G. Shakambari, B. Ashokkumar, S. Kathiresan, and P. Varalakshmi, “Biofilm engineering approaches for improving the performance of microbial fuel cells and bioelectrochemical systems,” *Front Energy Res*, vol. 6, p. 63, 2018.
[299] J. Greenman *et al.*, “Microbial fuel cells and their electrified biofilms,” *Biofilm*, vol. 3, p. 100057, 2021.
[300] R. H. Mahmoud, O. M. Gomaa, and R. Y. A. Hassan, “Bio-electrochemical frameworks governing microbial fuel cell performance: technical bottlenecks and proposed solutions,” *RSC Adv*, vol. 12, no. 10, pp. 5749–5764, 2022.
[301] X. Wu *et al.*, “Anode modification by biogenic gold nanoparticles for the improved performance of microbial fuel cells and microbial community shift,” *Bioresour Technol*, vol. 270, pp. 11–19, 2018.
[302] V. K. Magotra *et al.*, “Effect of gold nanoparticles laced anode on the bio-electro-catalytic activity and power generation ability of compost based microbial fuel cell as a coin cell sized device,” *Biomass Bioenergy*, vol. 152, p. 106200, 2021.
[303] A. Godain, N. Haddour, P. Fongarland, and T. M. Vogel, “Bacterial competition for the anode colonization under different external resistances in microbial fuel cells,” *Catalysts*, vol. 12, no. 2, p. 176, 2022.
[304] T. Liu, Y. Yu, D. Li, H. Song, X. Yan, and W. N. Chen, “The effect of external resistance on biofilm formation and internal resistance in Shewanella inoculated microbial fuel cells,” *RSC Adv*, vol. 6, no. 24, pp. 20317–20323, 2016.

[305] A. Vogl, F. Bischof, and M. Wichern, “Surface-to-surface biofilm transfer: a quick and reliable startup strategy for mixed culture microbial fuel cells,” *Water Science and Technology*, vol. 73, no. 8, pp. 1769–1776, 2016.
[306] N. J. Eyiuche, S. Asakawa, T. Yamashita, A. Ikeguchi, Y. Kitamura, and H. Yokoyama, “Community analysis of biofilms on flame-oxidized stainless steel anodes in microbial fuel cells fed with different substrates,” *BMC Microbiol*, vol. 17, no. 1, pp. 1–8, 2017.
[307] C.-Y. Wen *et al.*, “Efficient enrichment and analyses of bacteria at ultralow concentration with quick-response magnetic nanospheres,” *ACS Appl Mater Interfaces*, vol. 9, no. 11, pp. 9416–9425, 2017.
[308] Z. Li, J. Ma, J. Ruan, and X. Zhuang, “Using positively charged magnetic nanoparticles to capture bacteria at ultralow concentration,” *Nanoscale Res Lett*, vol. 14, no. 1, pp. 1–8, 2019.
[309] M. G. Sande, T. Çaykara, C. J. Silva, and L. R. Rodrigues, “New solutions to capture and enrich bacteria from complex samples,” *Med Microbiol Immunol*, vol. 209, no. 3, pp. 335–341, 2020.
[310] J. Chen, S. M. Andler, J. M. Goddard, S. R. Nugen, and V. M. Rotello, “Integrating recognition elements with nanomaterials for bacteria sensing,” *Chem Soc Rev*, vol. 46, no. 5, pp. 1272–1283, 2017.
[311] D. A. Rodionov *et al.*, “Genomic encyclopedia of sugar utilization pathways in the Shewanella genus,” *BMC Genomics*, vol. 11, no. 1, pp. 1–19, 2010.
[312] J. T. S. Irvine, G. P. G. Corre, and X. Xu, “Fuel Cells and the Hydrogen Economy,” in *The World Scientific Handbook of Energy*, World Scientific, 2013, pp. 427–454.
[313] V. D. Rajput *et al.*, “Insights into the Biosynthesis of Nanoparticles by the Genus Shewanella,” *Appl Environ Microbiol*, vol. 87, no. 22, pp. e01390-21, 2021.
[314] R. L. Kimber *et al.*, “Biosynthesis and characterization of copper nanoparticles using Shewanella oneidensis: application for click chemistry,” *Small*, vol. 14, no. 10, p. 1703145, 2018.
[315] G. F. Vettese *et al.*, “Multiple lines of evidence identify U (V) as a key intermediate during U (VI) reduction by shewanella oneidensis MR1,” *Environ Sci Technol*, vol. 54, no. 4, pp. 2268–2276, 2020.
[316] K. Revati and B. D. Pandey, “Microbial synthesis of iron-based nanomaterials—A review,” *Bulletin of Materials Science*, vol. 34, no. 2, pp. 191–198, 2011.
[317] Z. Sharafi, B. Bakhshi, J. Javidi, and S. Adrangi, “Synthesis of silica-coated iron oxide nanoparticles: preventing aggregation without using additives or seed pretreatment,” *Iran J Pharm Res*, vol. 17, no. 1, p. 386, 2018.
[318] M. A. Malvindi *et al.*, “Toxicity assessment of silica coated iron oxide nanoparticles and biocompatibility improvement by surface engineering,” *PLoS One*, vol. 9, no. 1, p. e85835, 2014.
[319] B. Frølund, R. Palmgren, K. Keiding, and P. H. Nielsen, “Extraction of extracellular polymers from activated sludge using a cation exchange resin,” *Water Res*, vol. 30, no. 8, pp. 1749–1758, 1996.
[320] M. H. Serres and M. Riley, “Genomic analysis of carbon source metabolism of Shewanella oneidensis MR-1: predictions versus experiments,” *J Bacteriol*, vol. 188, no. 13, pp. 4601–4609, 2006.
[321] F. Golipour, R. Habibipour, and L. Moradihaghgou, “Investigating effects of superparamagnetic iron oxide nanoparticles on Candida albicans biofilm formation,” *Medical Laboratory Journal*, vol. 13, no. 6, pp. 44–50, 2019.
[322] P. Mathieu *et al.*, “Silica coated iron/iron oxide nanoparticles as a nano-platform for T2 weighted magnetic resonance imaging,” *Molecules*, vol. 24, no. 24, p. 4629, 2019.

[323] C. Turrina, A. Oppelt, M. Mitzkus, S. Berensmeier, and S. P. Schwaminger, “Silica-coated superparamagnetic iron oxide nanoparticles: New insights into the influence of coating thickness on the particle properties and lasioglossin binding,” *MRS Commun*, vol. 12, no. 5, pp. 632–639, 2022.
[324] S. Kralj, D. Makovec, S. Čampelj, and M. Drofenik, “Producing ultra-thin silica coatings on iron-oxide nanoparticles to improve their surface reactivity,” *J Magn Magn Mater*, vol. 322, no. 13, pp. 1847–1853, 2010.
[325] E. S. D. T. de Mendonça *et al.*, “Effects of silica coating on the magnetic properties of magnetite nanoparticles,” *Surfaces and Interfaces*, vol. 14, pp. 34–43, 2019.
[326] P. S. Stewart, “Diffusion in biofilms,” *J Bacteriol*, vol. 185, no. 5, pp. 1485–1491, 2003.
[327] B. Gunes, “A critical review on biofilm-based reactor systems for enhanced syngas fermentation processes,” *Renewable and Sustainable Energy Reviews*, vol. 143, p. 110950, 2021.
[328] M. Krsmanovic, D. Biswas, H. Ali, A. Kumar, R. Ghosh, and A. K. Dickerson, “Hydrodynamics and surface properties influence biofilm proliferation,” *Adv Colloid Interface Sci*, vol. 288, p. 102336, 2021.
[329] C. K. Ng *et al.*, “Genetic engineering biofilms in situ using ultrasound-mediated DNA delivery,” *Microb Biotechnol*, vol. 14, no. 4, pp. 1580–1593, 2021.
[330] P. Stoodley, K. Sauer, D. G. Davies, and J. W. Costerton, “Biofilms as complex differentiated communities,” *Annu Rev Microbiol*, vol. 56, no. 1, pp. 187–209, 2002.
[331] R. U. Meckenstock *et al.*, “Biodegradation: updating the concepts of control for microbial cleanup in contaminated aquifers,” *Environ Sci Technol*, vol. 49, no. 12, pp. 7073–7081, 2015.
[332] B. Halan, K. Buehler, and A. Schmid, “Biofilms as living catalysts in continuous chemical syntheses,” *Trends Biotechnol*, vol. 30, no. 9, pp. 453–465, 2012.
[333] Z. Botyanszki, P. K. R. Tay, P. Q. Nguyen, M. G. Nussbaumer, and N. S. Joshi, “Engineered catalytic biofilms: Site-specific enzyme immobilization onto E. coli curli nanofibers,” *Biotechnol Bioeng*, vol. 112, no. 10, pp. 2016–2024, 2015.
[334] R. Singh, D. Paul, and R. K. Jain, “Biofilms: implications in bioremediation,” *Trends Microbiol*, vol. 14, no. 9, pp. 389–397, 2006.
[335] P. S. Stewart and M. J. Franklin, “Physiological heterogeneity in biofilms,” *Nat Rev Microbiol*, vol. 6, no. 3, pp. 199–210, 2008.
[336] S. Elias and E. Banin, “Multi-species biofilms: living with friendly neighbors,” *FEMS Microbiol Rev*, vol. 36, no. 5, pp. 990–1004, 2012.
[337] S. G. Hays, W. G. Patrick, M. Ziesack, N. Oxman, and P. A. Silver, “Better together: engineering and application of microbial symbioses,” *Curr Opin Biotechnol*, vol. 36, pp. 40–49, 2015.
[338] R. V. Joshi, C. Gunawan, and R. Mann, “We are one: multispecies metabolism of a biofilm consortium and their treatment strategies,” *Front Microbiol*, vol. 12, p. 635432, 2021.
[339] C. Beloin and D. McDougald, “Speciality Grand Challenge for ‘Biofilms,’” *Front Cell Infect Microbiol*, p. 99, 2021.
[340] I. Chattopadhyay, T. M. M. Usman, and S. Varjani, “Exploring the role of microbial biofilm for industrial effluents treatment,” *Bioengineered*, vol. 13, no. 3, pp. 6420–6440, 2022.
[341] S. J. Sørensen, M. Bailey, L. H. Hansen, N. Kroer, and S. Wuertz, “Studying plasmid horizontal transfer in situ: a critical review,” *Nat Rev Microbiol*, vol. 3, no. 9, pp. 700–710, 2005.

[342] H. Brim *et al.*, “Engineering Deinococcus radiodurans for metal remediation in radioactive mixed waste environments,” *Nat Biotechnol*, vol. 18, no. 1, pp. 85–90, 2000.
[343] D. Prakash, P. Gabani, A. K. Chandel, Z. Ronen, and O. v Singh, “Bioremediation: a genuine technology to remediate radionuclides from the environment,” *Microb Biotechnol*, vol. 6, no. 4, pp. 349–360, 2013.
[344] M. M. Clark, M. D. Paxhia, J. M. Young, M. P. Manzella, and G. Reguera, “Adaptive synthesis of a rough lipopolysaccharide in geobacter sulfurreducens for metal reduction and detoxification,” *Appl Environ Microbiol*, vol. 87, no. 20, pp. e00964-21, 2021.
[345] J.-M. Collard *et al.*, “Plasmids for heavy metal resistance in Alcaligenes eutrophus CH34: mechanisms and applications,” *FEMS Microbiol Rev*, vol. 14, no. 4, pp. 405–414, 1994.
[346] P. Diep, R. Mahadevan, and A. F. Yakunin, “Heavy metal removal by bioaccumulation using genetically engineered microorganisms,” *Front Bioeng Biotechnol*, vol. 6, p. 157, 2018.
[347] M. M. Al-Ansari *et al.*, “Effective removal of heavy metals from industrial effluent wastewater by a multi metal and drug resistant Pseudomonas aeruginosa strain RA-14 using integrated sequencing batch reactor,” *Environ Res*, vol. 199, p. 111240, 2021.
[348] S. P. Leonard *et al.*, “Genetic engineering of bee gut microbiome bacteria with a toolkit for modular assembly of broad-host-range plasmids,” *ACS Synth Biol*, vol. 7, no. 5, pp. 1279–1290, 2018.
[349] V. de Lorenzo, “Recombinant bacteria for environmental release: what went wrong and what we have learnt from it,” *Clinical Microbiology and Infection*, vol. 15, pp. 63–65, 2009.
[350] Y. Song *et al.*, “Ultrasound-mediated DNA transfer for bacteria,” *Nucleic Acids Res*, vol. 35, no. 19, p. e129, 2007.
[351] K. Tachibana, T. Uchida, K. Ogawa, N. Yamashita, and K. Tamura, “Induction of cell-membrane porosity by ultrasound,” *The Lancet*, vol. 353, no. 9162, p. 1409, 1999.
[352] H. Tang, C. C. J. Wang, D. Blankschtein, and R. Langer, “An investigation of the role of cavitation in low-frequency ultrasound-mediated transdermal drug transport,” *Pharm Res*, vol. 19, no. 8, pp. 1160–1169, 2002.
[353] Y. Chen, M. Du, Z. Yuan, Z. Chen, and F. Yan, “Spatiotemporal control of engineered bacteria to express interferon-γ by focused ultrasound for tumor immunotherapy,” *Nat Commun*, vol. 13, no. 1, pp. 1–15, 2022.
[354] J. F. Heidelberg *et al.*, “Genome sequence of the dissimilatory metal ion–reducing bacterium Shewanella oneidensis,” *Nat Biotechnol*, vol. 20, no. 11, pp. 1118–1123, 2002.
[355] B. Cao *et al.*, “Extracellular polymeric substances from Shewanella sp. HRCR-1 biofilms: characterization by infrared spectroscopy and proteomics,” *Environ Microbiol*, vol. 13, no. 4, pp. 1018–1031, 2011.
[356] D. Hanahan, “Studies on transformation of Escherichia coli with plasmids,” *J Mol Biol*, vol. 166, no. 4, pp. 557–580, 1983.
[357] S. Taghavi, D. van der Lelie, and M. Mergeay, “Electroporation of Alcaligenes eutrophus with (mega) plasmids and genomic DNA fragments,” *Appl Environ Microbiol*, vol. 60, no. 10, pp. 3585–3591, 1994.
[358] J. Sundaram, B. R. Mellein, and S. Mitragotri, “An experimental and theoretical analysis of ultrasound-induced permeabilization of cell membranes,” *Biophys J*, vol. 84, no. 5, pp. 3087–3101, 2003.

[359] M. Tomizawa, F. Shinozaki, Y. Motoyoshi, T. Sugiyama, S. Yamamoto, and M. Sueishi, "Sonoporation: Gene transfer using ultrasound," *World J Methodol*, vol. 3, no. 4, p. 39, 2013.
[360] D. J. Wells, "Electroporation and ultrasound enhanced non-viral gene delivery in vitro and in vivo," *Cell Biol Toxicol*, vol. 26, no. 1, pp. 21–28, 2010.
[361] A. Delalande, M. Postema, N. Mignet, P. Midoux, and C. Pichon, "Ultrasound and microbubble-assisted gene delivery: recent advances and ongoing challenges," *Ther Deliv*, vol. 3, no. 10, pp. 1199–1215, 2012.
[362] J. N. Belling *et al.*, "Acoustofluidic sonoporation for gene delivery to human hematopoietic stem and progenitor cells," *Proceedings of the National Academy of Sciences*, vol. 117, no. 20, pp. 10976–10982, 2020.
[363] T. P. McCreery, R. H. Sweitzer, and E. C. Unger, "DNA delivery to cells in culture using ultrasound," in *Gene Delivery to Mammalian Cells*, Springer, 2004, pp. 287–291.
[364] Q. Liu, J. Jiang, L. Tang, and M. Chen, "The effect of low frequency and low intensity ultrasound combined with microbubbles on the sonoporation efficiency of MDA-MB-231 cells," *Ann Transl Med*, vol. 8, no. 6, 2020.
[365] H. L. Røder *et al.*, "Biofilms can act as plasmid reserves in the absence of plasmid specific selection," *NPJ Biofilms Microbiomes*, vol. 7, no. 1, pp. 1–6, 2021.
[366] G. A. Metzger *et al.*, "Biofilms preserve transmissibility of a multi-drug resistance plasmid," *bioRxiv*, 2022.
[367] C. Hennequin, C. Aumeran, F. Robin, O. Traore, and C. Forestier, "Antibiotic resistance and plasmid transfer capacity in biofilm formed with a CTX-M-15-producing Klebsiella pneumoniae isolate," *Journal of Antimicrobial Chemotherapy*, vol. 67, no. 9, pp. 2123–2130, 2012.
[368] S. Mitragotri, D. Blankschtein, and R. Langer, "Ultrasound-mediated transdermal protein delivery," *Science (1979)*, vol. 269, no. 5225, pp. 850–853, 1995.
[369] H. Tang, D. Blankschtein, and R. Langer, "Effects of low-frequency ultrasound on the transdermal permeation of mannitol: Comparative studies with in vivo and in vitro skin," *J Pharm Sci*, vol. 91, no. 8, pp. 1776–1794, 2002.
[370] M. R. Prausnitz, S. Mitragotri, and R. Langer, "Current status and future potential of transdermal drug delivery," *Nat Rev Drug Discov*, vol. 3, no. 2, pp. 115–124, 2004.
[371] M. Erriu *et al.*, "Microbial biofilm modulation by ultrasound: current concepts and controversies," *Ultrason Sonochem*, vol. 21, no. 1, pp. 15–22, 2014.
[372] N. Vyas *et al.*, "Which parameters affect biofilm removal with acoustic cavitation? A review," *Ultrasound Med Biol*, vol. 45, no. 5, pp. 1044–1055, 2019.
[373] T. G. Leighton, "The acoustic bubble: Ocean, cetacean and extraterrestrial acoustics, and cold water cleaning," in *Journal of Physics: Conference Series*, 2017, vol. 797, no. 1, p. 012001.
[374] C. C. Coussios and R. A. Roy, "Applications of acoustics and cavitation to noninvasive therapy and drug delivery," *Annu Rev Fluid Mech*, vol. 40, 2008.
[375] S. Wuertz *et al.*, "Extracellular redox activity in activated sludge," *Water Science and Technology*, vol. 37, no. 4–5, pp. 379–384, 1998.
[376] J. Wimpenny, W. Manz, and U. Szewzyk, "Heterogeneity in biofilms," *FEMS Microbiol Rev*, vol. 24, no. 5, pp. 661–671, 2000.
[377] H.-C. Flemming, T. R. Neu, and D. J. Wozniak, "The EPS matrix: the 'house of biofilm cells,'" *J Bacteriol*, vol. 189, no. 22, pp. 7945–7947, 2007.
[378] E. Alpkvist, C. Picioreanu, M. C. M. van Loosdrecht, and A. Heyden, "Three-dimensional biofilm model with individual cells and continuum EPS matrix," *Biotechnol Bioeng*, vol. 94, no. 5, pp. 961–979, 2006.

[379] M. Rahimzadeh, M. Sadeghizadeh, F. Najafi, S. Arab, and H. Mobasheri, “Impact of heat shock step on bacterial transformation efficiency,” *Mol Biol Res Commun*, vol. 5, no. 4, p. 257, 2016.
[380] E. Sokołowska and A. U. Błachnio-Zabielska, “A critical review of electroporation as a plasmid delivery system in mouse skeletal muscle,” *Int J Mol Sci*, vol. 20, no. 11, p. 2776, 2019.
[381] L. Patil and P. R. Gogate, “Ultrasound assisted synthesis of stable oil in milk emulsion: Study of operating parameters and scale-up aspects,” *Ultrason Sonochem*, vol. 40, pp. 135–146, 2018.
[382] P. R. Gogate, V. S. Sutkar, and A. B. Pandit, “Sonochemical reactors: important design and scale up considerations with a special emphasis on heterogeneous systems,” *Chemical Engineering Journal*, vol. 166, no. 3, pp. 1066–1082, 2011.
[383] V. S. Sutkar and P. R. Gogate, “Design aspects of sonochemical reactors: techniques for understanding cavitational activity distribution and effect of operating parameters,” *Chemical Engineering Journal*, vol. 155, no. 1–2, pp. 26–36, 2009.
[384] Z. Dong, C. Delacour, K. Mc Carogher, A. P. Udepurkar, and S. Kuhn, “Continuous ultrasonic reactors: design, mechanism and application,” *Materials*, vol. 13, no. 2, p. 344, 2020.
[385] A. S. Mhetre and P. R. Gogate, “New design and mapping of sonochemical reactor operating at capacity of 72 L,” *Chemical Engineering Journal*, vol. 258, pp. 69–76, 2014.
[386] T. Lippert, J. Bandelin, F. Schlederer, J. E. Drewes, and K. Koch, “Effects of ultrasonic reactor design on sewage sludge disintegration,” *Ultrason Sonochem*, vol. 68, p. 105223, 2020.
[387] G. Reguera, K. D. McCarthy, T. Mehta, J. S. Nicoll, M. T. Tuominen, and D. R. Lovley, “Extracellular electron transfer via microbial nanowires,” *Nature*, vol. 435, no. 7045, pp. 1098–1101, 2005.
[388] C. M. Metallo and M. G. vander Heiden, “Understanding metabolic regulation and its influence on cell physiology,” *Mol Cell*, vol. 49, no. 3, pp. 388–398, 2013.
[389] H. A. Shah, J. Liu, Z. Yang, and J. Feng, “Review of machine learning methods for the prediction and reconstruction of metabolic pathways,” *Front Mol Biosci*, p. 567, 2021.
[390] L. Sin Yi, T. Li Chin, M. Saberi Mohamad, S. Deris, S. Subair, and Z. Ibrahim, “A Review on Metabolic Pathway Analysis in Biological Production,” *Mini Rev Org Chem*, vol. 12, no. 6, pp. 506–523, 2015.
[391] B. E. Logan, “Exoelectrogenic bacteria that power microbial fuel cells,” *Nat Rev Microbiol*, vol. 7, no. 5, pp. 375–381, 2009.
[392] D. R. Lovley, “Electromicrobiology,” *Annu Rev Microbiol*, vol. 66, pp. 391–409, 2012.
[393] L. Shi, K. M. Rosso, T. A. Clarke, D. J. Richardson, J. M. Zachara, and J. K. Fredrickson, “Molecular underpinnings of Fe (III) oxide reduction by Shewanella oneidensis MR-1,” *Front Microbiol*, vol. 3, p. 50, 2012.
[394] M. Shi, Y. Jiang, and L. Shi, “Electromicrobiology and biotechnological applications of the exoelectrogens Geobacter and Shewanella spp.,” *Sci China Technol Sci*, vol. 62, no. 10, pp. 1670–1678, 2019.
[395] Q. Cheng and D. F. Call, “Developing microbial communities containing a high abundance of exoelectrogenic microorganisms using activated carbon granules,” *Science of The Total Environment*, vol. 768, p. 144361, 2021.
[396] D.-F. Liu and W.-W. Li, “Potential-dependent extracellular electron transfer pathways of exoelectrogens,” *Curr Opin Chem Biol*, vol. 59, pp. 140–146, 2020.

[397] K. P. Nevin and D. R. Lovley, “Lack of production of electron-shuttling compounds or solubilization of Fe (III) during reduction of insoluble Fe (III) oxide by Geobacter metallireducens,” *Appl Environ Microbiol*, vol. 66, no. 5, pp. 2248–2251, 2000.
[398] D. P. Lies, M. E. Hernandez, A. Kappler, R. E. Mielke, J. A. Gralnick, and D. K. Newman, “Shewanella oneidensis MR-1 uses overlapping pathways for iron reduction at a distance and by direct contact under conditions relevant for biofilms,” *Appl Environ Microbiol*, vol. 71, no. 8, pp. 4414–4426, 2005.
[399] A. D. Corts, R. T. Gill, and J. A. Gralnick, “Development of a conjugation-based genome editing tool in shewanella oneidensis MR-1 using CRISPR/Cas9 and recombineering,” in *Synthetic Biology Conference: Engineering, Evolution, and Design, SEED 2017*, 2017, pp. 136–137.
[400] Y. Suzuki, A. Kouzuma, and K. Watanabe, “CRISPR/Cas9-mediated genome editing of Shewanella oneidensis MR-1 using a broad host-range pBBR1-based plasmid,” *J Gen Appl Microbiol*, vol. 66, no. 1, pp. 41–45, 2020.
[401] H. H. Hau, A. Gilbert, D. Coursolle, and J. A. Gralnick, “Mechanism and consequences of anaerobic respiration of cobalt by Shewanella oneidensis strain MR-1,” *Appl Environ Microbiol*, vol. 74, no. 22, pp. 6880–6886, 2008.
[402] E. A. H. Mohamed, “Biophysical remediation of vanadium by Shewanella sp. E1,” 2017.
[403] B. E. Igiri, S. I. R. Okoduwa, G. O. Idoko, E. P. Akabuogu, A. O. Adeyi, and I. K. Ejiogu, “Toxicity and bioremediation of heavy metals contaminated ecosystem from tannery wastewater: a review,” *J Toxicol*, vol. 2018, 2018.
[404] N. Ghorbanzadeh, R. Kumar, S. Lee, H.-S. Park, and B.-H. Jeon, “Impact of Shewanella oneidensis on heavy metals remobilization under reductive conditions in soil of Guilan Province, Iran,” *Geosciences Journal*, vol. 22, no. 3, pp. 423–432, 2018.
[405] B. E. Logan, R. Rossi, A. Ragab, and P. E. Saikaly, “Electroactive microorganisms in bioelectrochemical systems,” *Nat Rev Microbiol*, vol. 17, no. 5, pp. 307–319, 2019.
[406] D. R. Lovley, “The microbe electric: conversion of organic matter to electricity,” *Curr Opin Biotechnol*, vol. 19, no. 6, pp. 564–571, 2008.
[407] H.-R. Yuan *et al.*, “Significant enhancement of electron transfer from Shewanella oneidensis using a porous N-doped carbon cloth in a bioelectrochemical system,” *Science of The Total Environment*, vol. 665, pp. 882–889, 2019.
[408] A. Hirose, A. Kouzuma, and K. Watanabe, “Hydrogen-dependent current generation and energy conservation by Shewanella oneidensis MR-1 in bioelectrochemical systems,” *J Biosci Bioeng*, vol. 131, no. 1, pp. 27–32, 2021.
[409] S. Ikeda *et al.*, “Shewanella oneidensis MR-1 as a bacterial platform for electro-biotechnology,” *Essays Biochem*, vol. 65, no. 2, pp. 355–364, 2021.
[410] G. E. Pinchuk *et al.*, “Pyruvate and lactate metabolism by Shewanella oneidensis MR-1 under fermentation, oxygen limitation, and fumarate respiration conditions,” *Appl Environ Microbiol*, vol. 77, no. 23, pp. 8234–8240, 2011.
[411] Y. J. Tang, A. L. Meadows, J. Kirby, and J. D. Keasling, “Anaerobic central metabolic pathways in Shewanella oneidensis MR-1 reinterpreted in the light of isotopic metabolite labeling,” *J Bacteriol*, vol. 189, no. 3, pp. 894–901, 2007.
[412] J. Zhang *et al.*, “Construction of an acetate metabolic pathway to enhance electron generation of engineered Shewanella oneidensis,” *Front Bioeng Biotechnol*, vol. 9, 2021.
[413] D. R. Lovley, E. J. P. Phillips, and D. J. Lonergan, “Hydrogen and formate oxidation coupled to dissimilatory reduction of iron or manganese by Alteromonas putrefaciens,” *Appl Environ Microbiol*, vol. 55, no. 3, pp. 700–706, 1989.

[414] K. L. Duhl and M. A. TerAvest, “Shewanella oneidensis NADH dehydrogenase mutants exhibit an amino acid synthesis defect,” *Front Energy Res*, vol. 7, p. 116, 2019.
[415] S. Yoon, R. A. Sanford, and F. E. Löffler, “Shewanella spp. use acetate as an electron donor for denitrification but not ferric iron or fumarate reduction,” *Appl Environ Microbiol*, vol. 79, no. 8, pp. 2818–2822, 2013.
[416] D.-H. Park and B.-H. Kim, “Growth properties of the iron-reducing bacteria, Shewanella putrefaciens IR-1 and MR-1 coupling to reduction of Fe (III) to Fe (II),” *Journal of Microbiology*, vol. 39, no. 4, pp. 273–278, 2001.
[417] S.-L. Li, Y.-J. Wang, Y.-C. Chen, S.-M. Liu, and C.-P. Yu, “Chemical characteristics of electron shuttles affect extracellular electron transfer: shewanella decolorationis NTOU1 simultaneously exploiting acetate and mediators,” *Front Microbiol*, vol. 10, p. 399, 2019.
[418] H. N. Dai, T.-A. D. Nguyen, L.-P. M. LE, M. van Tran, T.-H. Lan, and C.-T. Wang, “Power generation of Shewanella oneidensis MR-1 microbial fuel cells in bamboo fermentation effluent,” *Int J Hydrogen Energy*, vol. 46, no. 31, pp. 16612–16621, 2021.
[419] S. L. Calderon, P. G. Avelino, A. M. Baena-Moncada, A. L. Paredes-Doig, and L. Rosa-Toro, “Electrical energy generation in a double-compartment microbial fuel cell using Shewanella spp. strains isolated from Odontesthes regia,” *Sustainable Environment Research*, vol. 30, no. 1, pp. 1–10, 2020.
[420] T. Ito, K. Yoshiguchi, H. D. Ariesyady, and S. Okabe, “Identification of a novel acetate-utilizing bacterium belonging to Synergistes group 4 in anaerobic digester sludge,” *ISME J*, vol. 5, no. 12, pp. 1844–1856, 2011.
[421] H. Weber, K. D. Kulbe, H. Chmiel, and W. Trösch, “Microbial acetate conversion to methane: kinetics, yields and pathways in a two-step digestion process,” *Appl Microbiol Biotechnol*, vol. 19, no. 4, pp. 224–228, 1984.
[422] X. Pan *et al.*, “Deep insights into the network of acetate metabolism in anaerobic digestion: focusing on syntrophic acetate oxidation and homoacetogenesis,” *Water Res*, vol. 190, p. 116774, 2021.
[423] D. Pant, G. van Bogaert, M. de Smet, L. Diels, and K. Vanbroekhoven, “Use of novel permeable membrane and air cathodes in acetate microbial fuel cells,” *Electrochim Acta*, vol. 55, no. 26, pp. 7710–7716, 2010.
[424] D. Z. Khater, K. M. El-Khatib, and H. M. Hassan, “Microbial diversity structure in acetate single chamber microbial fuel cell for electricity generation,” *Journal of Genetic Engineering and Biotechnology*, vol. 15, no. 1, pp. 127–137, 2017.
[425] Y. Zhang, B. Min, L. Huang, and I. Angelidaki, “Generation of electricity and analysis of microbial communities in wheat straw biomass-powered microbial fuel cells,” *Appl Environ Microbiol*, vol. 75, no. 11, pp. 3389–3395, 2009.
[426] R. O. N. Grosz and G. Stephanopoulos, “Statistical mechanical estimation of the free energy of formation of E. coli biomass for use with macroscopic bioreactor balances,” *Biotechnol Bioeng*, vol. 25, no. 9, pp. 2149–2163, 1983.
[427] J. Glazyrina *et al.*, “High cell density cultivation and recombinant protein production with Escherichia coli in a rocking-motion-type bioreactor,” *Microb Cell Fact*, vol. 9, no. 1, pp. 1–11, 2010.
[428] X. Zhang, W. He, L. Ren, J. Stager, P. J. Evans, and B. E. Logan, “COD removal characteristics in air-cathode microbial fuel cells,” *Bioresour Technol*, vol. 176, pp. 23–31, 2015.

[429] S. F. Ketep, E. Fourest, and A. Bergel, “Experimental and theoretical characterization of microbial bioanodes formed in pulp and paper mill effluent in electrochemically controlled conditions,” *Bioresour Technol*, vol. 149, pp. 117–125, 2013.
[430] A. G. Capodaglio *et al.*, “Microbial fuel cells for direct electrical energy recovery from urban wastewaters,” *The Scientific World Journal*, vol. 2013, 2013.
[431] S. Freguia, K. Rabaey, Z. Yuan, and J. Keller, “Electron and carbon balances in microbial fuel cells reveal temporary bacterial storage behavior during electricity generation,” *Environ Sci Technol*, vol. 41, no. 8, pp. 2915–2921, 2007.
[432] F. Yu, C. Wang, and J. Ma, “Applications of graphene-modified electrodes in microbial fuel cells,” *Materials*, vol. 9, no. 10, p. 807, 2016.
[433] S. Kerzenmacher, “Engineering of microbial electrodes,” *Bioelectrosynthesis*, pp. 135–180, 2017.
[434] R. Kaur, A. Marwaha, V. A. Chhabra, K.-H. Kim, and S. K. Tripathi, “Recent developments on functional nanomaterial-based electrodes for microbial fuel cells,” *Renewable and Sustainable Energy Reviews*, vol. 119, p. 109551, 2020.
[435] R. Toczyłowska-Mamińska *et al.*, “Evolving microbial communities in cellulose-fed microbial fuel cell,” *Energies (Basel)*, vol. 11, no. 1, p. 124, 2018.
[436] J. Wang, K. Ren, Y. Zhu, J. Huang, and S. Liu, “A Review of Recent Advances in Microbial Fuel Cells: Preparation, Operation, and Application,” *BioTech*, vol. 11, no. 4, p. 44, 2022.
[437] M. Abbaszadeh Amirdehi, S. Saem, M. P. Zarabadi, J. M. Moran-Mirabal, and J. Greener, “Microstructured anodes by surface wrinkling for studies of direct electron transfer biofilms in microbial fuel cells,” *Adv Mater Interfaces*, vol. 5, no. 13, p. 1800290, 2018.
[438] N. S. Malvankar, M. T. Tuominen, and D. R. Lovley, “Biofilm conductivity is a decisive variable for high-current-density Geobacter sulfurreducens microbial fuel cells,” *Energy Environ Sci*, vol. 5, no. 2, pp. 5790–5797, 2012.
[439] A. Salabat and F. Mirhoseini, “A novel and simple microemulsion method for synthesis of biocompatible functionalized gold nanoparticles,” *J Mol Liq*, vol. 268, pp. 849–853, 2018.
[440] A. K. Suresh *et al.*, “Monodispersed biocompatible silver sulfide nanoparticles: facile extracellular biosynthesis using the γ-proteobacterium, Shewanella oneidensis,” *Acta Biomater*, vol. 7, no. 12, pp. 4253–4258, 2011.
[441] S. Singh, J. Kaur, A. Tovstolytkin, and G. Singh, “Superparamagnetic β-NaFeO2: a novel, efficient and biocompatible nanoparticles for treatment of cancer by nanohyperthermia,” *Mater Res Express*, vol. 6, no. 8, p. 0850a6, 2019.

Appendices

Appendix A: Detailed designs of MFC double-compartment reactor (250 mL)

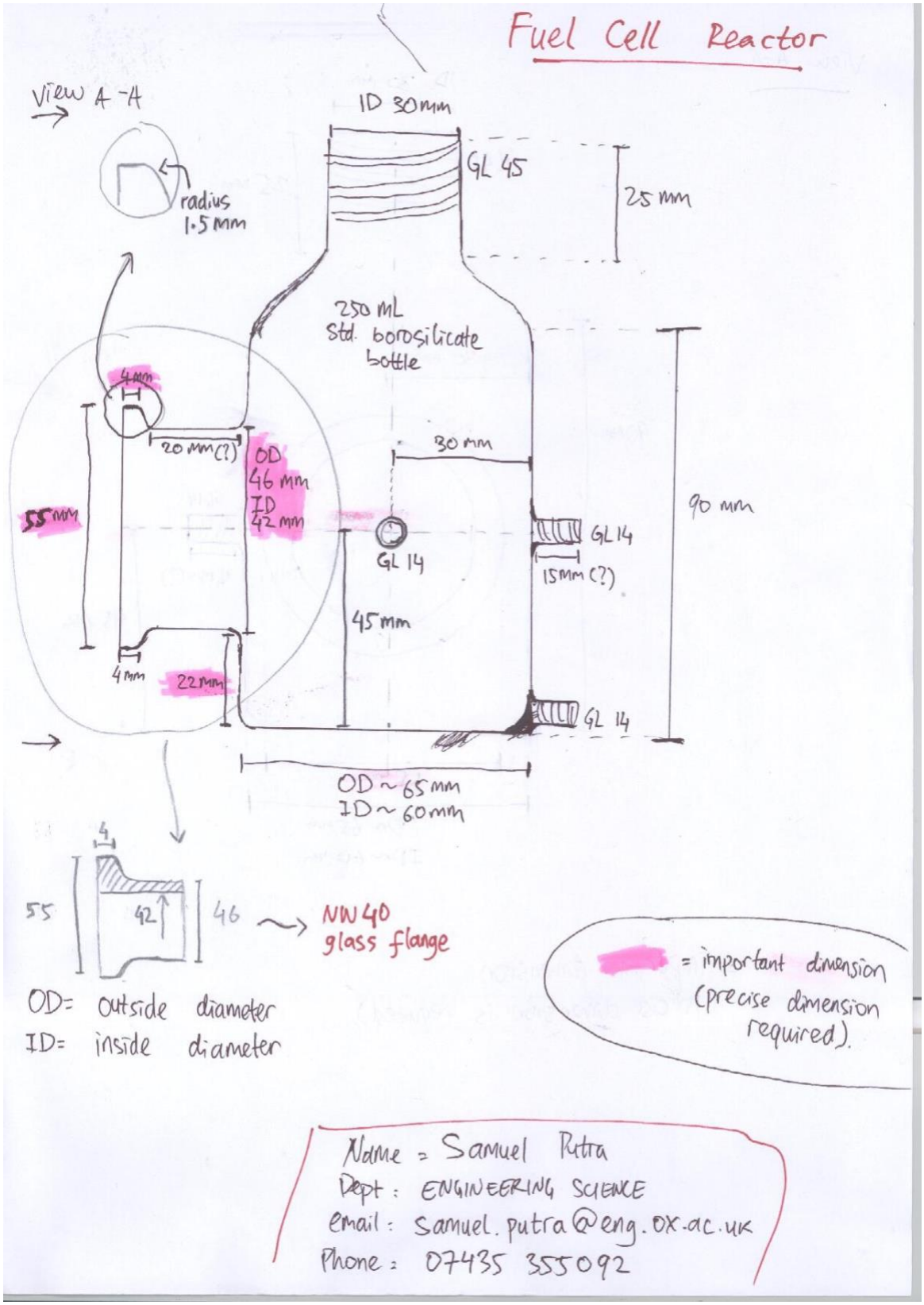

Appendix A (continued)

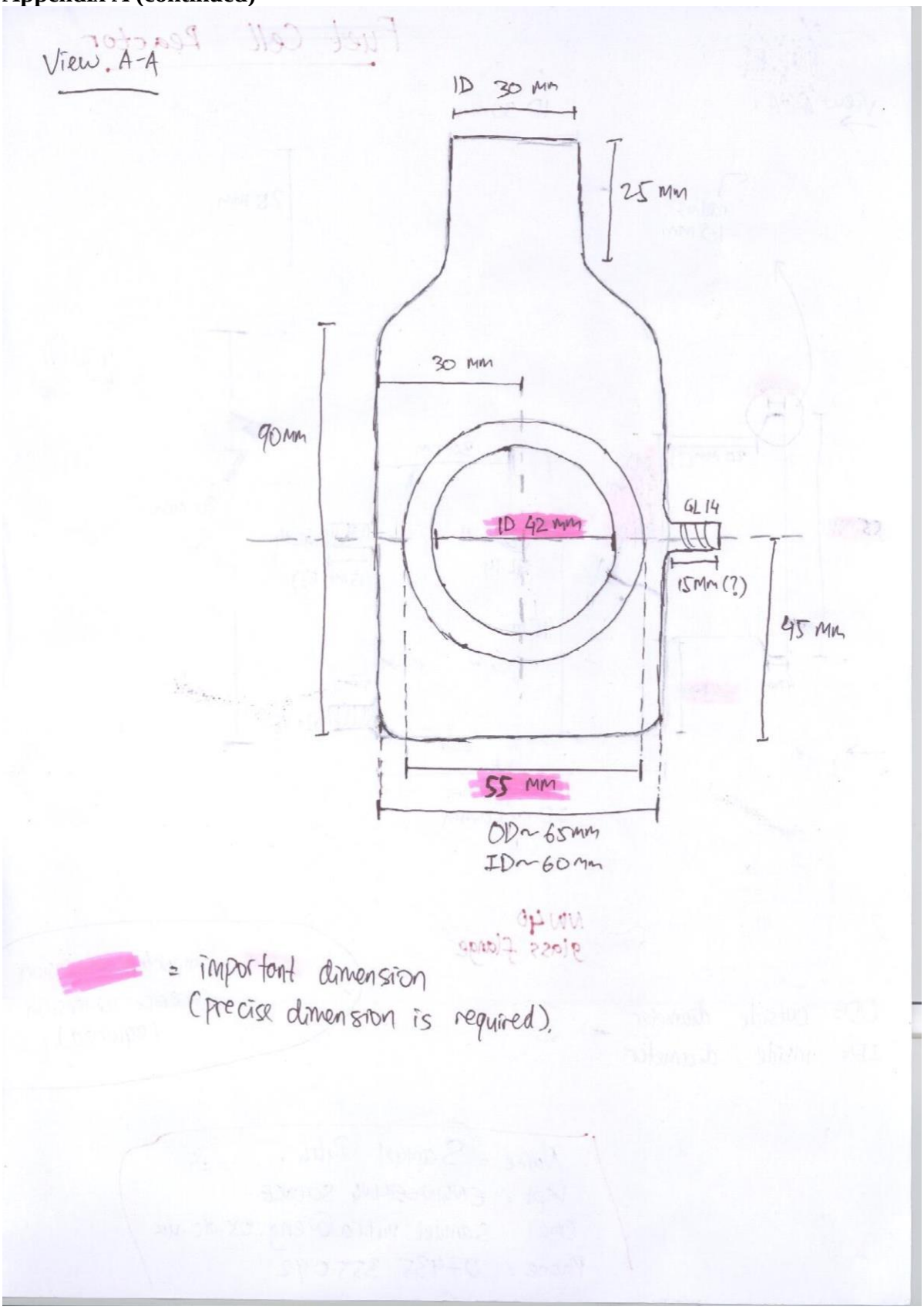

Appendix B: Engineering drawing of MFC double-compartment reactor (50 mL)

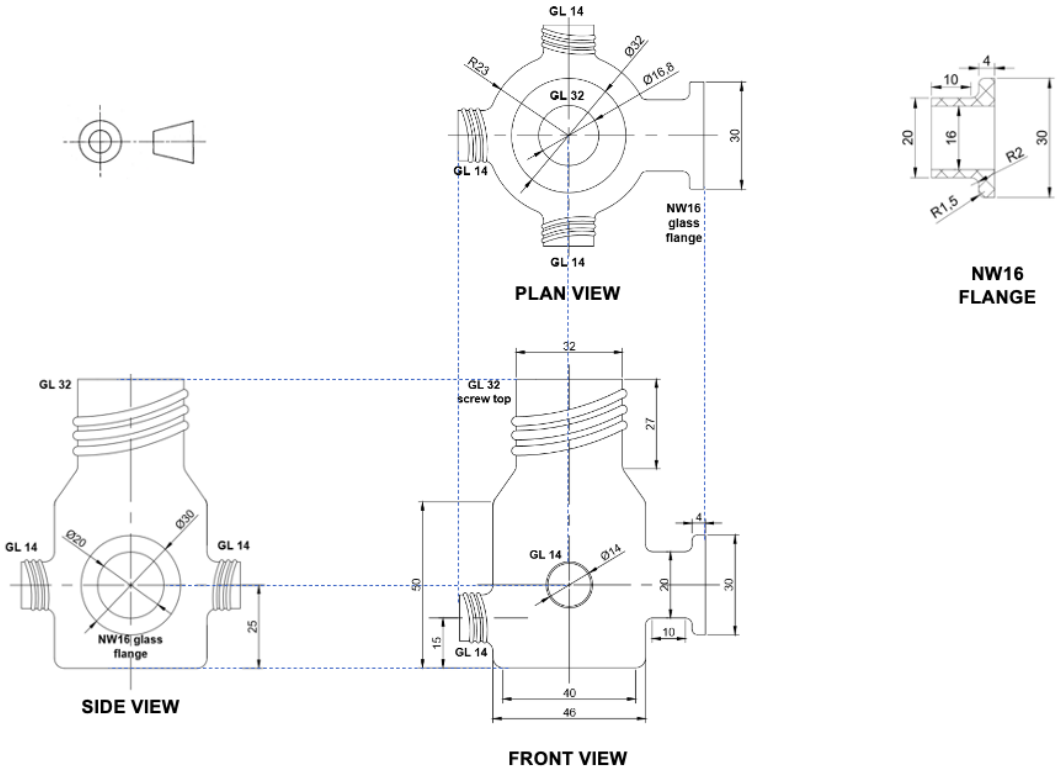

Table S1: Ingredients of vitamin stock (x100)

Chemical	**FW**	**mg/L**
Biotin (d-biotin)	244.3	2
Folic acid	441.1	2
Pyridoxine HCl	205.6	10
Riboflavin	376.4	5
Thiamine HCl 1.0 H_2O	355.3	5
Nicotinic acid	123.1	5
d-Pantothenic acid, hemicalcium salt	238.3	5
B12	1355.4	0.1
p-Aminobenzoic acid	137.13	5
Thioctic acid (or lipoic acid)	206.3	5

Table S2: Ingredients of mineral stock (x100)

Chemical	**FW**	**g/L**
Nitrilotriacetic acid	199.1	1.5
MgSO4.7H2O	246.48	3
MnSO4.H2O	169.02	0.5
NaCl	58.44	1
FeSO4.7H2O	277.91	0.1
CaCl2.2H2O	146.99	0.1
CoCl2.6H2O	237.93	0.1
ZnCl2	136.28	0.13
CuSO4.5H2O	249.68	0.01
AlK(SO4)2.12H2O	474.38	0.01
H3BO3	61.83	0.01
Na2MoO4.2H2O	241.95	0.025
NiCl2.6H2O	237.6	0.024
Na2WO4.2H2O	329.86	0.025

Table S3: Ingredients of amino acid stock (x100)

Chemical	**FW**	**g/L**
L-Glutamic acid	147.13	2
L-arginine	174.2	2
DL-serine	105.09	2

Sequencing results

pYYDT-C5 fragment to be detected by *PRTac-SF3_for* and *ribC-02_R8_rev* for UDD confirmation in MFC

Forward:

NNNNGGNNNNNNNNAGAGGAGAATCTAGTATGTTCCACCCAATCGAAGAAGCTT
TAGATGCTTTAAAAAAAGGTGAAGTTATCATCGTTGTTGATGATGAAGATCGTGA
AAACGAAGGTGATTTCGTTGCTTTAGCTGAACACGCTACTCCAGAAGTTATCAAC
TTCATGGCTACTCACGGTCGTGGTTTAATCTGTACTCCATTATCTGAAGAAATCG
CTGATCGTTTAGATTTACACCCAATGGTTGAACACAACACTGATTCTCACCACAC
TGCTTTCACTGTTTCTATCGATCACCGTGAAACTAAAACTGGTATCTCTGCTCAAG
AACGTTCTTTCACTGTTCAAGCTTTATTAGATTCTAAATCTGTTCCATCTGATTTC
CAACGTCCAGGTCACATCTTCCCATTAATCGCTAAAAAAGGTGGTGTTTTAAAAC
GTGCTGGTCACACTGAAGCTGCTGTTGATTTAGCTGAAGCTTGTGGTTCTCCAGG
TGCTGGTGTTATCTGTGAAATCATGAACGAAGATGGTACTATGGCTCGTGTTCCA
GAATTAATCGAAATCGCTAAAAAACACCAATTAAAAATGATCACTATCAAAGAT
TTAATCCAATACCGTTACAACTTAACTACTTTAGTTGAACGTGAAGTTGATATCA
CTTTACCAACTGATTTCGGTACTTTCAAAGTTTACGGTTACACTAACGAAGTTGA
TGGTAAAGAACACGTTGCTTTCGTTATGGGTGATGTTCCATTCGGTGAANAACCA
GTTTTAGTTCGTGTTCNNTCTGAATGTTTAACTGGTGATGTTTTCGGTTCTCANCG
TTGTGATTGTGGTCCACAATTACNCGCTGCTTTAAACCAAATCGCTGCTGAAGGT
CGNGGNGTTTNNTAAACTTACGTCANNNAGGTCNNNGTATCGGTTTAATCANNA
AATTAAAAGCTTANAAATTANNNNAACAAGGTTANAANNNNGNTNNNNCTANN
NNNNNNTNNNNNNNNNNNNNNNNNNNNNNNNNNNNNNNNNNNNNNNNNNNNN
NNNNNNNNNNNNNNNNNNNANNNNNNNNNNNNNNNNNNNCNNNNANNNNN
NNNNNTANNNNNNNNNNNNNNNNNNNNNNNNNNNNNNNNNNNNNNNNNNNN
NNNAA

Reverse:

NNNNNGCTTCNNNGTNNNCCNTTTTCNNNTTGTTCAGTTAATTCTTTTGATACCG
TTGAATTTACGTTCAGAACGGATACGTTTGTACCATTCGATTTTGATAGCAGCAC
CGTAAACTTCTTTGGTTGAAATCGAATAAGTTAACTTCGATAGATGGTTGTTTCT
GGACGTTTTTCGTAGAAAGTTGGTTTGTAACCGATGTTACAAACACCGTTTGTAA
ACTTCACCGTTAACTTCAGCTTTAACAGCGTAAACACCAGTTGGTGGAACGATGT
AAGAGTTGTTTAAACCAACGTTAGCAGTTGGGAAACCGATAGTACGACCACGTT
TATCACCGTGGATAACGATACCTTTGATGAAGTATGGTTGACCTAATAAAACGTT
AGCTAATTCAACATCACCGTTTTGTAAAGCAGTACGGATGTAAGAAGAAGAGAT
TTTTTTATCTTGTTCAGTTAATTTTTCAACCATAGTACAACCAGCTTTACCATCTA
AATCATCTGGCATAGTTTTCATAGTACCTTTACCGTATTTACCGTAAGTGAAATC
GAAACCAGCAACAGCGTGTTGAACGTTTAAACCGATGATGTATTGATCGATGAA
TTGTTTTGGAGATAAAGAAGCGAAAACTTCGTTGAATTTAACAACGTATAAAACT
TCAGTACCTAATTGTTCGATTTGGTTGATTTTATCTTCTAATGGAGTGATTAAATC
TTTTGGTTCTTTATCACGACCTAAAACGTGAGATGGGTGTGGGTGGAAAGTCATA
ACAGCTAAAGTTAAACCTTTTTCTTCAGCGATTTGTTTAGCAGTACCGATAACTTT
TTGGTGACCTAAGTGAANNCCATCGAAGTAACCTAAAGCCNNAACAGATTTAGC
TTGNTCTCNTTGATAATGGNGGGGNNNNNNNNNNGGGGAAANTNTNNNCNNNA
GTTNNNNCNNNNNNNNNNNNNTANNNNAAANAACGGTTANNTNNNNNNTNNNN
NNNNNNNNNNTTGACTANNNNACANATNNNNNNN

Sequencing result of UDD-treated MFC-biofilm plasmid

Forward:

NNNNGGGNNNNGAAGAGGAGAATCTAGTATGTTCCACCCAATCGAAGAAGCTTT
AGATGCTTTAAAAAAAGGTGAAGTTATCATCGTTGTTGATGATGAAGATCGTGA
AAACGAAGGTGATTTCGTTGCTTTAGCTGAACACGCTACTCCAGAAGTTATCAAC
TTCATGGCTACTCACGGTCGTGGTTTAATCTGTACTCCATTATCTGAAGAAATCG
CTGATCGTTTAGATTTACACCCAATGGTTGAACACAACACTGATTCTCACCACAC
TGCTTTCACTGTTTCTATCGATCACCGTGAAACTAAAACTGGTATCTCTGCTCAAG
AACGTTCTTTCACTGTTCAAGCTTTATTAGATTCTAAATCTGTTCCATCTGATTTC
CAACGTCCAGGTCACATCTTCCCATTAATCGCTAAAAAAGGTGGTGTTTTAAAAC
GTGCTGGTCACACTGAAGCTGCTGTTGATTTAGCTGAAGCTTGTGGTTCTCCAGG
TGCTGGTGTTATCTGTGAAATCATGAACGAAGATGGTACTATGGCTCGTGTTCCA
GAATTAATCGAAATCGCTAAAAAACACCAATTAAAAATGATCACTATCAAAGAT
TTAATCCAATACCGTTACAACTTAACTACTTTAGTTGAACGTGAAGTTGATATCA
CTTTACCAACTGATTTCGGTACTTTCAAAGTTTACGGTTACACTAACGAAGTTGA
TGGTAAAGAACACGTTGCTTTCGTTATGGGTGATGTTCCATTCGGTGAANAACCA
GTTTTAGTTCGNGTTCACTCTGAATGTTTAACTGNNGATGTTTTCGGTTCTNACCG
TTGTGATTGTGGTCCACAATTACNCGNTGCTTTAAACCAAATCGCTGCTGAAGGT
CGNNNTNTTTTATNANACTTACGTCANNNAGGTNNNGGTNTCGGTTNAATCAAC
AAATTAAAAGCTTACAATTACANNNACAAGGTTANAAANNNNNNNNNNNTAAN
NANNNNNNNNNNNNNNNNNNNNNNNNNNNNNNNNNNNNNNNNNNNNNNNNN
NNNNNNNNNNNNNNNNNNNNNNNNNNANNNNNNNCNNNNNNNNNNNNNNANN
NNNNNNNNNNNNNNNNNNNNNNNNNNNNNNNNNA

Reverse:

NNNNNCTTCTTTGTTTATCTTTTTCGATTTGTTCAGTTAATTCTTTGATACCGTTGA
ATTTACGTTCAGAACGGATACGTTTGTACCATTCGATTTTGATAGCAGCACCGTA
AACTTCTTGGTTGAAATCGAATAAGTTAACTTCGATAGATGGTTGTTCTGGACGT
TTTTCGTAGAAAGTTGGTTTGTAACCGATGTTACAAACACCGTTGTAAACTTCAC
CGTTAACTTCAGCTTTAACAGCGTAAACACCAGTTGGTGGAACGATGTAAGAGTT
GTTTAAACCAACGTTAGCAGTTGGGAAACCGATAGTACGACCACGTTTATCACCG
TGGATAACGATACCTTTGATGAAGTATGGTTGACCTAATAAAACGTTAGCTAATT
CAACATCACCGTTTTGTAAAGCAGTACGGATGTAAGAAGAAGAGATTTTTTTATC
TTGTTCAGTTAATTTTTCAACCATAGTACAACCAGCTTTACCATCTAAATCATCTG
GCATAGTTTTCATAGTACCTTTACCGTATTTACCGTAAGTGAAATCGAAACCAGC
AACAGCGTGTTGAACGTTTAAACCGATGATGTATTGATCGATGAATTGTTTTGGA
GATAAAGAAGCGAAAACTTCGTTGAATTTAACAACGTATAAAACTTCAGTACCT
AATTGTTCGATTTGGTTGATTTTATCTTCTAATGGAGTGATTAAATCTTTTGGTTC
TTTATCACGACCTAAAACGTGAGATGGGGTGTGGGGTGGAAAGTCATAACAGCT
AAAGTTAAACCTTTTTCTTCAGCGATTTGTTTAGCAGTACCGATAACTTTTTGGTG
ACCTAAGTGAACACCATCGAAGTAACCTAAAGCNATAACNNNTTTAGNTTGNTC
TTCTTTGATTAANNGNGGGGGTGAATGANNNNNAAAANTTT

Figures

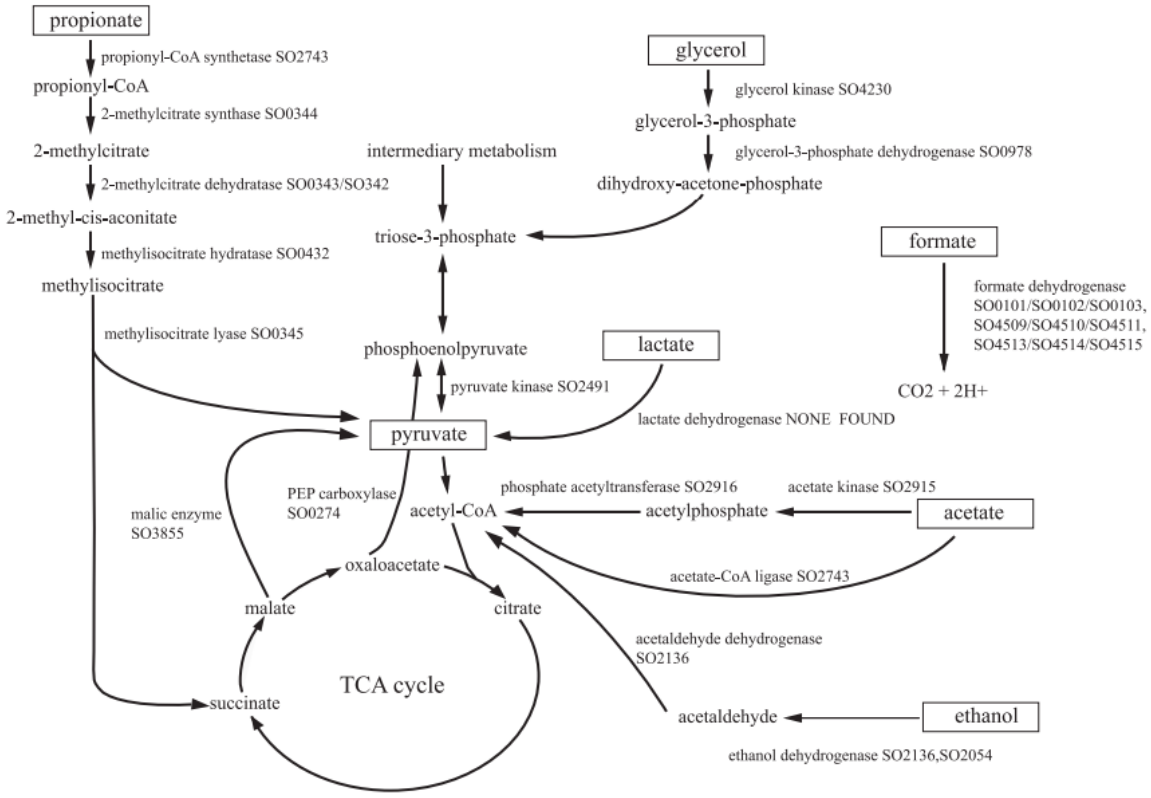

Fig. S1: Enzymes in S. oneidensis MR-1 for utilization of one-, two-, and three-carbon compounds. Enzymes involved in the degradation of compounds with one carbon (formate), two carbons (acetate, ethanol), and three carbons (propionate, glycerol, lactate, and pyruvate) are shown by their names and predicted S. oneidensis locus tags (SO number). The function predictions were based on sequence similarity to proteins with experimentally verified functions. Predicted isozymes are shown as SO numbers separated by a comma. Enzyme complexes are indicated by SO numbers separated by a forward slash. TCA, tricarboxylic acid.

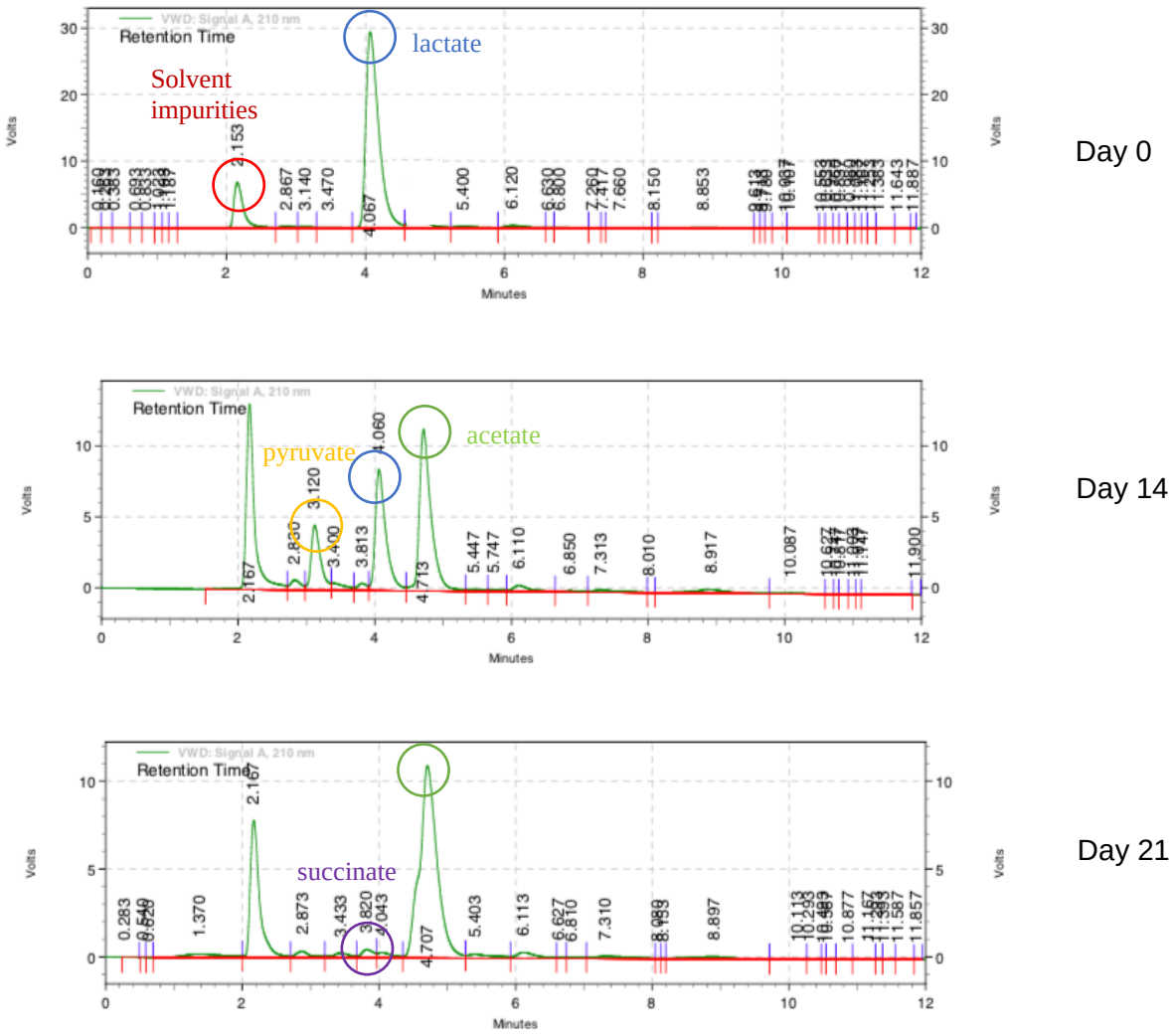

Fig. S2: HPLC chromatogram of lactate-fed MFC anodic media at a) start of the experiment; b) day 14 and c) day 21. Pyruvate (retention time = 3.12 min) was detected as an intermediate product at day 14; succinate was detected in trace amount (retention time = 3.82 min). Other peaks: lactate = 4.06 min; acetate = 4.71 min; solvent impurities = 2.16 min